DEVELOPMENT AND PERFORMANCE EVALUATION OF A TRAY COLUMN UNDER VERTICAL AND TILT CONDITIONS

BY

OKECHUKWU ELECHI ONYELUCHEYA (M. ENG.)

20044449929

A THESIS SUBMITTED TO THE POST GRADUATE SCHOOL, FEDERAL UNIVERSITY OF TECHNOLOGY, OWERRI.

IN PARTIAL FULFILLMENT OF THE REQUIREMENTS FOR THE AWARD OF A DOCTOR OF PHILOSOPHY (PhD) DEGREE IN CHEMICAL ENGINEERING

JUNE 2013

CERTIFICATION

I certify that this work "DEVELOPMENT AND PERFORMANCE EVALUATION OF A TRAY COLUMN UNDER VERTICAL AND TILT CONDITIONS" was carried out by Engr. Okechukwu Elechi Onyelucheya (20044449929) in partial fulfillment for award of the degree of PhD in Chemical Engineering in the Department of Chemical Engineering, Federal University of Technology, Owerri.

Signature_____ Date_____
Engr. Prof K. O. Okpala (Supervisor)

Signature_____ Date_____
Dr. O. C. Ndukwe (Co-Supervisor)

Signature_____ Date_____
Late Professor I. A. Njiribeako (Co-Supervisor)

Signature_____ Date_____
Engr. Dr. M. S. Nwakaudu
(Head, Dept. of Chemical Engineering)

Signature_____ Date_____
Engr.Professor. E. E. Anyanwu
(Dean, School of Engineering & Eng. Tech.)

Signature_____ Date_____
Engr.Professor. K. B. Oyoh
(Dean, School of Post Graduate Studies)

Signature_____ Date_____

Engr.Professor. F. O. Chukwuma
(External Examiner)

DEDICATION

This work is dedicated to the Almighty God who gave me wisdom, and to my lovely wife Chioma who was always there for me.

ACKNOWLEDGEMENT

The conclusion of this research would not have been possible without the contributions received from numerous individuals at various stages of the work. First in line is Professor I. A. Njiribeako who intimated me of the industrial challenge that formed the basis for this research, and also painstakingly monitored and supervised the work to its conclusion. It is very painful that he did not live to see the defence of the work. I am also indebted to my other supervisors Professor K. O. Okpala, and Dr O. C. Ndukwe for their valuable contributions. Worthy of mention is the assistance of Engr. Obinna Otu, Mr. Agbada Solomon and Mr. Ugwu Hyginus of the Scientific Equipment Development Institute Enugu (SEDI-E) who fabricated the intricate aspects of the work. I am also grateful to Mr. John Emeana and Mr. Martins Anyanwu of the Centre for Industrial Studies, FUTO for their assistance with the fabrication. I finally want to acknowledge my family, friends, colleagues and well wishers for their support, encouragement, and incessant harassment over none completion of the PhD which all contributed to the completion of the work.

TABLE OF CONTENTS

NOMENCLATURE

x_1 —Gas flowrate, in litres per minute

x_2 — Liquid flowrate, in litres per minute

x_3 —Angle of tilt, in degrees

$x_{1,0}$ —Gas flowrate experimental centre point

$x_{2,0}$ —Liquid flowrate experimental centre point

$x_{3,0}$ —Experimental centre point for angle of tilt

Δx_1 —Experimental variation interval for gas flowrate

Δx_2 —Experimental variation interval for liquid flowrate

Δx_3 —Experimental variation interval for angle of tilt

y_1 —Experimental response value from first run

y_2 —Experimental response value from replicate run

y —Average experimental response

x_0 —The fictional variable (value = +1) used to estimate b_0 (the free member) in the regression equation

$b_1, b_2, b_3, \ldots, b_9$ —Regression coefficients

R^2 —Coefficient of determination

Adj R^2 —Adjusted coefficient of determination

Mse —Mean square of error

ANOVA —Analysis of variance

P-value —Probability value of student's t-test and ANOVA

t-value —Indicative value of student's t-test

F-value —Indicative value of Fisher's F-test

$F_{calculated}$ —F-value obtained from ANOVA

$F_{tabulated}$ —F-value obtained from the table

H_0 —Null hypothesis

LIST OF TABLES

LIST OF FIGURES/CHARTS

ABSTRACT

In this work, the operation and performance of a novel Separation Tray Column under Vertical and Tilt conditions is presented. The Tray Column used for the work is a Downcomerless liquid initiated and controlled Valve Tray with capacity to shut portions of the tray lacking liquid at any time. To evaluate the mass transfer performance of this column, an oxidation experiment was conducted at 30^0C and the percentage of Fe (II) oxidised to Fe (III) from contaminated water by air was chosen as the system response. The influence of the Gas flowrate (x_1 in litres per minute), the Liquid flowrate(x_2 in litres per minute) and the Angle of tilt (x_3 in degrees) on the response was represented by polynomial models and their effects were studied using the Student's t-test and Fischer's F-test for the Analysis of Variance (ANOVA) for each model. Out of the 5 models, the experimental data were found to be best represented by a linear polynomial model with Coefficient of Determination R^2 = 0.9635. The test of significance of the individual coefficients in the model based on the Student's t-test showed that only parameters x_1 and x_2 (i.e. the gas and liquid flowrates) are significant at 95% confidence level. The angle of tilt (with p=0.18) had no significant influence on the amount of Iron (II) oxidised. The ANOVA of this model showed that the model was significant as the calculated F-value (F-model = 17.60) exceeded the tabulated F-value (6.16), and also from its probability value (p=0.008) which is less than 0.05. From this test also, the model parameters x_1 and x_2 had significant influence as their calculated F-values (164.57 and 45.38 respectively) were much higher than their tabulated F-values (F=7.71). The parameter x_3 and their interaction effects were still not significant from this test as their calculated F-values (5.42 for x_3, 0.06 for x_1x_3 and 0.2 for x_2x_3) are less than their tabulated F-values of 7.71. These findings were further validated by the x-y scatter plots which showed that for all the liquid flowrates, the % Fe (II) oxidised increased with increasing vapour flowrates but the impact of the angles of tilt was minimal. The implication of these is that the operational efficiency of this novel tray column will not be compromised by column tilt of up to 20 degrees from the vertical.

Keywords: Gas to Liquid Processes, Stripping Ships, Tray Column Tilt and Motion, Novel Separation Tray Column, Mobile and Floating Platforms.

CHAPTER ONE

INTRODUCTION

1.1 BACKGROUND OF STUDY

Gas-liquid operations constitute one of the major modes of mass transfer encountered in chemical engineering applications (Sinnot, 1993). The following gas-liquid mass transfer systems are listed by Perry and Green (1997): distillation, flashing, rectification, absorption, stripping, evaporation, humidification, and spray drying. All these operations are designed to contact liquid and gas (vapour) phases for the purpose of mass, heat and momentum transfer between them (Hanley, 2012). According to Treybal (1981) "the rate of mass transfer is directly dependent upon the interfacial surface exposed between the phases, hence the nature and degree of dispersion of one fluid in the other are therefore of prime importance". Most mass transfer operations are motivated by the need to make maximum contact between phases in which mass transfer is expected to occur (Benitez, 2009, Nnolim, 1993).Properly designed gas-liquid mass transfer equipment should therefore provide efficient interphase diffusional interchange by dispersing the gas phase, liquid phase or both phases during operation in a cost effective manner (Fard et al, 2007, Liu et al, 2011, Naziri et al, 2012, Smith, 1963). The fields of application of mass transfer theories have become widespread, from traditional

chemical industries to bioscience and environmental industries, where the design of new processes, the optimization of existing processes, and solving pollution problems are all heavily dependent on knowledge of mass transfer (Asano, 2006, Negrea et al, 2008, Zang et al, 2012).

1.2 PROBLEM STATEMENT

Mass transfer equipment are designed with suitable internals, either tray/plates or packings which increase the surface area available for contact of the gas and liquid phases (Baehr & Stephan, 2006, Hoon et al, 2011).The overall column efficiency, defined as the ratio of the number of theoretical plates to actual plates required for a given separation is of ultimate concern during the design and operation of contacting devices. For a properly designed column, the efficiency depends almost entirely on proper contact between vapour and liquid streams. Any condition which leads to poor liquid distribution or short-circuiting will therefore lower the efficiency of the column. One way of avoiding liquid channelling is by ensuring the column remains vertical and does not sway during operation. The need may however arise to operate contacting devices on moving platforms. The term "moving platform," implies that the column may not always be vertical, but can sway depending on the motion of the platform. Such sways will result in tilting of

the Vapor Liquid Equilibrium (VLE) equipment mounted on the platforms and lead to a loss or total collapse of the efficiency of such equipment (Lockett & Billingham, 2003; Locket & Billingham, 2002; Tanner et al, 1996; Waldie, 1996). The design of VLE equipment which can operate under such conditions without loss of efficiency still remains a major Chemical Engineering challenge and forms the forms the basis of this research.

1.3 RESEARCH OBJECTIVES

The objectives of this research are as follows;

1. To design and construct a Separation Tray which can operate without loss of efficiency on mobile platforms.
2. To evaluate the mass transfer performance of this tray using the amount of Fe (II) oxidized to Fe (III) as the system response.
3. To test the tray in both vertical and tilted positions to determine the significance of the following key parameters;
    - The gas flowrate x_1 (in litres per minute)
    - The liquid flowrate x_2 (in litres per minute)
    - The angle of column tilt x_3 (in degrees)

1.4 RESEARCH HYPOTHESIS

Polynomial models will be developed from the experimental data to be obtained that will have the 3 key parameters as variables. The p-values in the student's t-test will be used as a tool to check the significance of each of the coefficients which in turn may indicate the pattern of the interactions between the variables. The Null Hypothesis as defined in Appendix 3 will be used as the Research Hypothesis.

1.5 JUSTIFICATION OF STUDY

Offshore oil and gas exploration activities have in recent times been on the increase. This is because as the number of new discoveries of oil and gas reserves decreases, there is need to fully exploit existing resources (Lye et al, 2007). These offshore exploration activities have their concomitant technological challenges, which are quite different from those experienced during onshore exploration. These challenges have led to the rampant use of Floating production, Storage and Offloading (FPSO) platforms, and major modifications of the process equipment used on these platforms such as coil-wound heat exchangers and contacting columns. A typical offshore exploration challenge is the need to economically recover "stranded gas". "Stranded gas" refers to gas reserves in offshore locations that cannot be transported to shore via pipelines due to the prohibitive and uneconomic cost of such a venture. These gases also cannot be flared due to the

deleterious environmental consequences of such large scale gas flaring. According to Goldstone et al (1998), remote conversion of natural gas to liquid fuels presents a unique set of challenges where offshore locations are involved. The lack of infrastructure, field marginality, inability or undesirability to flare gas, etc may require a floating production, storage and offloading installation to process the associated crude oil, convert gas to liquid fuel, store, and subsequently offload all products into shuttle tankers to the mainland.

The solution therefore lies in the conversion of such gases to high density liquids on a floating production plant either by refrigeration to Liquefied Natural Gases (LNG) or by Gas to Liquid (GTL) chemical conversion to higher molecular weight liquids which can be economically transported in shuttle tankers. In both cases, the process plant would have to be mounted on a large ship, barge, or other tethered support and hence would be subjected to tilt and motion from wave and wind forces (Waldie, 2004). A further desirable feature of such a floating platform is that it can be moved from one stranded gas source to another thus taking full advantage of a series of small reserves (Lye et al, 2007).

Although Baker and Waldie (1996) have developed a packed column which can operate in tilt and motion conditions with better efficiency than conventional packed columns, there is to date no plate column design for such operations.

The need to develop a plate column that can operate without loss of efficiency under vertical, tilt and motion conditions is the motivation for this research work.

The scope of applications of columns that can operate on mobile platforms without loss of efficiency is wide. Another classic example of this need is seen in "Stripping Ships". Stripping ships are vessels used to convey crude oil from offshore rigs to onshore refineries. These ships are equipped with stripping columns. After each discharge, the tanks are washed to avoid vaporization of the left over crude when tanks get heated (by sunlight, for example) in transit. These volatile oils are inflammable and pose fire and explosion hazards. Because of the large capacity of these tanks, the amount of oil washed down is substantial. This oil is usually recovered by stripping the wash liquid. The ship must however be docked until the stripping operation is completed. With a stripping column operating efficiently on a moving platform, no time need be lost since the separation can be carried out while the ship is in motion.

With this technology also, it will be possible if desired to erect columns on floating platforms, which may not remain rigidly vertical continuously. Hence if there should be a marine tilt or motion due to a typhoon, tsunami, tidal wave, or any other violent and adverse condition that causes the column to sway/tilt, the column would still be operating efficiently despite the sways these may cause.

Apart from these needs described above, because the operation of this novel plate column will be liquid controlled as described in the next chapter, such a column will also compete favorably with others during normal operation. It may even be found to offer certain operational efficiency advantages over the conventional plate columns in normal operating conditions

1.6 SCOPE OF STUDY

The scope of this research is to design, construct and test a separation tray which can operate without loss of efficiency on mobile platforms. The novel tray being proposed will achieve this by ensuring that intimate contact of the vapour and liquid phases is maintained at all times even if the tray experiences a tilt from its normal horizontal position.

The operation dynamics and performance of the novel tray will be evaluated on air-water system to determine its vapour and liquid flow capacity, and its tray efficiency will be evaluated based on oxidation of Fe (II) to Fe (III) in water. This test will be carried out in both vertical and tilted positions to determine the impact of the following key parameters:

- The gas flowrate
- The liquid flowrate

- The angle of column tilt

To achieve this, a Factorial Design of Experiment will be used to afford simultaneous varying of all 3 factors during the experimental runs as against the one factor at a time method where excessive amount of experimentation will be required to evaluate the simultaneous impact of the 3 factors. The experimental runs will be done in replicates to reduce random experimental errors and the data obtained will be fitted to polynomial models. The adequacy of the models will be ascertained statistically and the effects of the model parameters will also be ascertained both statistically and otherwise. From these analyses we will be able to assess the tray column performance over a range of operating conditions including tilting.

CHAPTER TWO

LITERATURE REVIEW

2.1 PLATE COLUMNS WITH DOWNCOMERS

Plate columns are vertical cylinders containing plates or trays for stage by stage contact of liquid and gas. Each plate of the tower represents a stage on which interphase transfer and separation take place. The liquid flows down the column and contacts the gas on each plate as the gas passes upward through the holes of the plate. The overall effect is a multiple stage contact of the liquid and gas.

The distinguishing feature of cross flow plate from the counterflow is the presence of downcomers in the former. The number of downcomers used and the liquid flow pattern can be varied to meet certain design specifications. Such variations can yield reverse-flow, double-pass and even four-pass liquid flow patterns.

The principal types of cross-flow plates in use are bubble cap plates, sieve plates and valve plates (floating cap plates). Schematic diagrams of these plates are shown in figs 2.1 and 2.2.

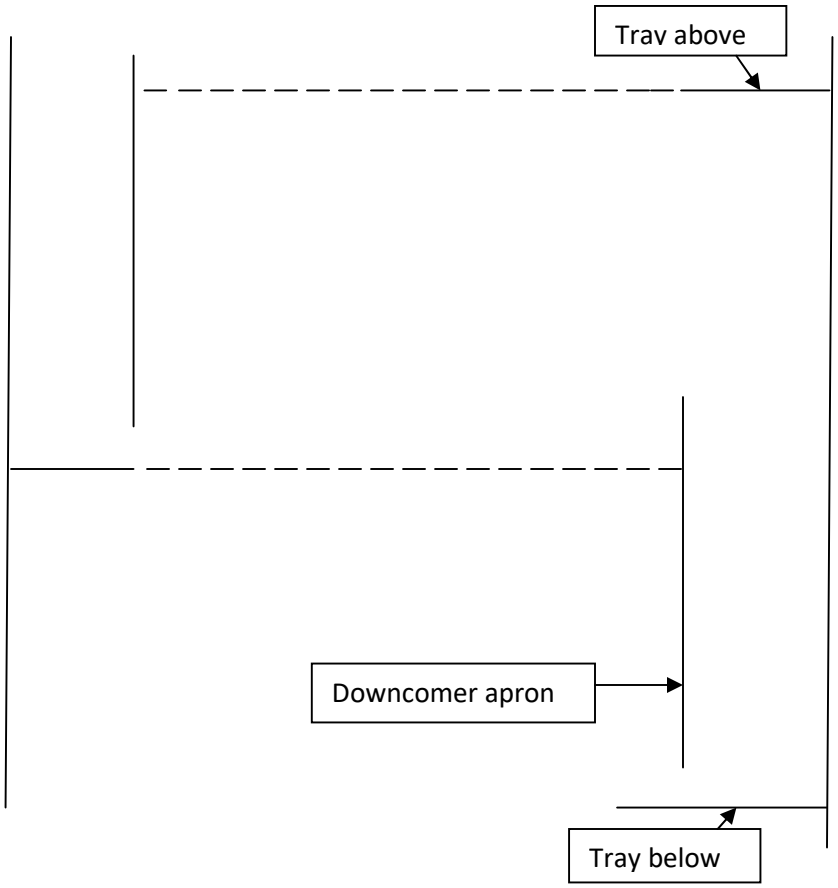

Fig 2.1: Schematic diagram of sieve tray with downcomer

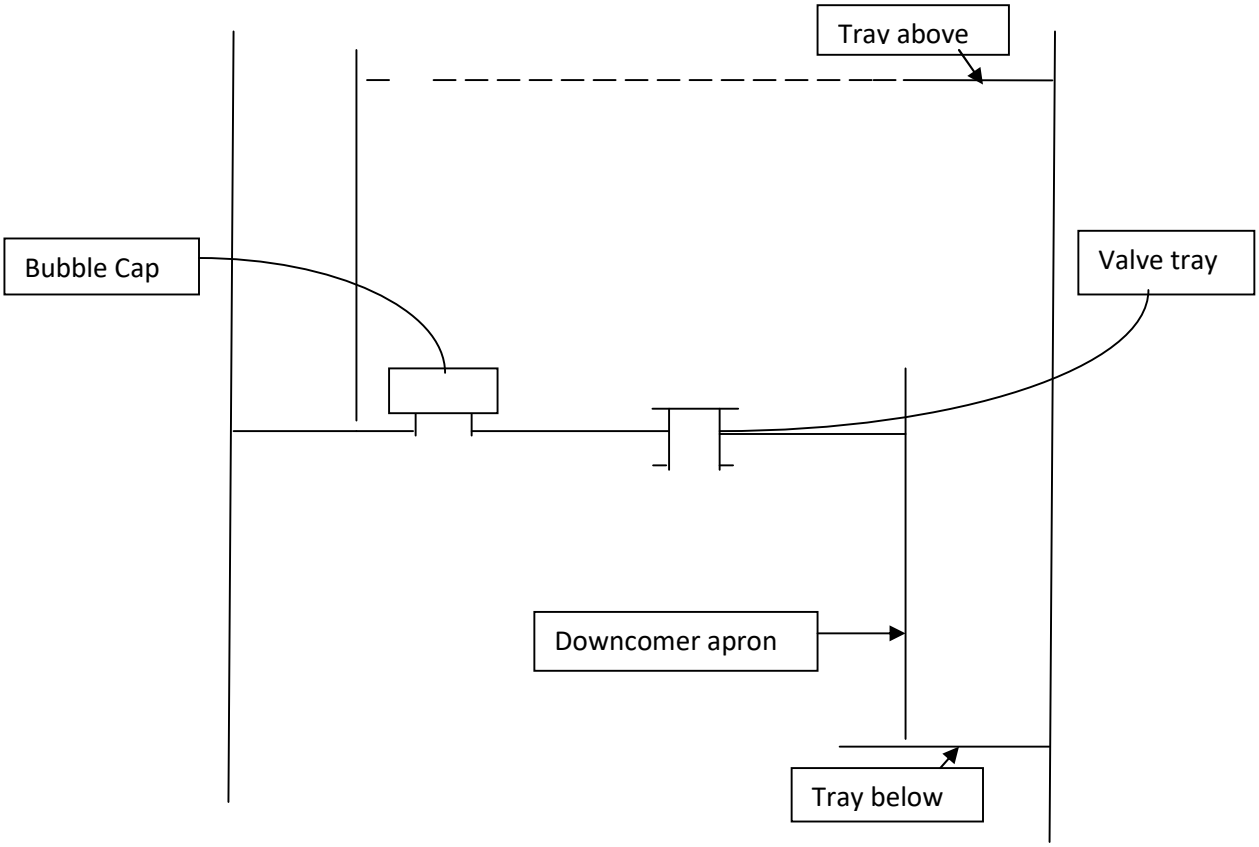

Fig 2.2: Schematic diagram of bubble cap tray and valve tray

Bolles(1963) describes bubble caps as “caps or inverted cups located above risers through which vapour enters from below the tray and is dispersed under the surface of the liquid as bubbles by means of slots in the caps”. This is the oldest design of cross-flow plates with its major advantage being the liquid seal maintained on each tray by the risers hence checking tray weeping even at low vapour rates. Liquid flows over caps, outlet weir and downcomer to the tray below.

The sieve plate is simply a perforated plate across which the liquid flows. The cross-flow pattern is ensured by the vapour, which prevents flow of liquid through the holes (weeping). At low vapor rates, the efficiency of the plate drops because some or all of the liquid drains through the perforations without proper contact.

The valve plates on the other hand are basically sieve plates with floating caps fitted with legs providing variable hole size as they open or close. The valves are operated to open or close positions by the vapour flow rate and offers improved performance over conventional sieve plates when the prevailing vapour rates are low.

2.2 PLATE COLUMNS WITHOUT DOWNCOMERS

In counter flow plates, the vapour and liquid streams flow counter currently and not in cross flow pattern as those in the previous section. Two classes of this design exist and are detailed sections 2.2.1 and 2.2.2.

2.2.1 PERFORATED TRAYS WITHOUT DOWNCOMERS

These are columns which have no downcomers and in which the tray occupies the entire column cross-section with liquid and vapour utilizing the same openings for flow. The tray openings are usually long slots or round holes and there is no cross flow of liquid but the vapour and liquid flow counter currently through the same openings intermittently. In the words of Fair (1963), during operation, "liquid dumps momentarily through one or more sections of the tray and the locations of liquid passage move about the tray in a random fashion". The implication of this is that each of the openings on the tray is either passing vapour or liquid at any given time and not the 2 fluids simultaneously (Weiland, 2001). The liquid head on the tray and the pressure of the vapour approaching the tray determine if a particular section of the tray will be passing vapour or liquid at any given time. During operation, there is usually a level of relatively clear liquid on the tray followed on top by a bubbling, agitated mass, part of which becomes frothy and/or foamy in appearance depending upon the tray operation and the fluid system properties. This results in wavelets of froth-liquid mixture moving from one place to another over the tray (Billet, 2001, Ludwig, 1997, Xu et al, 1994). The performance data for this kind of tray tower are relatively scarce and mostly proprietary.

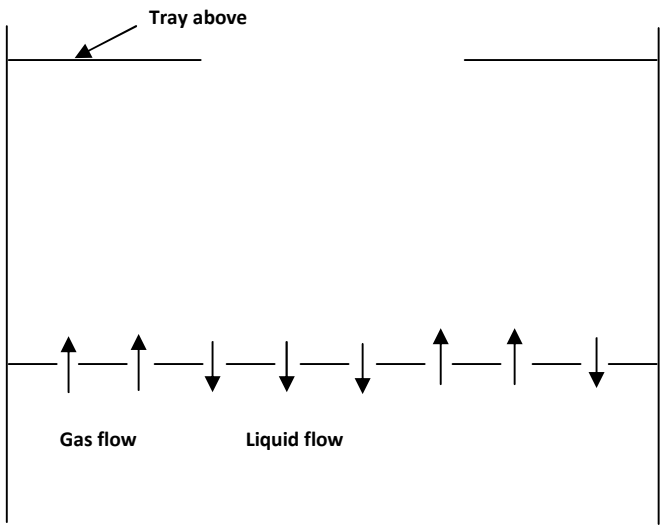

Fig 2.3 Downcomerless Counterflow plate

2.2.2 BAFFLE TRAY COLUMNS

The baffle tray column, also known as "splash/shower deck" column is another type of counter flow tray column. In these columns, the liquid cascades down from one tray to the one below thereby forming a curtain of liquid which the gas must flow through as it moves upward. The arrangement of the baffles can be the simply segmental pattern for small diameter columns or "disk and doughnut" pattern for large diameter column as shown in figs 2.4 and 2.5.

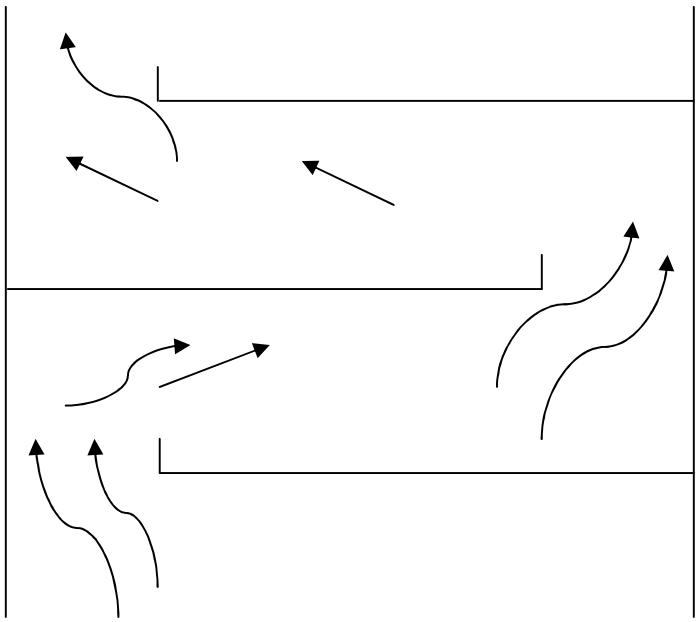

Fig 2.4 Baffle tray column

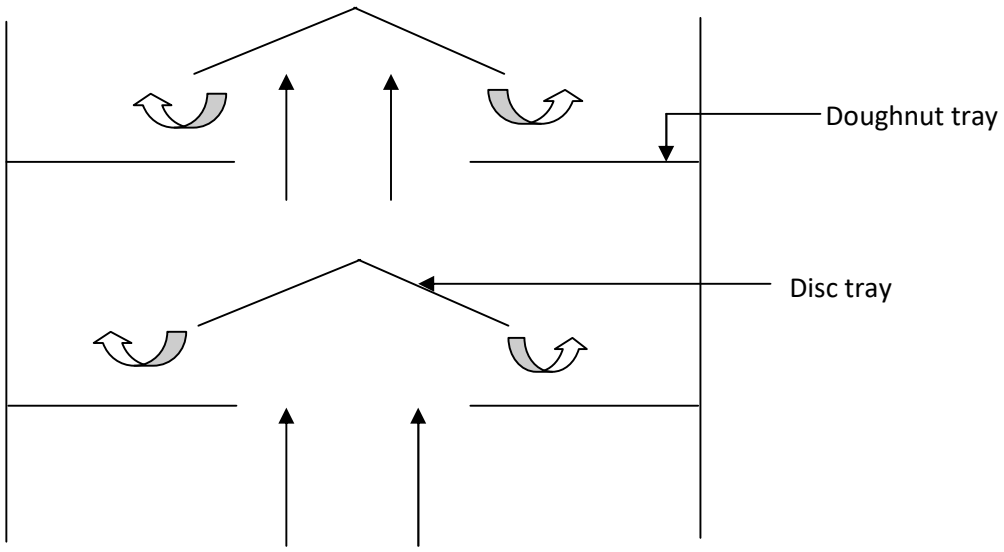

Fig 2.5 Disc and Doughnut Counterflow tray

2.3 VALVE TRAY DESIGNS USED ON CROSSFLOW TRAYS

The following are diagrams of some conventional valve tray designs currently in use for VLE separations as given by Ludwig (1997).

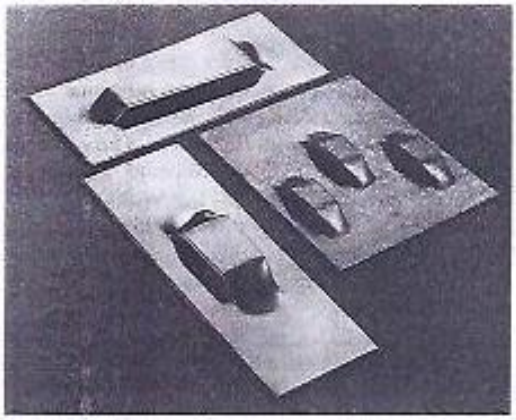

Figure 2.6 – Nutter LVG long, SVG short and MVG tray slots.

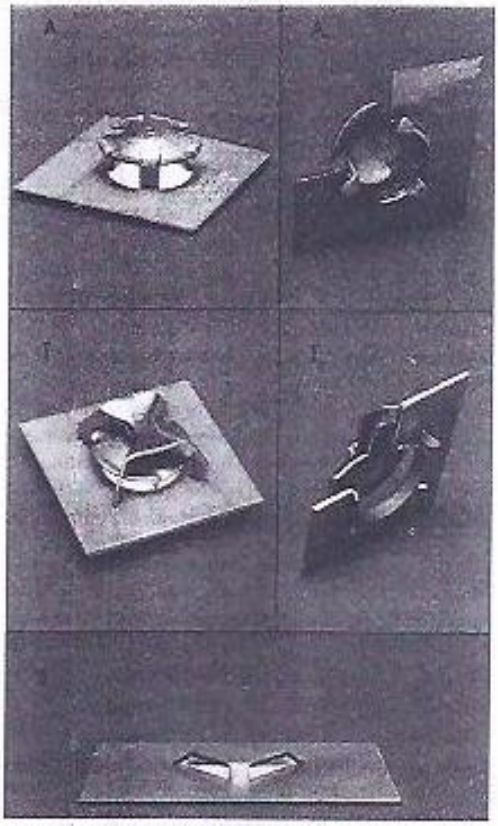

Figure 2.7 – Types of standard Koch valves.

Figure 2.8 – Type "T" Flexitray

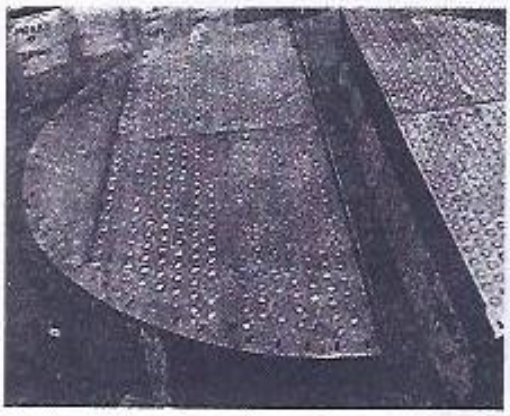

Figure 2.9 – Type "A" Flexitray

A Standard valve with integral legs used for most services, utilizing a sharp-edged orifice in the tray floor.

A_o Same "A" valve, but with a contoured hole in the tray floor for lower operating pressure drop.

T Round valve retained by a fixed holddown and a sharp-edged hole in the tray floor for all services, including fouling, slurry and corrosive applications.

T_o The same "T" valve and holddown with a contoured, low-pressure drop hole in the tray floor.

S Stationary valve punched up from the tray floor.

The A, A_o, T and T_o valves can be supplied either with a flat periphery for tightest shutoff against liquid weepage at turndown rates or with a three-dimpled periphery to minimize contact with the tray deck for fouling or corrosive conditions.

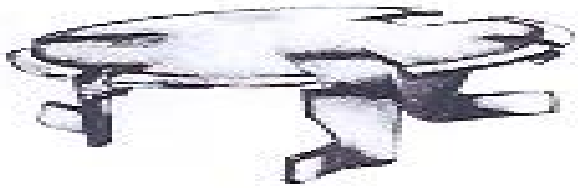

Standard Dimensions:
Diameter: 1"m"
Initial Opening: 0.10"

Figure 2.10 – Glitsch Ballast Valves, V-series

Standard Dimensions:
Diameter: 1"m"
Initial Opening: none (flush seating)

Figure 2.11 – Glitsch Ballast Valves, V-series

V-1 TYPE
(Flat Orifice)

Figure 2.12 – Glitsch Ballast Valves, V-series

Diameter of Orifice Opening: 1 17/32"

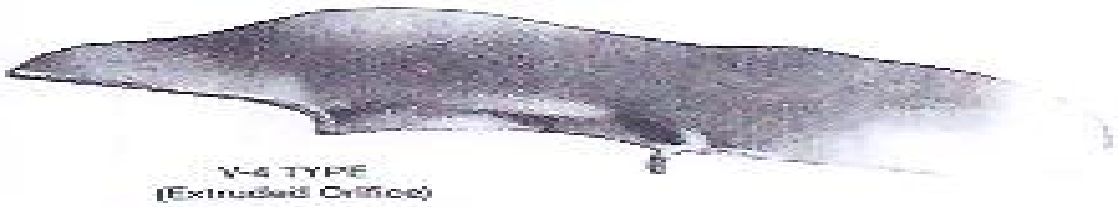

V-4 TYPE
(Extruded Orifice)

Figure 2.13 – Glitsch Ballast Valves, V-series

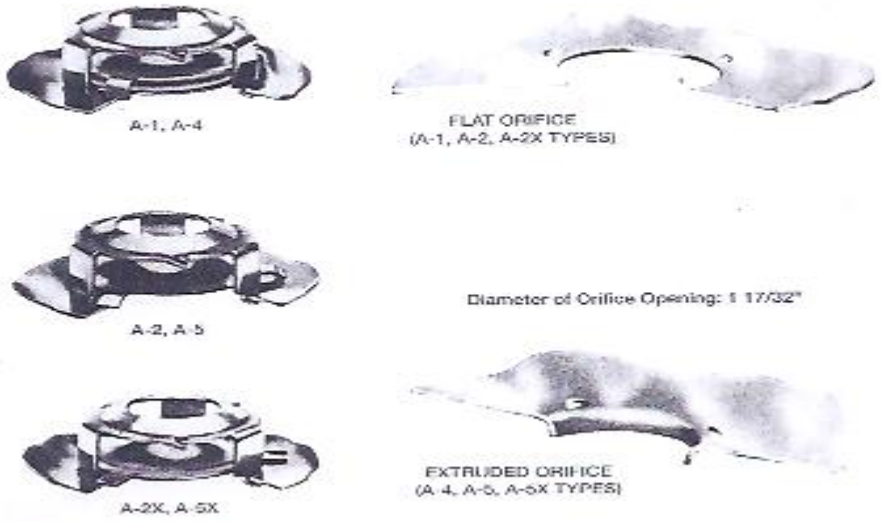

Figure 2.14 – Glitsch Ballast Valves, A-series

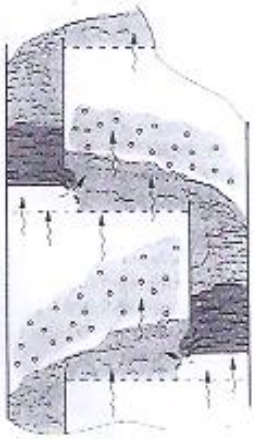

Figure 2.15 – Glitsch Nye Tray action to improve conventional sieve and valve tray performance by 10-20%.

The Nye Tray increases the area available for disengagement of this light froth. In addition to the normal perforated section, vapor can now flow into the inlet area below the downcomer. Vapor enters the contact zone of the Nye Tray through the perforated face of the inlet panel, under the liquid coming out of the downcomer.

Specifically, the Nye Tray achieves this improvement by using a patented inlet area on a sieve or valve tray, which increases the area available for vapor-liquid disengagement.

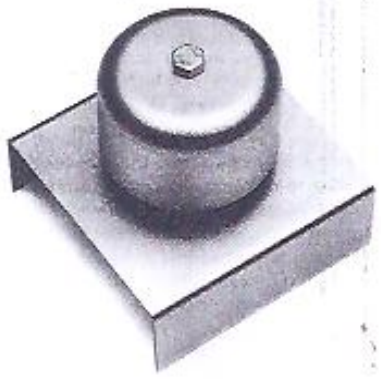

Figure 2.16 – Norton FRI Plain Bubble Cap

The Norton standard bubble cap is the Fractionation Research Inc. (FRI) plain cap. It is available in 3-in. and 4-in. OD and custom sizes as well.
The FRI cap has a plain skirt; however, we also manufacture caps with various cap slot designs. Caps and risers can also be offered to our clients' specific requirements.

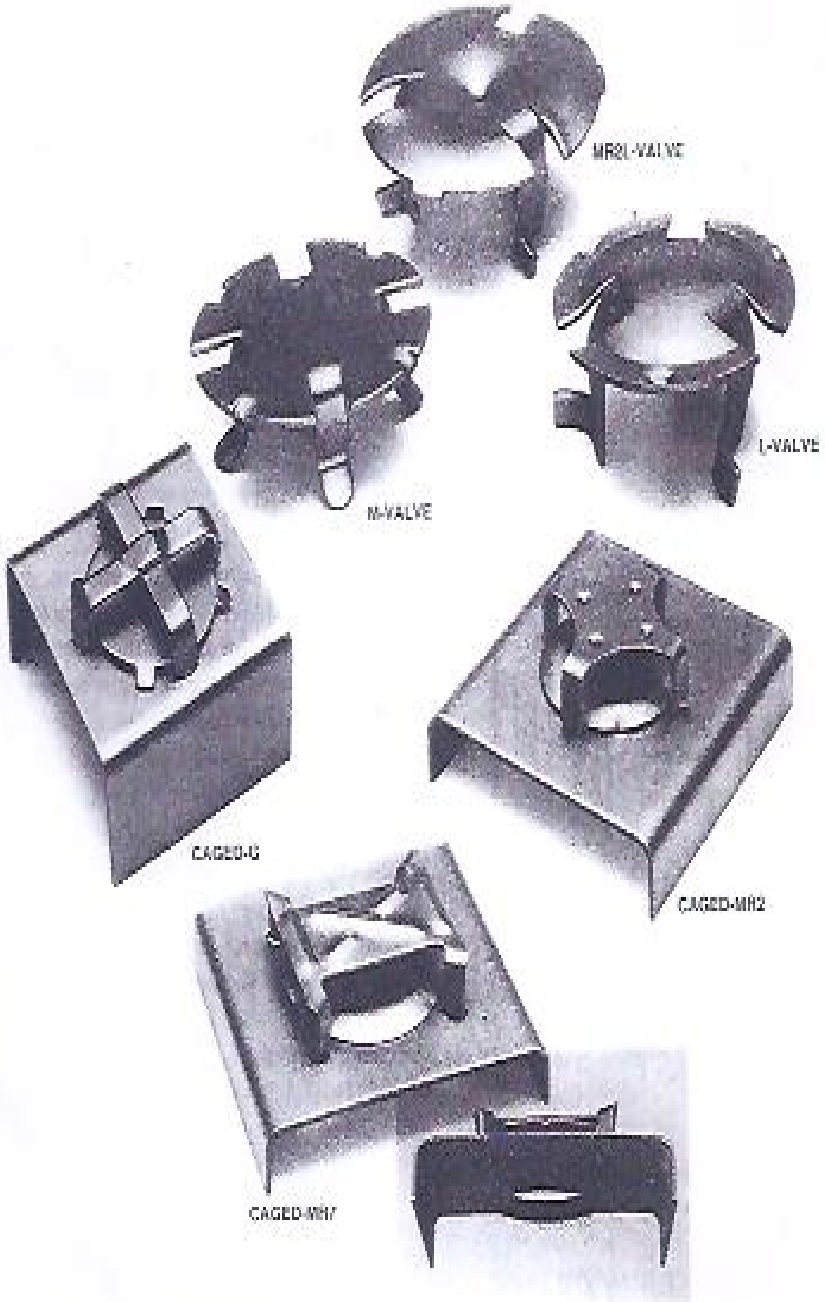

Figure 2.17 – Typical Norton Valve Tray Valves

A catalogue of the some developed tray types and improvements on existing trays as compiled by Wijn (1998) is also reviewed and presented in Appendix 4. Also listed there are existing facilities for tray testing, development and trouble shooting.

Apart from these facilities, Bandyopadhyay and Biswas (2011) investigated the interfacial hold up in a tapered bubble column using air-water, while Sultana et al (2010) evaluated mass transfer using aeration of water. Baker and Waldie (1996) also evaluated the mass transfer performance of their novel column by using it to run experiments on deoxygenation of water. Tray columns can be used for both distillation and absorption duties (Richardson & Harker, 2002).

CHAPTER THREE
RESEARCH METHODOLOGY

3.1 CONCEPTION OF THE PROPOSED TRAY CONFIGURATION AND DESCRIPTION OF ITS MODE OF OPERATION

Before identifying those features needed for efficient operation of a column on a moving platform and proposing a design, it is necessary to illustrate schematically the shortcomings of the conventional columns on moving platforms. The following diagrams (figs. 3.1, 3.2 & 3.3) show the column flow dynamics when platform motion causes a sway of 10^0 from the vertical position.

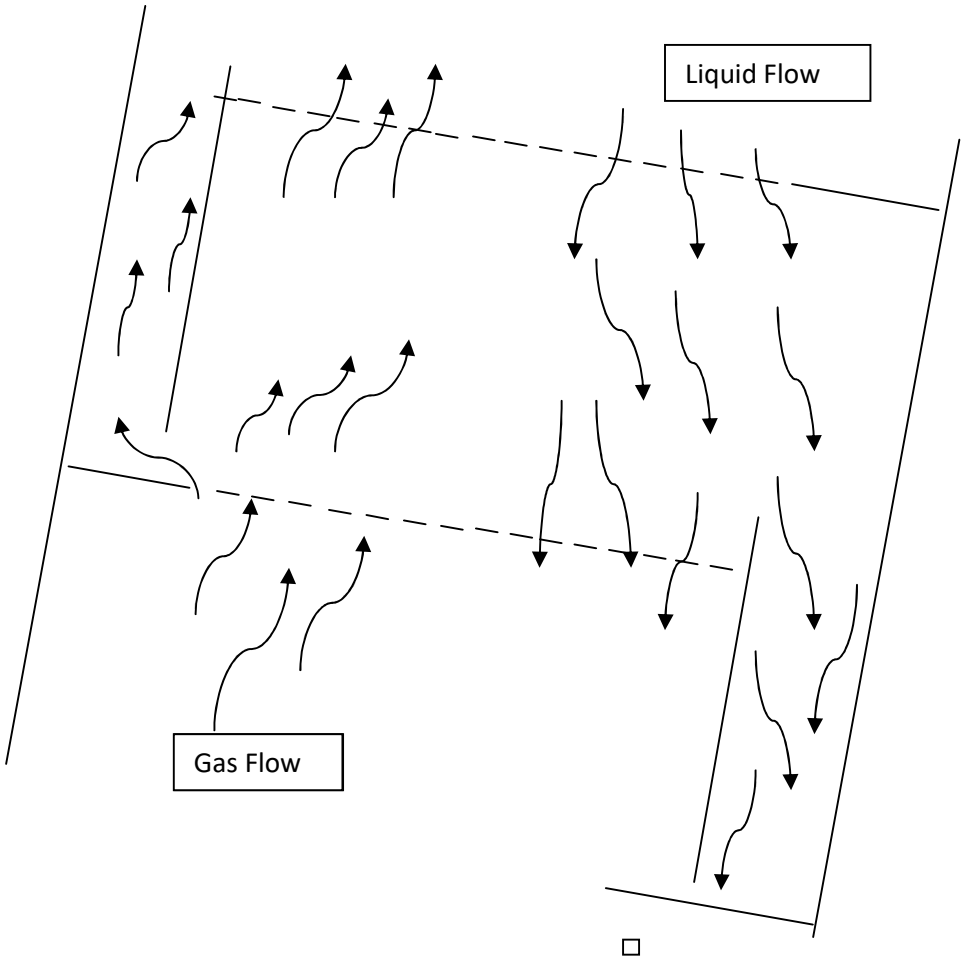

Fig 3.1: Tilted Cross flow tray showing fluid flow distribution

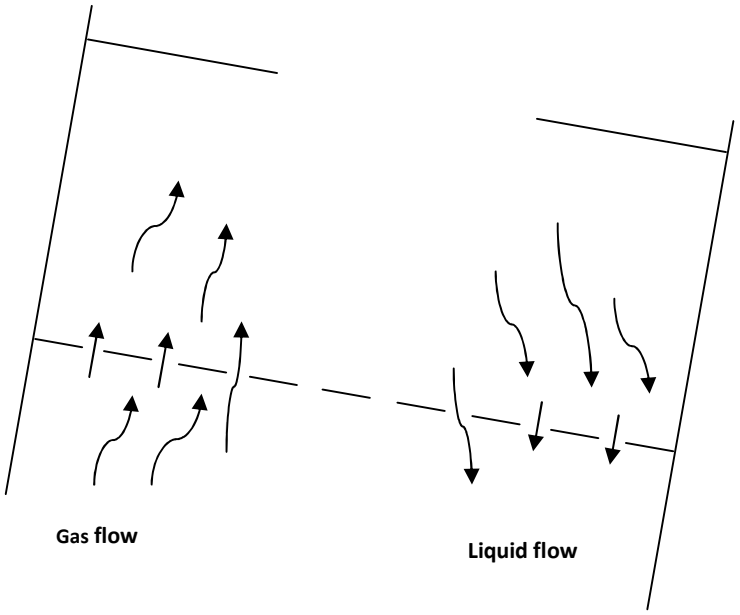

Fig 3.2 Tilted downcomerless counterflow tray showing fluid flow distribution

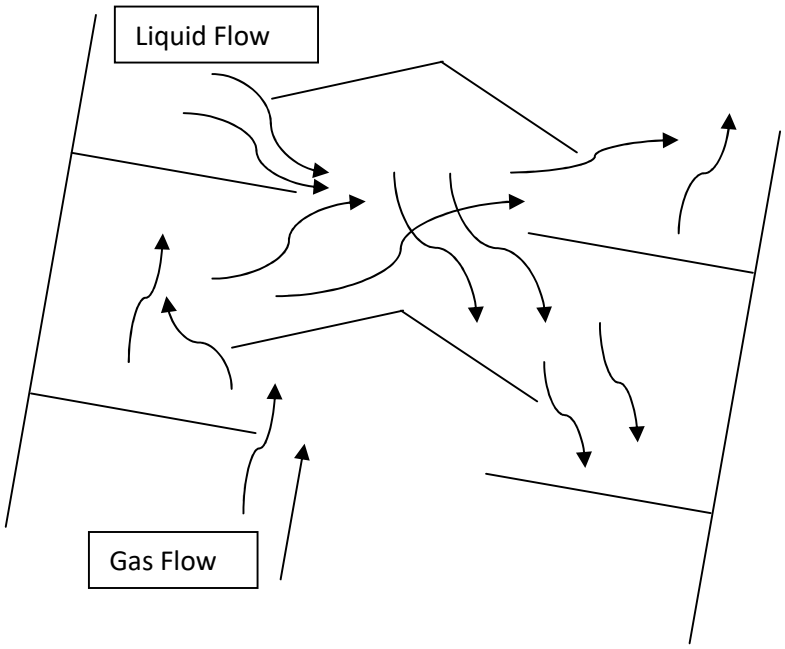

Fig 3.3 Tilted downcomerless counterflow tray showing fluid flow distribution

For cross-flow trays (bubble cap, sieve and valve trays) and counter flow trays, severe gas/liquid misdistribution which is the fundamental drawback is noticed leading to a collapse of tray efficiency. This is to be expected because the gas will naturally follow the path of least resistance (i.e. where there is no liquid). Remesat et al (2005) have reported that there can be a negative economic impact when operating a column with permanently tilted trays whether it is reduced throughput, purity or increased utility consumption.

To overcome this problem, a novel separation column having the following features is proposed:

(1) A plate column of the counter-flow type (counter flow trays are downcomerless). This is essential because the downcomer of a cross flow tray under tilt condition may be starved of liquid or conversely flooded with liquid and thereby compromises the column efficiency.

(2) The operation of the counter flow valve tray must be LIQUID INITIATED AND CONTROLLED. This is a most important factor because the valves should **open** in any part(s) of the tray containing a certain minimum liquid level and **shut** in any portion(s) of the tray lacking liquid. This is the only way to ensure stable operation under all conditions.

During start up of the novel column, liquid will have to be passed first through the column to open the valves before the vapour is allowed in. The conventional valve tray types (e.g. Glitsch Ballast valve tray, Koch Flexitray, Nutter Float valve, etc) are all vapour controlled. For these trays vapour is passed first through the columns during start up to open and operate the valve and the liquid refluxed until stable operating conditions are attained.

Figures 3.4a and 3.4b are cross sectional diagrams of a liquid controlled valve tray called *"Plunger-cap Multifloat Valve Tray"* having four floats per valve with arrows showing the movement of the parts in closed and open positions.

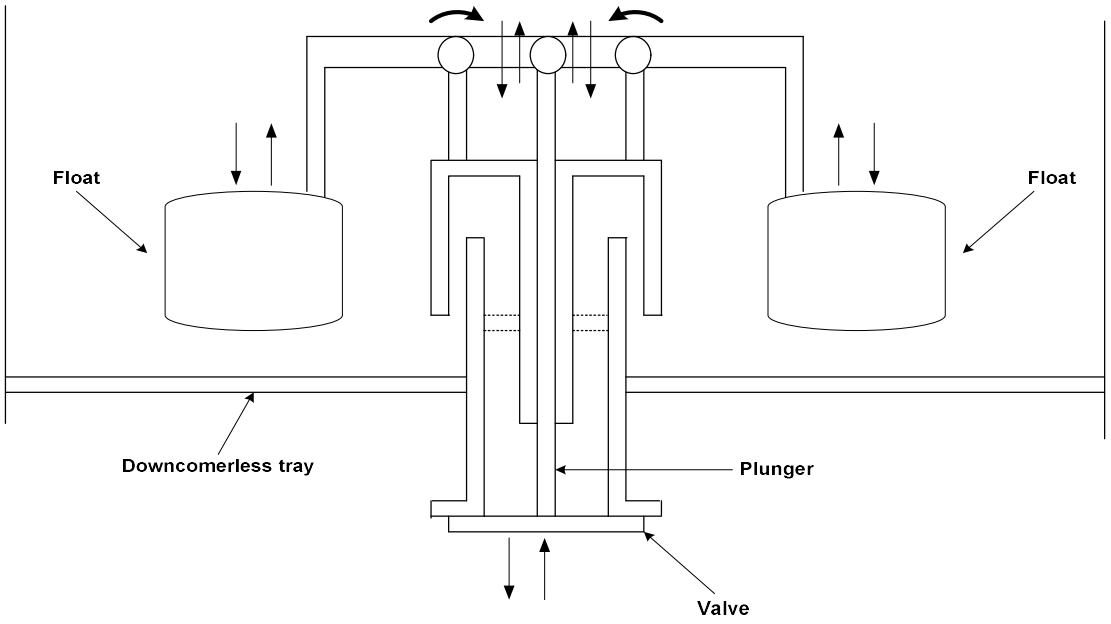

Fig 3.4a: Liquid controlled multi-float plunger-cap valve tray in closed position

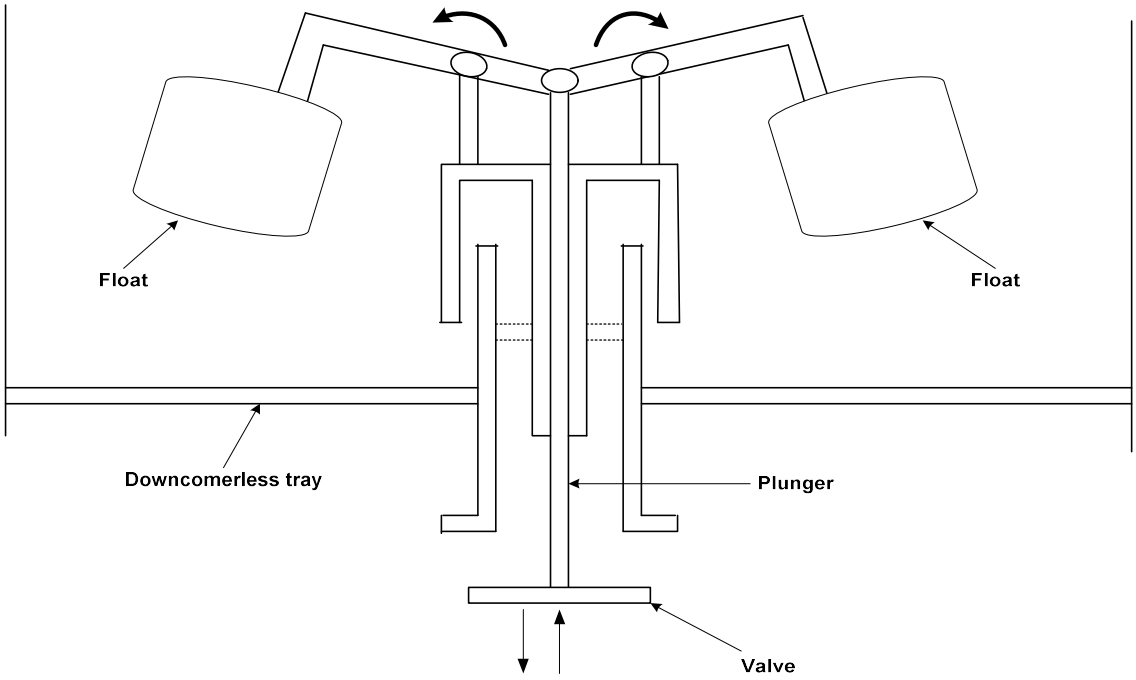

Fig 3.4b: Liquid controlled multi-float plunger-cap valve tray in open position

3.2 MECHANICAL DESIGN OF PLUNGER-CAP MULTI-FLOAT VALVE TRAY

The complete mechanical design of this valve involves several stages which are enumerated in the following sub sections.

3.2.1 FORMULATION OF A WEIGHT VOLUME RELATIONSHIP MODEL FOR THE FLOAT VALVE.

A vital prerequisite to the actual design and construction of the float valve is the building of a suitable empirical model relating the float volume and weight. Such a model is important because it will help avoid repetitive experimentation and observations to ascertain the float behaviour. In model building, the objective is to obtain a model which exhibits the least error between the actual data and the predicted response. The degree of accuracy needed and the potential uses of the model influence the structure and complexity of the model. In the absence of any constraint, the simplest adequate model (with the fewest number of coefficients) should be used. Some typical relations for empirical models are;

$$Y = a_0 + a_1x_1 + a_2x_2 + \ldots \quad 3.1$$

,and

$$Y = a_0 + a_1x + a_2x^2 + \ldots \quad 3.2$$

For the purpose of this study, a cylindrically shaped float will be used. This choice is informed by the ease of construction of such a float.

3.2.2 OPTIMISATION OF THE CYLINDRICAL FLOAT DIMENSIONS

The 3 basic steps involved in the optimisation of any system are;

- Clear identification of the objective: the criterion to be used to judge the system performance.
- Determination of the objective function: the system of equations and other relationships, which relate the objective with the variable to be manipulated to optimize the function.
- Obtaining the values of the variables that give the optimum value of the objective function. The best technique to be used for this step will depend on the complexity of the system and on the mathematical model used to represent the system.

When the objective function can be expressed as a function of one variable, the function can be differentiated, or plotted to find the maximum or minimum. Though this will be possible for only a few practical design problems, the problem at hand (optimisation of the cylindrical float dimensions) falls among these few.

The objective of this optimisation is to determine the dimensions of the cylinder (length and diameter) that will give the minimum surface area required to enclose a given volume.

The total surface area, A, of a closed cylinder is

$$A = \pi DL + 2\pi D^2/4 \qquad 3.3$$

Where D is the diameter and L is the length or height. This total surface area is the objective function which is to be minimised. Equation 3.3 can be written as

$f(\text{D x L}) = DL + D^2/2$ 3.4

For a given volume, the diameter and length are related by

$V = \pi D^2 L/4$ or $L = 4V/\pi D^2$ 3.5

Putting equation 3.5 in 3.4 gives the objective function in terms of D only as

$f(D) = 4V/\pi D + D^2/2$ 3.6

Differentiating this function and equating the differential to zero gives the optimum value of D as

$- 4V/\pi D^2 + D = 0$, and this implies that $D = (4V/\pi)^{1/3}$ 3.7

From equation 3.5, the corresponding length will be,

$L = 4V/\pi \div (4V/\pi)^{2/3} = (4V/\pi)^{1/3}$ 3.8

Hence from equation 3.7 and 3.8, the length and diameter are equal. We deduce from this result, for a cylindrical container, the minimum surface area required to enclose a given volume is obtained when the length is made equal to the diameter. Based on this finding, 5 cylindrical floats were constructed with diameters (D) of 3.0, 3.5, 4.0, 4.5, and 5.0 cm. Their volumes (V) were calculated and they were weighed to obtain their individual weights (W). The data obtained is represented in table 3.1 below.

Table 3.1: Empirical data for modelling the cylindrical float weight and volume.

D (L), cm	V, cm3	W, g
3.0	21.21	30
3.5	33.67	37
4.0	50.27	48
4.5	71.57	57
5.0	98.17	64

3.2.3 FITTING MODELS TO THE EMPIRICAL DATA

The data in table 3.1 above will be fitted with models that are linear in coefficients and the coefficients of the models estimated using the method of least squares.. The data in table 3.1 is fitted to the models;

$$W = a_0 + a_1 V \qquad 3.9$$

$$W = a_0 + a_1 V + a_2 V^2 \qquad 3.10$$

Using the curve fitting toolbox of Matlab 7.5 the results in tables 3.2 and 3.3 were obtained.

Table 3.2: Predicted responses and coefficient of Determination for model $W = a_0 + a_1V$ ($W = 22.58 + 0.448V$)

Volume of Cylindrical float, cm3	Experimentally Obtained weight of cylindrical float, g	Statistically predicted Weight of cylindrical Float, g	Statistical parameters
21.21	30	32.08	$R^2 = 0.9675$
33.67	37	37.66	Adj $R^2 = 0.9567$
50.27	48	45.10	
71.57	57	54.64	
98.17	64	66.56	

Table 3.3: Predicted responses and coefficient of Determination for model $W = a_0 + a_1V + a_2V^2$ ($W = 12.5601 + 0.8747V - 0.0036V^2$)

Volume of Cylindrical float, cm3	Experimentally Obtained weight of cylindrical float, g	Statistically predicted Weight of cylindrical Float, g	Statistical parameters
21.21	30	29.52	$R^2 = 0.9982$
33.67	37	37.98	Adj $R^2 = 0.9963$
50.27	48	47.54	
71.57	57	56.92	
98.17	64	64.10	

From these results, the second model $W = 12.5601 + 0.8747V - 0.0036V^2$ with Coefficient of Correlation of 0.9982 correlates the data very well and will be used for this analysis.

3.2.4 DESIGN CALCULATIONS

3.2.4.1 Determination of Cylindrical Float Dimensions

Consider the diagram of the Multi-float plunger-cap valve tray shown below with the forces that will be acting on it indicated;

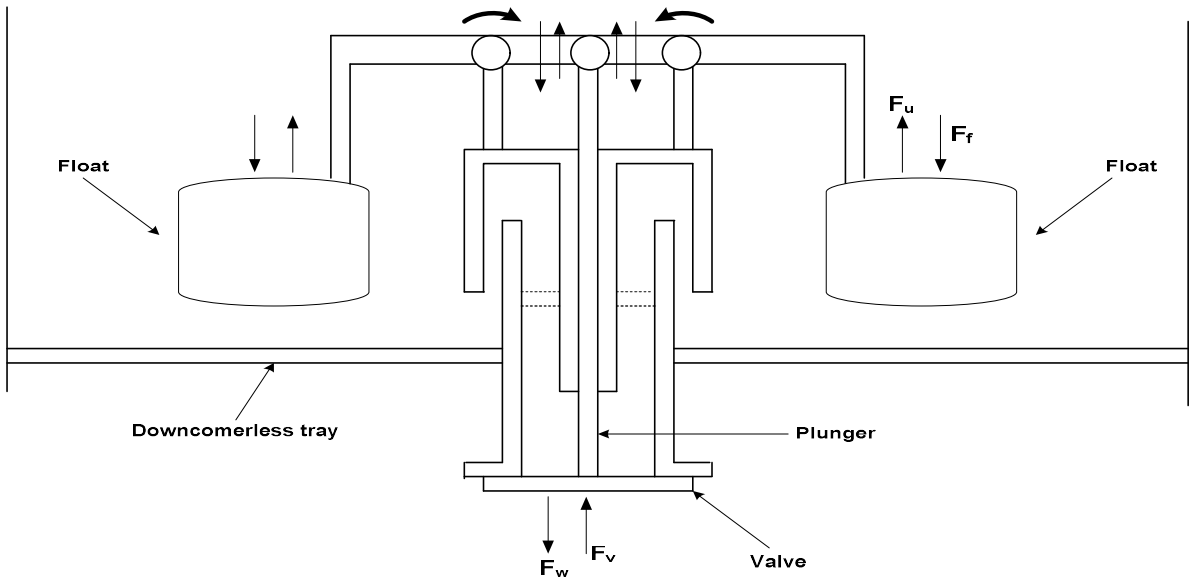

Fig 3.5: Liquid controlled multi-float plunger-cap valve tray showing force components

The float behaviour depends on the following force components indicated in figure 3.5 above:

1. Upthrust experienced by the valve F_u which is dependent on the fraction of the float covered by water, *x*, according to Archimedes Principle (see Appendix 5).

2. Weight of the valve assembly, F_w.
3. Force exerted by the vapour on each valve, F_v.
4. Weight of the float F_f.

For the floats to rise and the valve to open, $F_u + F_w$ must be greater than $F_v + F_f$ at the specified float fraction (x) covered by liquid. The minimum float size required for efficient operation will be used for the construction. We specify that at least 75% of the float must be covered by the liquid before the valve will open. This is to ensure that there is enough liquid head for effective mass transfer. Water is used as the liquid and air as the vapour for this design. The first step here is to evaluate the magnitude of the constant force terms viz. F_v and F_w.

The weight of the float is 5 g and the force exerted by the weight of the float F_w is 0.0491N.

The force exerted by the air on the valve is $\rho AV^2 = \rho V(AV)$

Where ρ is the air density, V is the air velocity and AV is the air volumetric flowrate, Q.

The density of air is 1.225 Kg/m^3. To obtain the velocity of the air in the column, we note that the volumetric flow rate $Q = A_1V_1$ (in pipe) $= A_2V_2$ (in column). We assume a very high air flow rate of 1000 litres/ minute for this calculation to accommodate all possible operating ranges.

1000 Litres/minute = 0.0167 m^3/s = A_2V_2

A_2 is the cross sectional area of the column = $\pi (0.5)^2/4 = 0.196$ m^2.

Therefore $V_2 = 0.0167/0.196 = 0.0852$ m/s

And $F_v = \rho V(AV) = 1.225 \times 0.0852 \times 0.0167 = 1.743 \times 10^{-3}$ (Kg.m/s^2 or N)

From this analysis of the 2 forces, F_v is less than F_w and hence the air velocity cannot stop the valve from opening once the floats rise. The opening of the valve will now depend on the F_u and F_f which vary with the liquid height *x* and the cylindrical float size. The algorithm for this calculation involves the following steps:

- Choosing a starting value for the cylindrical float diameter D
- Calculating the volume V_1 of the liquid that will be displaced by the float at this diameter.
- Calculating the volume of the liquid that will be displaced by the float at this diameter when the fraction submerged is 0.75, V_2.
- Using the value of V_1 in the earlier obtained weight volume relationship model, $W = 12.5601 + 0.8747V - 0.0036V^2$ to obtain the weight of the float and subsequently the force exerted by the float F_f.
- Calculating the Upthrust that will be exerted on the cylindrical float by V_2.
- Compare F_f and F_u, if F_u is less than F_f, then we return to the first step and increase the value of the diameter D for the next iteration. If it is not, we terminate the calculations and use the diameter value for this iteration as the least required for the float to rise.

The Matlab computer program that executes this algorithm is given below with the results obtained.

```
D=1;x=0.75;Denw=1000;Ff=1;Fu=0.5;
Dvalue=[];Ffvalue=[];Fuvalue=[];
while Fu<Ff
   v1=(pi*D^3)/4;
   v2=(x*pi*D^3)/4;
   Ff=9.81*(12.5601+0.8747*v1-0.0036*v1^2)/1000;
   M=v2*Denw/100^3;
   Fu=9.81*M;
   Dvalue=[Dvalue D];Ffvalue=[Ffvalue Ff];Fuvalue=[Fuvalue Fu];
   D=D+0.1*D;
end
solution=[Dvalue' Ffvalue' Fuvalue']
```

The following values were obtained and the calculation terminated after the 18^{th} iteration, i.e. when the value of F_u exceeded that of F_f.

Table 3.4: Iteration Results of Program for Determination of the Minimum Cylindrical Float Dimensions

Iteration No	D, cm	Ff, N	Fu, N
1	1.00	0.1299	0.0058
2	1.10	0.1321	0.0077
3	1.21	0.1351	0.0102
4	1.33	0.1390	0.0136
5	1.46	0.1442	0.0181
6	1.61	0.1510	0.0241
7	1.77	0.1600	0.0321
8	1.95	0.1719	0.0428
9	2.14	0.1875	0.0569
10	2.36	0.2078	0.0758
11	2.59	0.2342	0.1008
12	2.85	0.2680	0.1342
13	3.14	0.3107	0.1786
14	3.45	0.3636	0.2378
15	3.80	0.4270	0.3165
16	4.18	0.4987	0.4212
17	4.60	0.5720	0.5606
18	5.05	0.6302	0.7462

Based on these results, the cylindrical floats were constructed with the height and diameter equal to 50mm.

3.2.4.2 Determination of Liquid Flow Rate

Since we have specified the valve dimensions and the number of valves per tray, we cannot also specify the liquid flow rate but must calculate it. For scale up however, we will specify the desired liquid flowrate and determine the tray dimensions from this liquid flowrate.

The diameter of the riser from which liquid flows from one tray to the other is 25mm, but because of the plastic perforated support, only about 18mm is available for liquid flow. The liquid height that will be attained on the plate before the float will rise and the liquid begins to flow from the riser to the next tray is about 50mm, and about 10mm above the riser inlet. The water will accelerate at $9.81 m/s^2$ and the velocity at the riser exit is $V = 2zg$, where z = height of the fluid on the tray, and g = gravitational acceleration coefficient. The volumetric flowrate as stated previously is $Q = AV$, where A is the cross sectional area of the riser.

$A = (\pi \times 0.018^2)/4 = 2.545 \times 10^{-4} m^2$

$V = 2 \times 0.01 \times 9.81 = 0.1962 m^2/s$

$Q = AV = 2.545 \times 10^{-4} m^2 \times 0.1962 m^2/s = 4.993 \times 10^{-5} m^3/s = 2.99$ Litres per Min.

Since there are 4 valves per tray, the maximum liquid flowrate that this tray column should be operated at is 2.99 x 4 = 11.96 Litres per min. Therefore operating the column above this liquid flowrate will cause the column to be flooded with liquid. This serves as a guide in the choice of the liquid flow rates in the Design of the Experiments.

3.3 MECHANICAL DETAILS OF PLUNGER-CAP MULTI-FLOAT VALVE TRAY AND TEST COLUMN

Details of the mechanical design of the novel tray column are shown in the diagrams that follow. The test column is a 500mm diameter column with 2 trays, 4 valves per tray and a tray spacing of 450mm (18”).

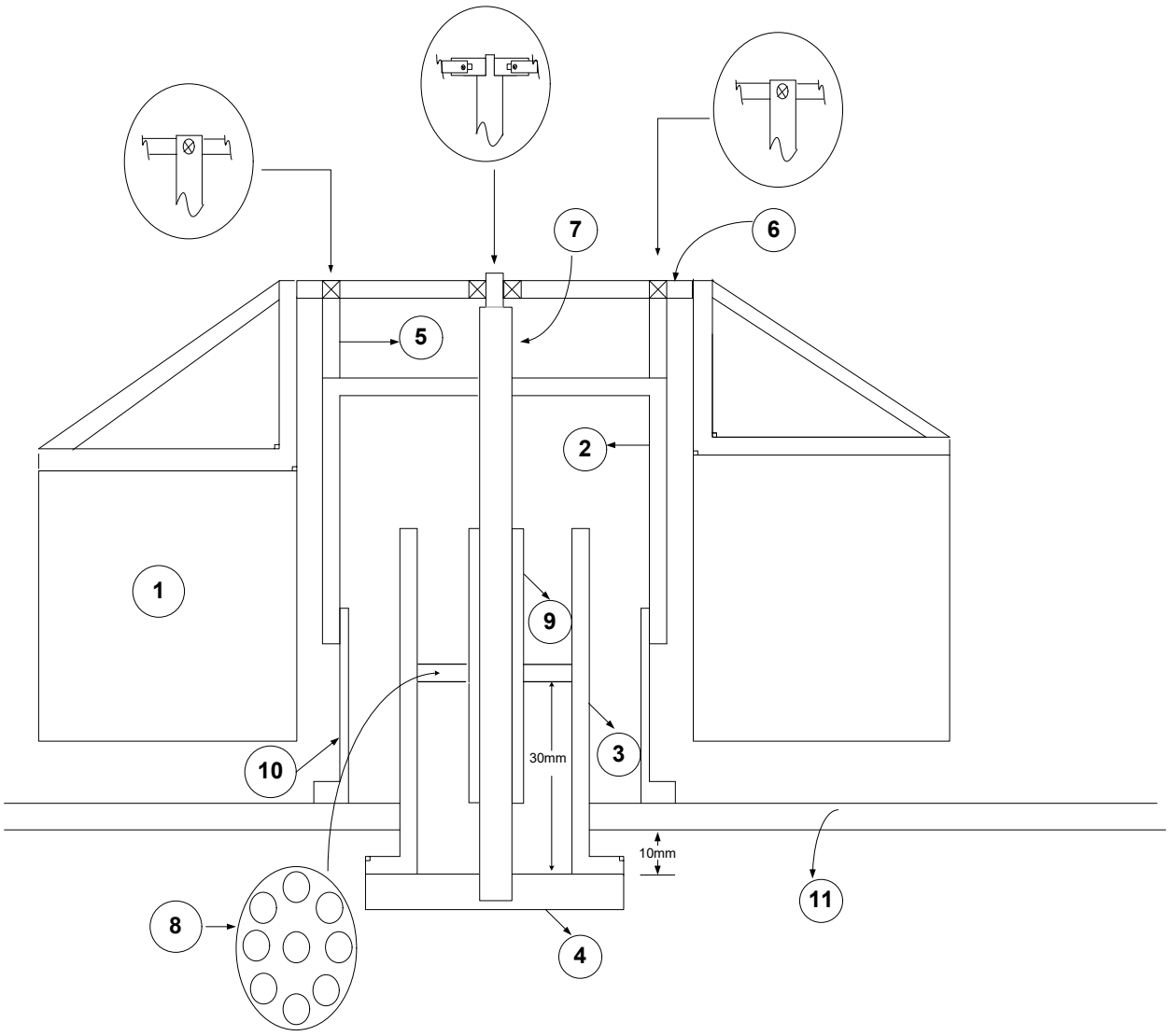

Figure 3.6: Front Elevation Showing Float and Valve Details

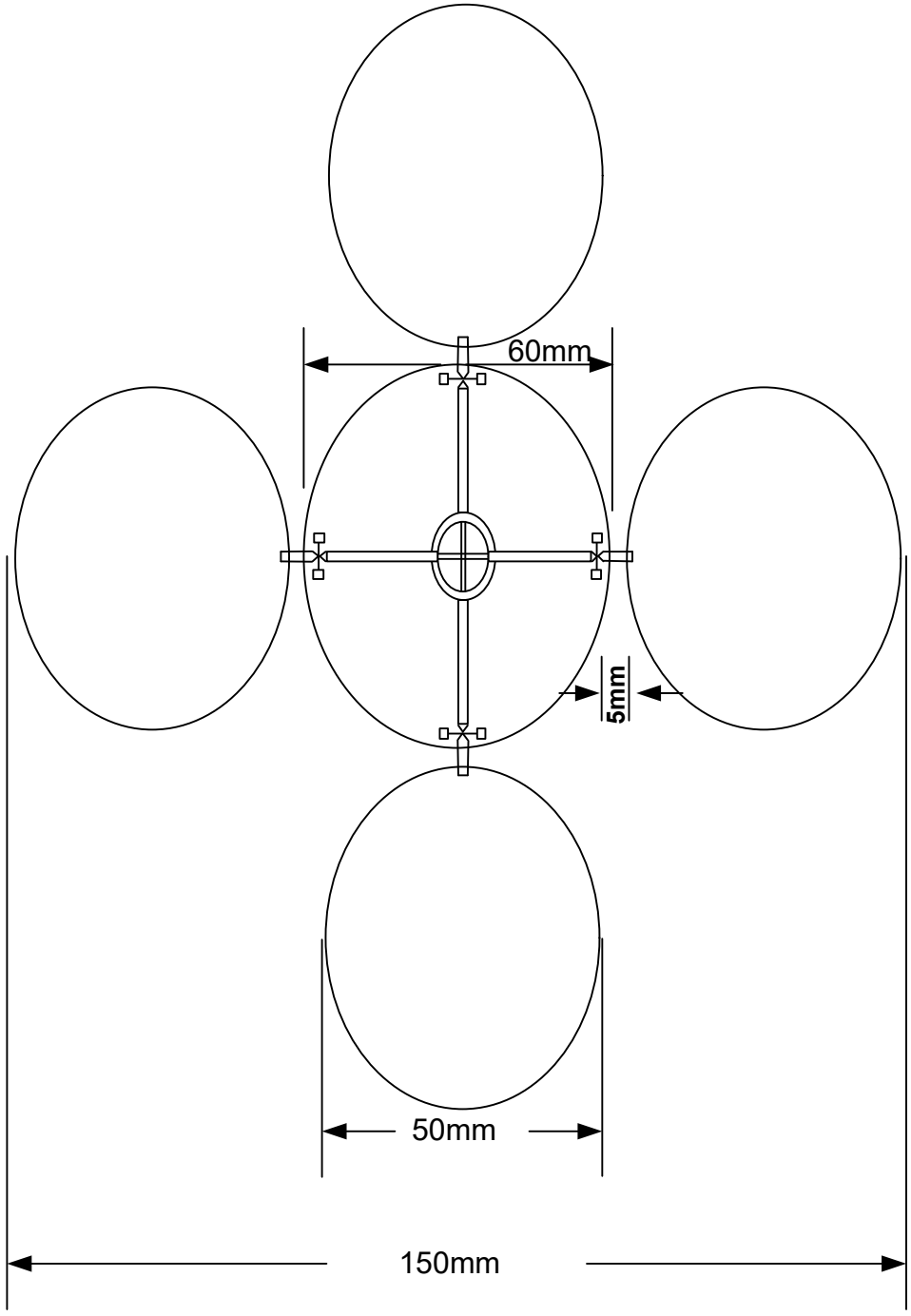

Figure 3.7: Top View Showing Float and Valve Details

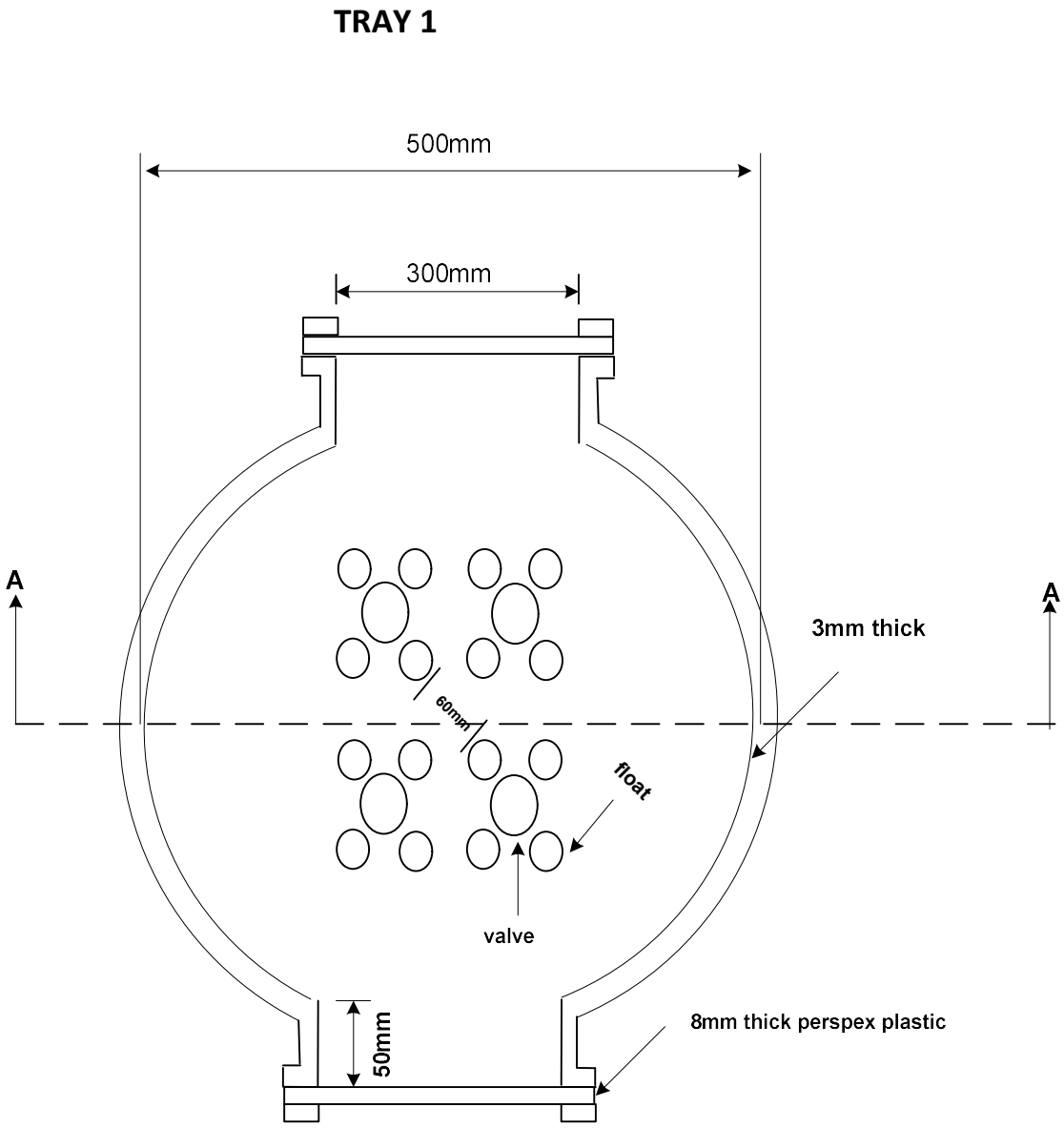

Figure 3.8: Top View of Horizontal Cut B-B above Tray 1 (See Figure 3.10)

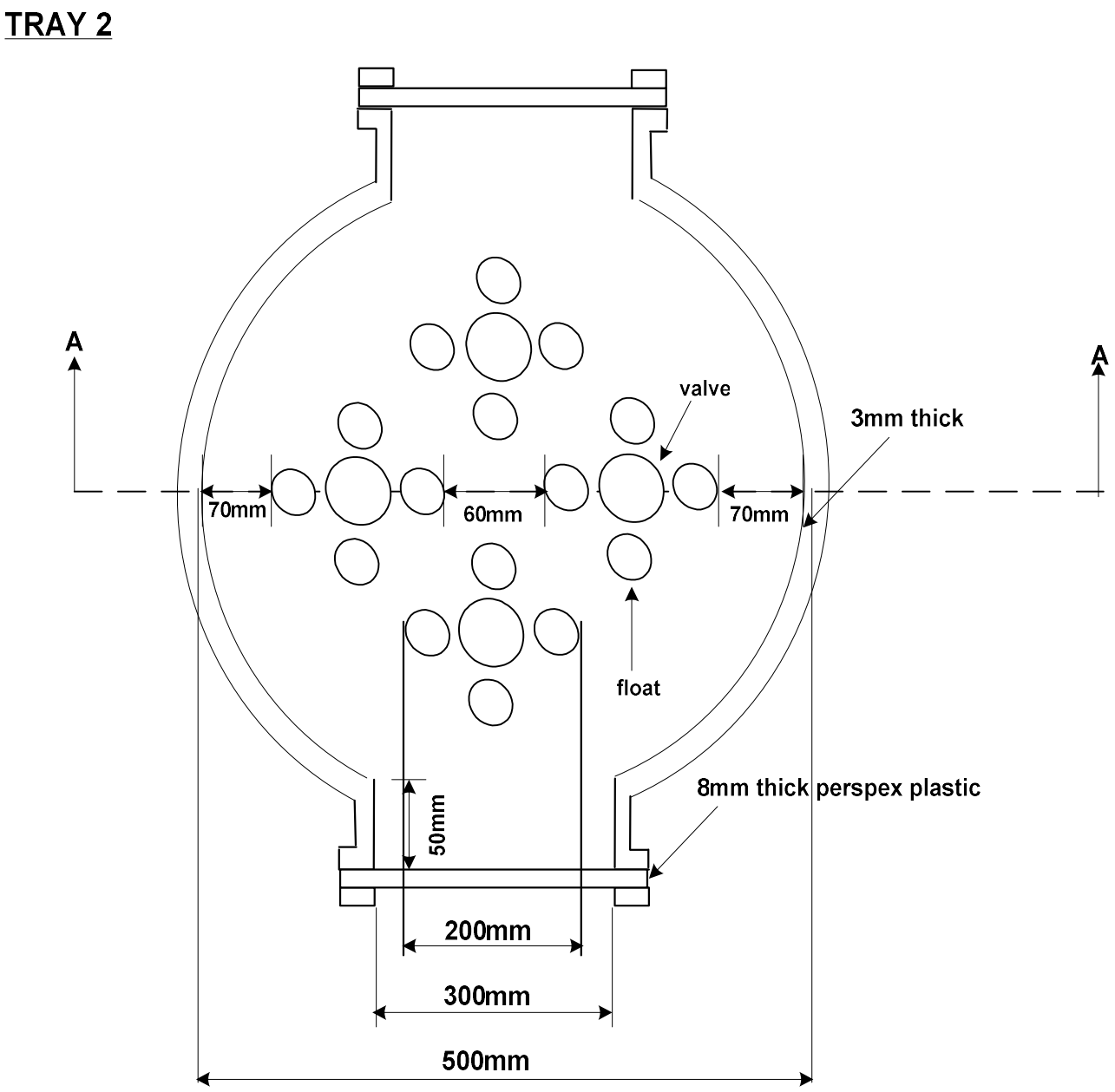

Figure 3.9: Top View of Horizontal Cut C-C above Plate 2 (See Figure 3.10)

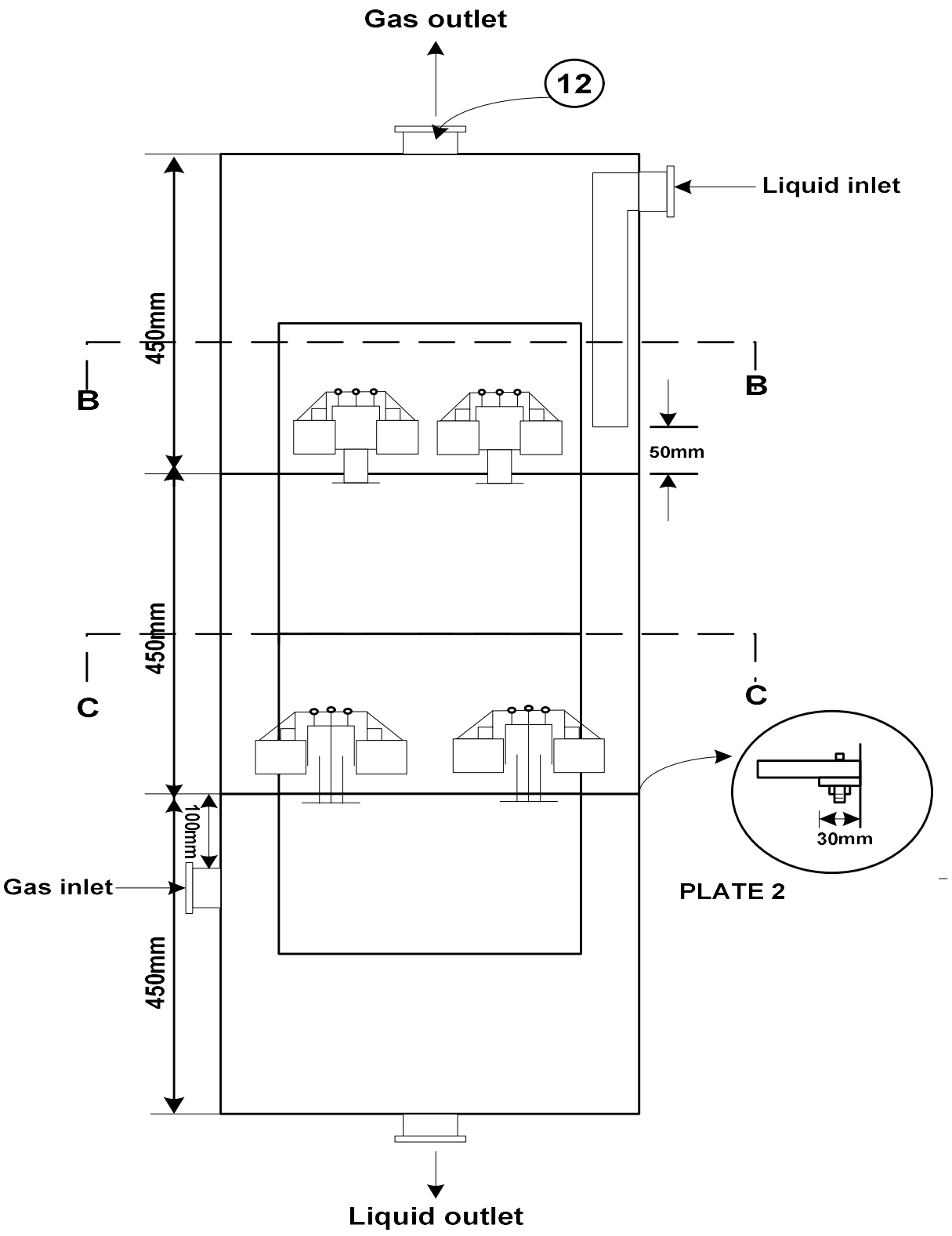

Figure 3.10: Section A-A of Figures 3.8 and 3.9

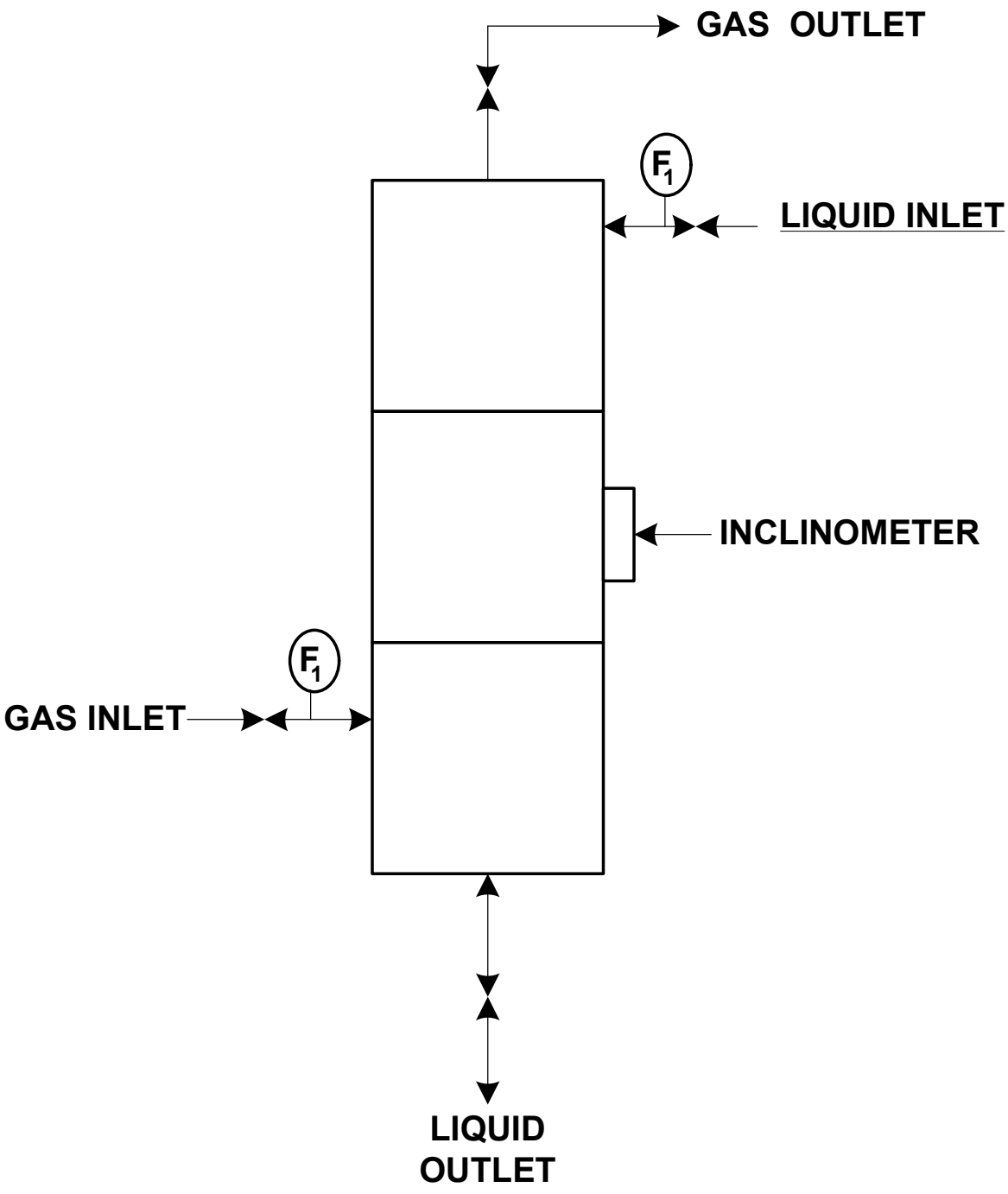

Figure 3.11: Schematic Diagram of Column Showing Instrumentation Details

3.4 MULTI FLOAT PLUNGER VALVE TRAY SPECIFICATIONS

The specifications and the number of items required in the preceding design diagrams (Figure 3.5 to 3.9) are contained in the table below.

Table 3.5: Specifications of the components of the valve tray

ITEM NO	DESCRIPTION	MATERIAL OF CONSTRUCTION	DIMENSION	NUMBER REQUIRED PER VALVE
1	Cylindrical floats that operate novel tray	0.5mm steel	Height = 50mm Diameter = 50mm	4 per valve
2	Bubble cap	2mm thick stainless steel	Height = 40mm Diameter = 60mm	1 per valve
3	Riser	2mm thick stainless steel	Height = 50mm Diameter = 25mm	1 per valve
4	Valve cover	10mm thick plastic	Diameter = 40mm	1 per valve
5	Bars supporting the pivot and connecting float to plunger	1mm thick stainless steel bars	Height = 40mm Width = 8mm	8 per valve
6	Bar connecting float to pivot	1mm thick stainless steel bar	Length = 30mm Width = 8mm	4 per valve
7	Plunger	5mm diameter stainless steel rod	Length = 95mm	1 per valve
8	Perforated support for plunger and also to aid liquid vapor contact	10mm thick plastic with 6mm diameter perforations	Diameter = 25mm	1 per valve
9	Guide/support for plunger	6mm internal diameter stainless steel pipe	Length = 40mm Thickness = 2mm	1 per valve
10	Bubble cap legs/support	1mm thick stainless steel bar	Length = 20mm Width = 8mm	3 per valve
11	Plate	3mm thick mild steel plate	Diameter = 500mm	2 for the column
12	Liquid and vapor inlet/outlet pipes (Fig. 3.10)	2mm thick pipes of mild steel	Diameter = 25mm for liquid pipes, and 12.5mm for vapour pipes	2 of each for the column

3.5 EXPERIMENTAL INVESTIGATION

Below is a picture of the novel column after installation.

Figure 3.12: Picture of Multi-float-plunger valve tray column

It conforms basically with the design previously described in section3.2 and 3.3 which has portions of the shell fitted with Perspex to permit observation of the workings of the tray internals during operation. Water supplied from a holding tank by a 0.5 Horsepower Electric pump was fed through the top of the column to the first tray. When the level of water on this tray was sufficient to lift the floats, the valves opened and allowed water to flow to the tray beneath. The response of the valves of the tray beneath was same as obtained with the tray above and the water flowed to the base of the column from where it was re-circulated by gravity to the holding tank. The air which was supplied by a 2.5 Horsepower Air Compressor was introduced beneath the second tray in the column. A head of liquid maintained at the base of the column served as a liquid seal and ensured that the air introduced flowed through the open valve to the second tray first, then to the first tray contacting liquid in each of these trays. It was released through a vent at the top of the column. The flow rates of both the water and air were measured by rotameters. The column assembly was also fitted with valves for controlling the flows at the desired rates and the entire column was mounted on a rig which could be tilted and operated at various angles.

3.6 FACTORIAL DESIGN OF THE EXPERIMENT

A Design of Experiment was done following the installation and carrying out of preliminary test runs on the novel column. Design of experiment is a means of determining the optimal experimental design or sequence to be used for simultaneous varying of all the factors to be analysed. The purpose of statistically designing an experiment is to collect the maximum amount of relevant information with a minimum expenditure of time and resources. The traditional approach demands considerable material expense and is more time consuming, for the effect of each factor experiment may be designed to investigate one factor at a time so that all other independent variables (factors) are held constant. (Lazic, 2004, Atkinson & Donev,1992) When properly utilized it yields more precise data and more complete information on the studied phenomenon with minimal number of experiments and the lowest possible material cost. Design of experiments has also been used to study the effects of process and geometrical variables in a sieve tray column (Gutierrez-Oppe et al, 2013).

3.6.1 SELECTION OF SYSTEM RESPONSE

To determine the efficiency of this column, an oxidation experiment was conducted on a synthetic contaminated water containing Fe (II). The percentage of Fe (II) oxidized to Fe (III) from the water by air at a fixed temperature was chosen as the system response. 200 litres of water containing 2.00 mg/L of Fe (II) was

subjected to air stripping at 30^0C for 30 minutes. Samples were collected before and after the stripping operation and the percentage Fe (II) oxidized to Fe (III) (as indicated by the percentage reduction in Fe (II) concentration) was taken as the system response. The experimental thrust was to evaluate the mass transfer performance of the column by analysis of the percentage Fe (II) oxidized to Fe (III) at various liquid and gas flow rates and in both vertical and tilt positions.

3.6.2 SELECTION OF FACTORS

The factors whose effects were investigated are:

1. Gas flowrate (x_1, in litres per minute)
2. Liquid flowrate, (x_2, in litres per minute)
3. Angle of tilt, (x_3, in degrees)

3.6.3 EXPERIMENTAL FACTOR SPACE, NULL LEVEL AND VARIATION INTERVAL

These limits were selected for all the factors based on the preliminary experiment and the maximum liquid flow rate earlier determined:

$(1 \leq x_1 \leq 5, 3 \leq x_2 \leq 11, -10 \leq x_3 \leq 30)$.

The experimental centre was chosen as,

$x_{1,0} = 2.7$; $x_{2,0} = 7.0$; $x_{3,0} = 10$.

The following variation intervals were chosen to realize the basic experiment:

$\Delta x_1 = 0.5$; $\Delta x_2 = 2$; $\Delta x_3 = 10$.

The experimental designs for the linear models and the quadratic models are as shown in tables 3.6 and 3.7 below. Details of how they were obtained and other information about them are given in Appendix 6.

Table 3.6: Experimental Design for Linear Model

TRIALS	x_0	DESIGN MATRIX			OPERATIONAL MATRIX			RESPONSE		
		x_1	x_2	x_3	x_1	x_2	x_3	y_1	y_2	y
1	+	-	-	-	2.2	5	0			
2	+	+	-	-	3.2	5	0			
3	+	-	+	-	2.2	9	0			
4	+	+	+	-	3.2	9	0			
5	+	-	-	+	2.2	5	20			
6	+	+	-	+	3.2	5	20			
7	+	-	+	+	2.2	9	20			
8	+	+	+	+	3.2	9	20			
9	+	0	0	0	2.7	7	10			
10	+	0	0	0	2.7	7	10			
11	+	0	0	0	2.7	7	10			

The models that were used are as follows:

$$y = b_0 + b_1x_1 + b_2x_2 + b_3x_3 \quad \ldots\ldots\ldots\ldots\ldots\ldots\ldots\ldots\ldots\ldots\ldots\ldots\ldots\ldots\ldots\ldots\ldots\ldots\ldots\ldots\ldots\ldots \quad (3.1)$$

$$y = b_0 + b_1x_1 + b_2x_2 + b_3x_3 + b_4x_1x_2 + b_5x_1x_3 + b_6x_2x_3 \ldots\ldots\ldots\ldots\ldots\ldots\ldots\ldots\ldots\ldots\ldots\ldots\ldots\ldots\ldots\ldots\ldots\ldots\ldots\ldots\ldots\ldots \quad (3.2)$$

$$y = b_0 + b_1x_1 + b_2x_2 + b_3x_3 + b_4x_1x_2 + b_5x_1x_3 + b_6x_2x_3 + b_7x_1x_2x_3 \ldots\ldots\ldots\ldots\ldots\ldots\ldots\ldots\ldots\ldots\ldots\ldots\ldots\ldots\ldots\ldots\ldots\ldots\ldots\ldots\ldots\ldots \quad (3.3)$$

Table 3.7: Experimental Design for Box Wilson Second Order Model

TRIALS	x_0	DESIGN MATRIX			OPERATIONAL MATRIX			RESPONSE		
		x_1	x_2	x_3	x_1	x_2	x_3	y_1	y_2	y
1	+	+	+	+	3.2	9	20			
2	+	+	+	-	3.2	9	0			
3	+	+	-	+	3.2	5	20			
4	+	+	-	-	3.2	5	0			
5	+	-	+	+	2.2	9	20			
6	+	-	+	-	2.2	9	0			
7	+	-	-	+	2.2	5	20			
8	+	-	-	-	2.2	5	0			
9	+	-1.68	0	0	1.9	7	10			
10	+	1.68	0	0	3.5	7	10			
11	+	0	-1.68	0	2.7	3.6	10			
12	+	0	1.68	0	2.7	10.4	10			
13	+	0	0	-1.68	2.7	7	-6.8			
14	+	0	0	1.68	2.7	7	26.8			
15	+	0	0	0	2.7	7	10			
16	+	0	0	0	2.7	7	10			
17	+	0	0	0	2.7	7	10			
18	+	0	0	0	2.7	7	10			
19	+	0	0	0	2.7	7	10			
20	+	0	0	0	2.7	7	10			

The models used are:

$$y = b_0 + b_1x_1 + b_2x_2 + b_3x_3 + b_4x_1^2 + b_5x_2^2 + b_6x_3^2 \ldots\ldots\ldots\ldots\ldots\ldots\ldots\ldots \quad (3.3)$$

$$y = b_0 + b_1x_1 + b_2x_2 + b_3x_3 + b_4x_1x_2 + b_5x_1x_3 + b_6x_2x_3 + b_7x_1^2 + b_8x_2^2 + b_9x_3^2 \ldots\ldots \quad (3.4)$$

The simplest possible model that best represents the system is normally used to analyse its behaviour (Ruzicka, 2013).

3.6.4 SAMPLE PREPARATION AND ANALYSIS

400 mg/L Fe (II) stock solution was prepared by dissolving 2.0g of Ferrous Sulphate ($FeSO_4.7H_2O$) in 1 litre of distilled water. This was further diluted to 200 litres for the actual experimental runs to give a contaminated water containing 2.0 mg/l of Fe (II). A sample of this water together with a second one collected at the end of each experimental run were analyzed using a HACH model DR/2010 portable datalogging spectrophotometer to ascertain their Fe(II) content and hence the percentage of Fe(II) oxidized to Fe(III).

CHAPTER FOUR

RESULTS AND DISCUSSION

4.1 EXPERIMENTAL RESULTS

The results from the oxidation studies based on the linear experimental design are shown in table 4.1 below.

Table 4.1: Results from oxidation studies based on Linear Experimental Design

Gas Flow Rate, LPM	Liquid Flow Rate, LPM	Angle of Tilt, Degrees	% Fe (II) Oxidised from First Experimental Run	% Fe(II) Oxidised from Replicate Experimental Run	Average % Fe(II) Oxidised
2.2	5	0	10.25	10.55	10.40
3.2	5	0	11.26	14.28	12.77
2.2	9	0	10.80	12.20	11.50
3.2	9	0	14.50	13.94	14.22
2.2	5	20	10.88	10.96	10.92
3.2	5	20	12.66	13.38	13.02
2.2	9	20	11.97	11.69	11.83
3.2	9	20	14.70	15.30	15.50
2.7	7	10	12.33	12.01	12.17
2.7	7	10	12.00	11.36	11.68
2.7	7	10	11.98	12.32	12.15

The results from the oxidation studies based on the Box-Wilson Experimental Design are shown in table 4.2 below.

Table 4.2: Results from oxidation studies based on Box-Wilson Experimental Design

Gas Flow Rate, LPM	Liquid Flow Rate, LPM	Angle of Tilt, Degrees	% Fe (II) Oxidised from First Experimental Run	% Fe(II) Oxidised from Replicate Experimental Run	Average % Fe(II) Oxidised
3.2	9	20	14.70	15.30	15.00
3.2	9	0	14.50	13.94	14.22
3.2	5	20	12.66	13.38	13.02
3.2	5	0	11.26	14.28	12.77
2.2	9	20	11.97	11.69	11.83
2.2	9	0	10.80	12.20	11.50
2.2	5	20	10.88	10.96	10.92
2.2	5	0	10.25	10.55	10.40
1.9	7	10	11.12	9.54	10.33
3.5	7	10	16.58	17.26	16.92
2.7	3.6	10	5.00	7.20	6.10
2.7	10.4	10	12.28	13.16	12.72
2.7	7	-6.8	10.89	12.71	11.80
2.7	7	26.8	13.43	11.32	12.38
2.7	7	10	12.33	12.01	12.17
2.7	7	10	12.00	11.36	11.68
2.7	7	10	11.98	12.32	12.15
2.7	7	10	10.45	12.34	11.40
2.7	7	10	10.69	11.77	11.23
2.7	7	10	11.71	12.07	11.89

4.1.1 ANALYSIS OF PURE LINEAR MODEL BASED ON FIRST ORDER LINEAR EXPERIMENTAL DESIGN

Table 4.3 below shows the Linear Experimental Design Matrix with the experimentally obtained responses included. The linear experimental design was first fitted with a linear model of the form

$$y = b_0 + b_1x_1 + b_2x_2 + b_3x_3 \quad (4.1)$$

The model correlation, coefficient of determination, the student's t-test, the fisher's F-test and other statistical parameters were determined using the statistics toolbox of Matlab 7.5 software.

Table 4.3: Linear experimental design and responses obtained

TRIALS	x_0	DESIGN MATRIX			OPERATIONAL MATRIX			RESPONSE		
		x_1	x_2	x_3	x_1	x_2	x_3	y_1	y_2	y
1	+	-	-	-	2.2	5	0	10.25	10.55	10.40
2	+	+	-	-	3.2	5	0	11.26	14.28	12.77
3	+	-	+	-	2.2	9	0	10.80	12.20	11.50
4	+	+	+	-	3.2	9	0	14.50	13.94	14.22
5	+	-	-	+	2.2	5	20	10.88	10.96	10.92
6	+	+	-	+	3.2	5	20	12.66	13.38	13.02
7	+	-	+	+	2.2	9	20	11.97	11.69	11.83
8	+	+	+	+	3.2	9	20	14.70	15.30	15.00
9	+	0	0	0	2.7	7	10	12.33	12.01	12.17
10	+	0	0	0	2.7	7	10	12.00	11.36	11.68
11	+	0	0	0	2.7	7	10	11.98	12.32	12.15

The results of the statistical analysis of the data shown in table 4.3 are shown in tables 4.4, 4.5, and 4.6 below.

Table 4.4. Predicted responses and coefficient of Determination for model $y = b_0 + b_1x_1 + b_2x_2 + b_3x_3$

Trial no	Experimental Response	Predicted Response	Statistical Parameters
1	10.40	10.12	
2	12.77	12.71	$R^2 = 0.9489$
3	11.50	11.48	
4	14.22	14.07	Adj $R^2 = 0.9270$
5	10.92	10.59	
6	13.02	13.18	Mse = 0.1351
7	11.83	11.95	
8	15.00	14.54	
9	12.17	12.33	
10	11.68	12.33	
11	12.15	12.33	

Table 4.5. Estimated regression coefficients, t-values and p-values for model $y = b_0 + b_1x_1 + b_2x_2 + b_3x_3$

Variable	Estimated Coefficients	t-value	p-value
Constant	12.33	111.28	< 0.001
$\mathbf{x_1}$	1.30	9.96	<0.001
$\mathbf{x_2}$	0.68	5.23	0.001
$\mathbf{x_3}$	0.24	1.81	0.114

Table 4.6. Analysis of variance (ANOVA) of model $y = b_0 + b_1x_1 + b_2x_2 + b_3x_3$

Source	Degree of Freedom (DF)	Sum of square (SS)	Mean square (MS)	F-value	p-value
Regression	3	17.557	0.135	43.31	<0.001
$\mathbf{x_1}$	1	13.416	13.416	164.57	<0.001
$\mathbf{x_2}$	1	3.699	3.699	45.38	<0.001
$\mathbf{x_3}$	1	0.442	0.442	5.42	0.059
Residual error	7	0.489	0.082		
Total	10	18.503			

4.1.2 ANALYSIS OF LINEAR MODEL WITH INTERACTIONS BASED ON FIRST ORDER LINEAR EXPERIMENTAL DESIGN

The linear experimental design matrix with experimental responses shown in table 4.3 was next fitted with a linear model with interactions of the form

$$y = b_0 + b_1x_1 + b_2x_2 + b_3x_3 + b_4x_1x_2 + b_5x_1x_3 + b_6x_2x_3 \qquad (4.2)$$

The model correlation, coefficient of determination, the student's t-test, the fisher's F-test and other statistical parameters were determined as previously using the statistics toolbox of Matlab 7.5 software.

Table 4.7. Predicted responses and coefficient of Determination for model $y = b_0 + b_1x_1 + b_2x_2 + b_3x_3 + b_4x_1x_2 + b_5x_1x_3 + b_6x_2x_3$

Trial no	Experimental Response	Predicted Response	Statistical Parameters
1	10.40	10.37	
2	12.77	12.56	$R^2 = 0.9635$
3	11.50	11.29	
4	14.22	14.19	Adj $R^2 = 0.9088$
5	10.92	10.71	
6	13.02	12.99	Mse = 0.1688
7	11.83	11.80	
8	15.00	14.79	
9	12.17	12.33	
10	11.68	12.33	
11	12.15	12.33	

Table 4.8. Estimated regression coefficients, t-values and p-values for model $y = b_0 + b_1x_1 + b_2x_2 + b_3x_3 + b_4x_1x_2 + b_5x_1x_3 + b_6x_2x_3$

Variable	Estimated Coefficients	t-value	p-value
Constant	12.33	99.55	<0.001
x_1	1.295	8.91	<0.001
x_2	0.68	4.68	0.009
x_3	0.235	1.62	0.18
x_1x_2	0.178	1.22	0.29
x_1x_3	0.023	0.15	0.88
x_2x_3	0.043	0.29	0.78

Table 4.9. Analysis of variance (ANOVA) of model $y = b_0 + b_1x_1 + b_2x_2 + b_3x_3 + b_4x_1x_2 + b_5x_1x_3 + b_6x_2x_3$

Source	Degree of Freedom (DF)	Sum of square (SS)	Mean square (MS)	F-value	p-value
Regression	6	17.828	0.169	17.60	0.008
x_1	1	13.416	13.416	164.57	<0.001
x_2	1	3.699	3.699	45.38	<0.001
x_3	1	0.442	0.442	5.42	0.059
x_1x_2	1	0.252	0.252	3.46	0.160
x_1x_3	1	0.004	0.004	0.06	0.823
x_2x_3	1	0.014	0.014	0.20	0.686
Residual error	4	0.219	0.073		
Total	10	18.503			

4.1.3 ANALYSIS OF LINEAR MODEL WITH TRIPLE FACTOR INTERACTIONS BASED ON FIRST ORDER LINEAR EXPERIMENTAL DESIGN

The linear experimental design with experimental response values shown in table 4.3 was next fitted with a linear model with triple factor interactions of the form

$$y = b_0 + b_1x_1 + b_2x_2 + b_3x_3 + b_4x_1x_2 + b_5x_1x_3 + b_6x_2x_3 + b_7x_1x_2x_3 \ldots\ldots\ldots \quad (4.3)$$

The model correlation, coefficient of determination, and the statistical parameters of the student's t-test were determined using the statistics toolbox of Matlab 7.5 software.

Table 4.10: Correlation coefficients, t-values and p-values for model $y = b_0 + b_1x_1 + b_2x_2 + b_3x_3 + b_4x_1x_2 + b_5x_1x_3 + b_6x_2x_3 + b_7x_1x_2x_3$

Variable	Estimated Coefficients	t-value	p-value
Constant	12.333		
x_1	1.295	4.872	0.008
x_2	0.680	1.500	0.015
x_3	0.235	0.469	0.335
x_1x_2	0.178	0.535	0.374
x_1x_3	0.023	0.044	0.484
x_2x_3	0.043	0.084	0.469
$x_1x_2x_3$	0.090	0.178	0.435

4.1.4 ANALYSIS OF PURE QUADRATIC MODEL FIT BASED ON BOX WILSONS SECOND ORDER EXPERIMENTAL DESIGN

The Box Wilson's second order experimental design with experimental responses is shown in table 4.11 below.

Table 4.11. Box Wilson's experimental design and responses obtained.

TRIALS	x_0	DESIGN MATRIX			OPERATIONAL MATRIX			RESPONSE		
		x_1	x_2	x_3	x_1	x_2	x_3	y_1	y_2	y
1	+	+	+	+	3.2	9	20	14.70	15.30	15.00
2	+	+	+	-	3.2	9	0	14.50	13.94	14.22
3	+	+	-	+	3.2	5	20	12.66	13.38	13.02
4	+	+	-	-	3.2	5	0	11.26	14.28	12.77
5	+	-	+	+	2.2	9	20	11.97	11.69	11.83
6	+	-	+	-	2.2	9	0	10.80	12.20	11.50
7	+	-	-	+	2.2	5	20	10.88	10.96	10.92
8	+	-	-	-	2.2	5	0	10.25	10.55	10.40
9	+	-1.68	0	0	1.9	7	10	11.12	9.54	10.33
10	+	1.68	0	0	3.5	7	10	16.58	17.26	16.92
11	+	0	-1.68	0	2.7	3.6	10	5.00	7.20	6.10
12	+	0	1.68	0	2.7	10.4	10	12.28	13.16	12.72
13	+	0	0	-1.68	2.7	7	-6.8	10.89	12.71	11.80
14	+	0	0	1.68	2.7	7	26.8	13.43	11.32	12.38
15	+	0	0	0	2.7	7	10	12.33	12.01	12.17
16	+	0	0	0	2.7	7	10	12.00	11.36	11.68
17	+	0	0	0	2.7	7	10	11.98	12.32	12.15
18	+	0	0	0	2.7	7	10	10.45	12.34	11.40
19	+	0	0	0	2.7	7	10	10.69	11.77	11.23
20	+	0	0	0	2.7	7	10	11.71	12.07	11.89

This was fitted with a pure quadratic model of the form

$y = b_0 + b_1x_1 + b_2x_2 + b_3x_3 + b_4x_1^2 + b_5x_2^2 + b_6x_3^2$ ……..(4.3)

The model correlation, coefficient of determination, the student's t-test, the fisher's F-test and other statistical parameters were determined as previously using the statistics toolbox of Matlab 7.5 software.

Table 4.12. Predicted responses and coefficient of Determination for model $y = b_0 + b_1x_1 + b_2x_2 + b_3x_3 + b_4x_1^2 + b_5x_2^2 + b_6x_3^2$

Trial no	Experimental Response	Predicted Response	Statistical Parameters
1	15.00	15.15	
2	14.22	14.73	$R^2 = 0.8812$
3	13.02	12.72	
4	12.77	12.31	Adj $R^2 = 0.8264$
5	11.83	12.01	
6	11.50	11.59	Mse = 0.7602
7	10.92	9.58	
8	10.40	9.16	
9	10.33	11.41	
10	16.92	16.69	
11	6.10	7.80	
12	12.72	11.87	
13	11.80	12.16	
14	12.38	12.87	
15	12.17	11.73	
16	11.68	11.73	
17	12.15	11.73	
18	11.40	11.73	
19	11.23	11.73	
20	11.89	11.73	

Table 4.13. Estimated regression coefficients, t-values and p-values for model $y = b_0 + b_1x_1 + b_2x_2 + b_3x_3 + b_4x_1^2 + b_5x_2^2 + b_6x_3^2$

Variable	Estimated Coefficients	t-value	p-value
Constant	11.73	32.99	<0.001
x_1	1.57	6.65	<0.001
x_2	1.21	5.14	<0.001
x_3	0.21	0.89	0.392
x_1^2	0.82	3.58	0.003
x_2^2	-0.67	-2.92	0.012
x_3^2	0.28	1.21	0.248

Table 4.14. Analysis of variance (ANOVA) of model $y = b_0 + b_1x_1 + b_2x_2 + b_3x_3 + b_4x_1^2 + b_5x_2^2 + b_6x_3^2$

Source	Degree of Freedom (DF)	Sum of square (SS)	Mean square (MS)	F-value	p-value
Regression	6	73.303	0.760	16.07	<0.001
x_1	3	40.385	13.462	111.24	<0.001
x_2	3	33.848	11.283	93.24	<0.001
x_3	3	0.78	0.26	2.15	0.164
Residual error	10	1.0891	0.121		
Total	19	83.1847			

4.1.5 ANALYSIS OF QUADRATIC MODEL WITH INTERACTION BASED ON BOX WILSONS SECOND ORDER EXPERIMENTAL DESIGN

The second order experimental design was then fitted to a quadratic model with interactions as follows;

$$y = b_0 + b_1x_1 + b_2x_2 + b_3x_3 + b_4x_1x_2 + b_5x_1x_3 + b_6x_2x_3 + b_7x_1^2 + b_8x_2^2 + b_9x_3^2 \quad .....(4.4)$$

Table 4.15. Predicted responses and coefficient of Determination for model $y = b_0 + b_1x_1 + b_2x_2 + b_3x_3 + b_4x_1x_2 + b_5x_1x_3 + b_6x_2x_3 + b_7x_1^2 + b_8x_2^2 + b_9x_3^2$

Trial no	Experimental Response	Predicted Response	Statistical Parameters
1	15.00	15.39	
2	14.22	14.85	$R^2 = 0.8845$
3	13.02	12.53	
4	12.77	12.15	Adj $R^2 = 0.7805$
5	11.83	11.85	
6	11.50	11.39	Mse = 0.9611
7	10.92	9.70	
8	10.40	9.41	
9	10.33	11.41	
10	16.92	16.69	
11	6.10	7.80	
12	12.72	11.87	
13	11.80	12.16	
14	12.38	12.86	
15	12.17	11.73	
16	11.68	11.73	
17	12.15	11.73	
18	11.40	11.73	
19	11.23	11.73	
20	11.89	11.73	

Table 4.16. Estimated regression coefficients, t-values and p-values for model $y = b_0 + b_1x_1 + b_2x_2 + b_3x_3 + b_4x_1x_2 + b_5x_1x_3 + b_6x_2x_3 + b_7x_1^2 + b_8x_2^2 + b_9x_3^2$

Variable	Estimated Coefficients	t-value	p-value
Constant	11.73	29.33	<0.001
x_1	1.57	5.92	<0.001
x_2	1.21	4.57	<0.001
x_3	0.21	0.79	0.449
x_1x_2	0.18	0.51	0.62
x_1x_3	0.02	0.06	0.95
x_2x_3	0.04	0.12	0.905
x_1^2	0.82	3.18	0.010
x_2^2	-0.67	-2.59	0.027
x_3^2	0.28	1.08	0.307

Table 4.17. Analysis of variance (ANOVA) of model $y = b_0 + b_1x_1 + b_2x_2 + b_3x_3 + b_4x_1x_2 + b_5x_1x_3 + b_6x_2x_3 + b_7x_1^2 + b_8x_2^2 + b_9x_3^2$

Source	Degree of Freedom (DF)	Sum of square (SS)	Mean square (MS)	F-value	p-value
Regression	9	73.573	0.9611	8.505	0.001
x_1	3	40.39	13.46	11.24	<0.001
x_2	3	33.85	11.28	93.24	<0.001
x_3	3	0.78	0.26	2.15	0.1641
x_1x_2	1	0.2521	0.252	1.85	0.223
x_1x_3	1	0.0041	0.004	0.03	0.869
x_2x_3	1	0.0144	0.014	0.11	0.756
Residual error	7	0.8185	0.136		
Total	19	83.185			

4.1.6 GRAPHICAL ANALYSIS OF THE VARIOUS MODELS

The graphical representations of the effects of the various factors on the response called surface plots were also developed using the statistics toolbox of Matlab7.5 software and interactions between any two variables on the % iron II oxidized were studied while the third variable was kept constant at its mid value. These results are presented in figures 4.1 to 4.12 below. Figures 4.13 to 4.48 are the x-y scatter plots showing the variation in percentage Fe (II) oxidised at constant liquid flowrates and various degrees of column tilt for the different models

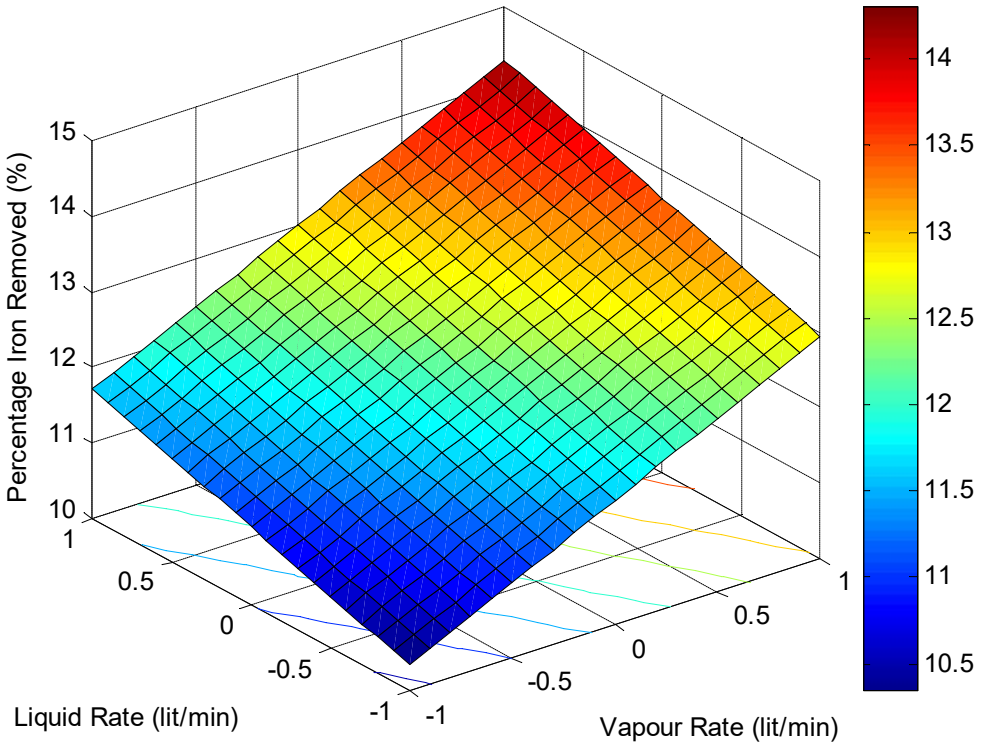

Figure 4.1: Response surface plot for model $y = b_0+b_1x_1+b_2x_2+b_3x_3$ showing the interaction effect between the liquid rate and vapour rate with the angle of tilt held at its mid value of 10 degrees.

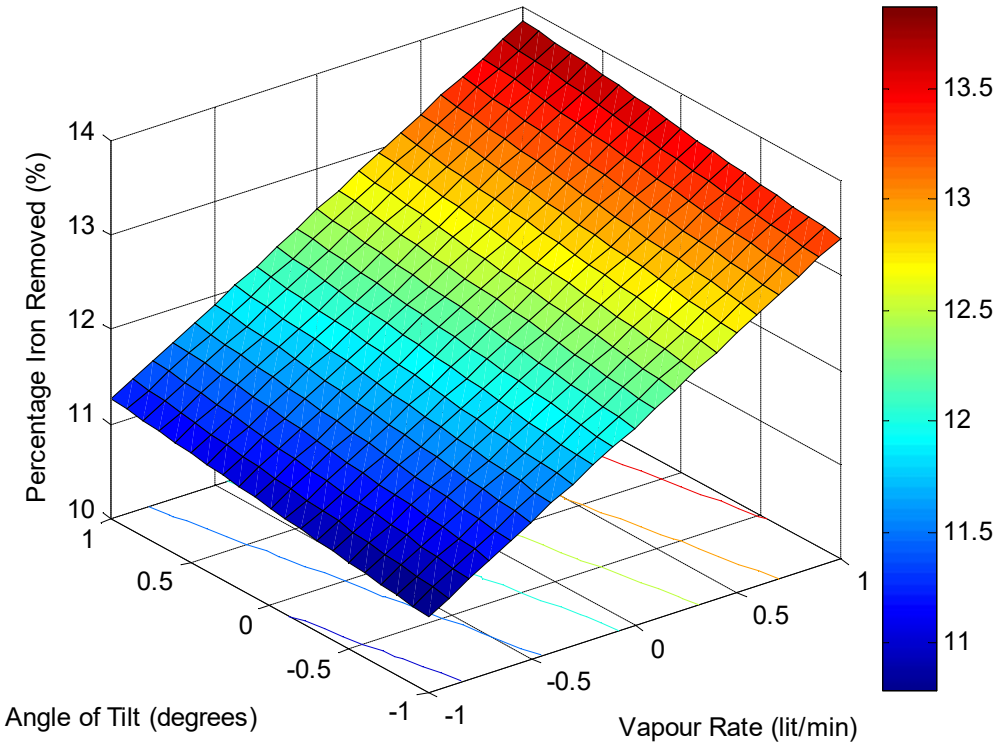

Figure 4.2: Response surface plot for model; $y = b_0+b_1x_1+b_2x_2+b_3x_3$ showing the interaction effect between the vapour rate and angle of tilt with the liquid rate held at its mid value of 7.0 litres/minute.

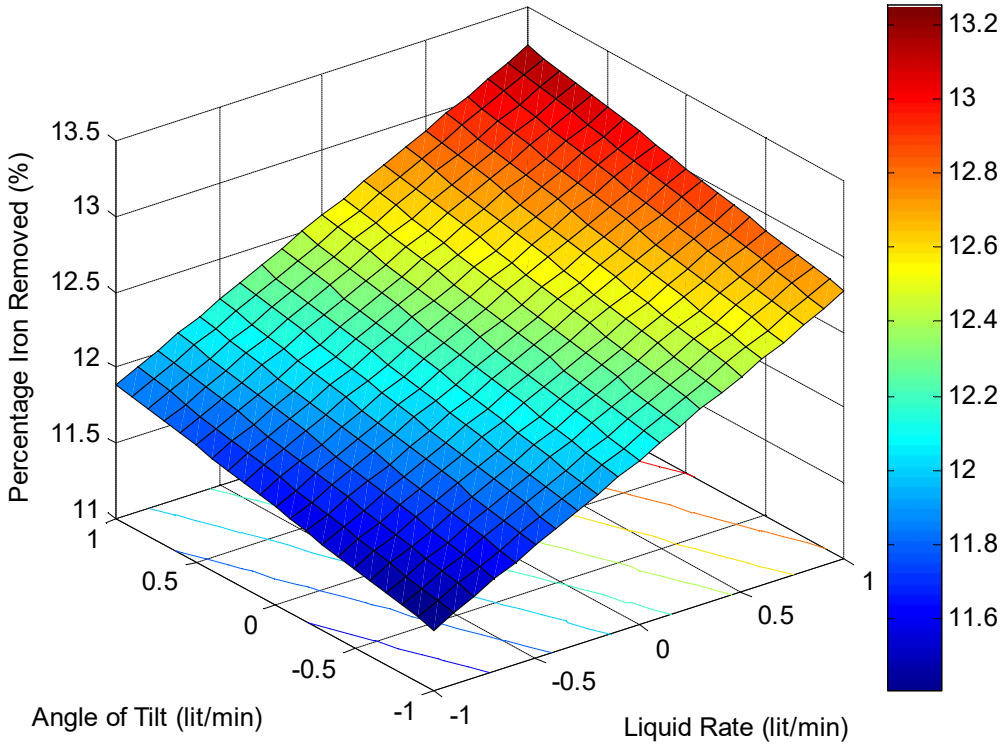

Figure 4.3: Response surface plot for model; $y = b_0+b_1x_1+b_2x_2+b_3x_3$ showing the interaction effect between the liquid rate and angle of tilt with the vapour rate held at its mid value of 2.7 litres/minute.

.

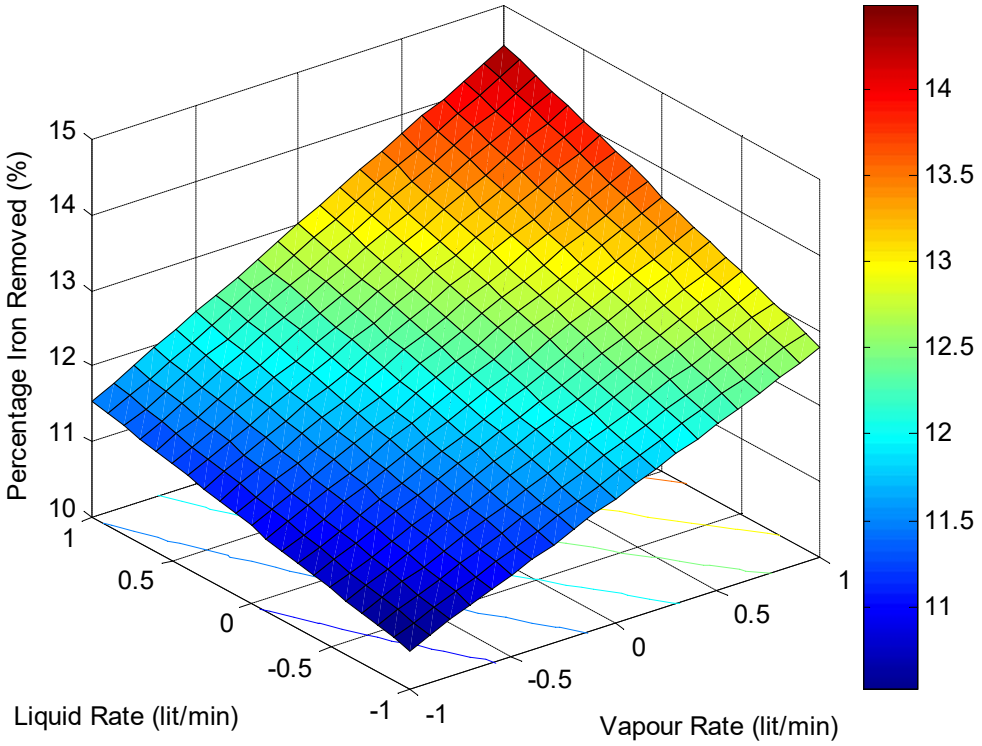

Figure 4.4: Response surface plot for model; $y = b_0+b_1x_1+b_2x_2+b_3x_3+b_4x_1x_2+b_5x_1x_3+b_6x_2x_3$ showing the interaction effect between the liquid rate and the vapour rate with the angle of tilt with held at its mid value of 10 degrees.

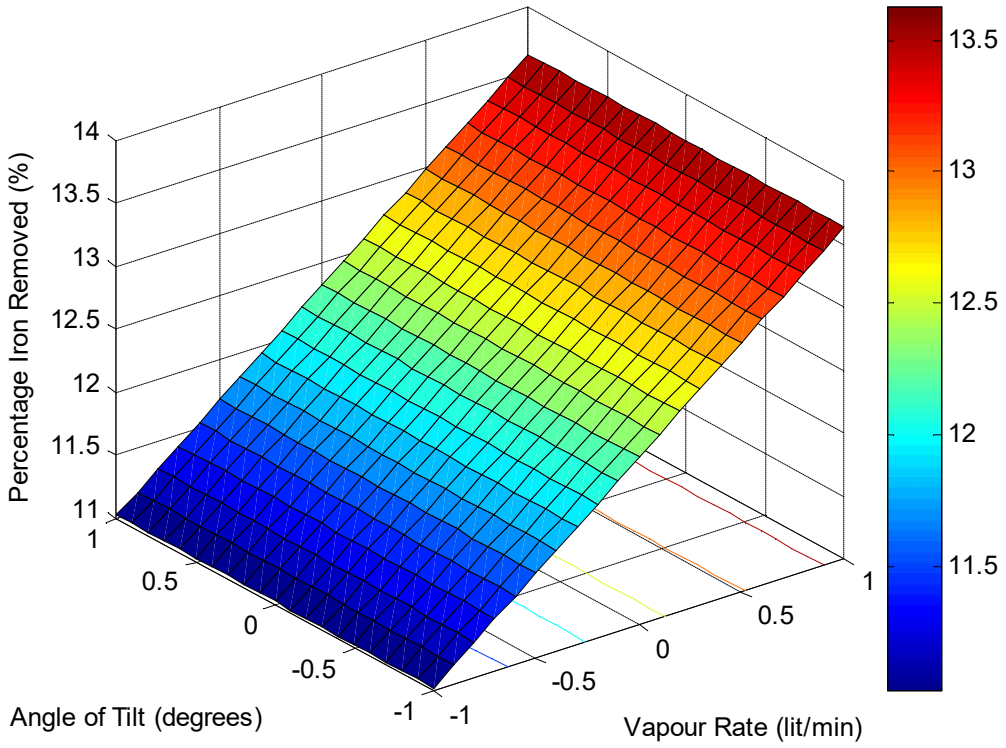

Figure 4.5: Response surface plot for model; $y = b_0+b_1x_1+b_2x_2+b_3x_3+b_4x_1x_2+b_5x_1x_3+b_6x_2x_3$ showing the interaction effect between the vapour rate and angle of tilt with the liquid rate held at its mid value of 7 litres/minute.

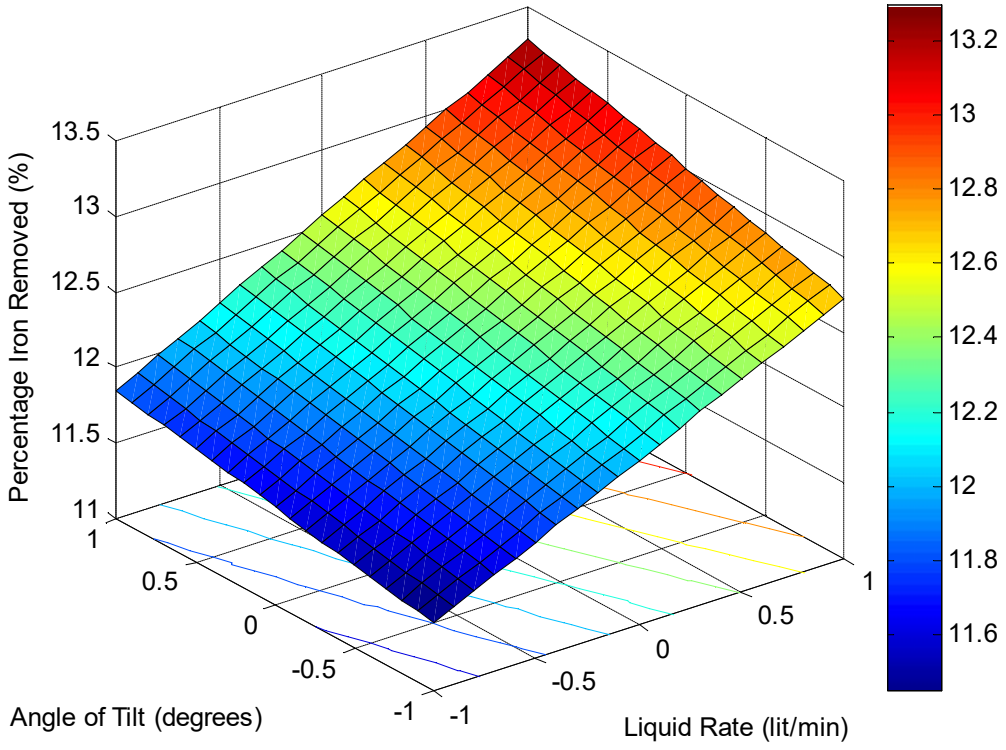

Figure 4.6: Response surface plot for model; $y = b_0+b_1x_1+b_2x_2+b_3x_3+b_4x_1x_2+b_5x_1x_3+b_6x_2x_3$ showing the interaction effect between the liquid rate and angle of tilt with the vapour rate held at its mid value of 2.7 litres/minute.

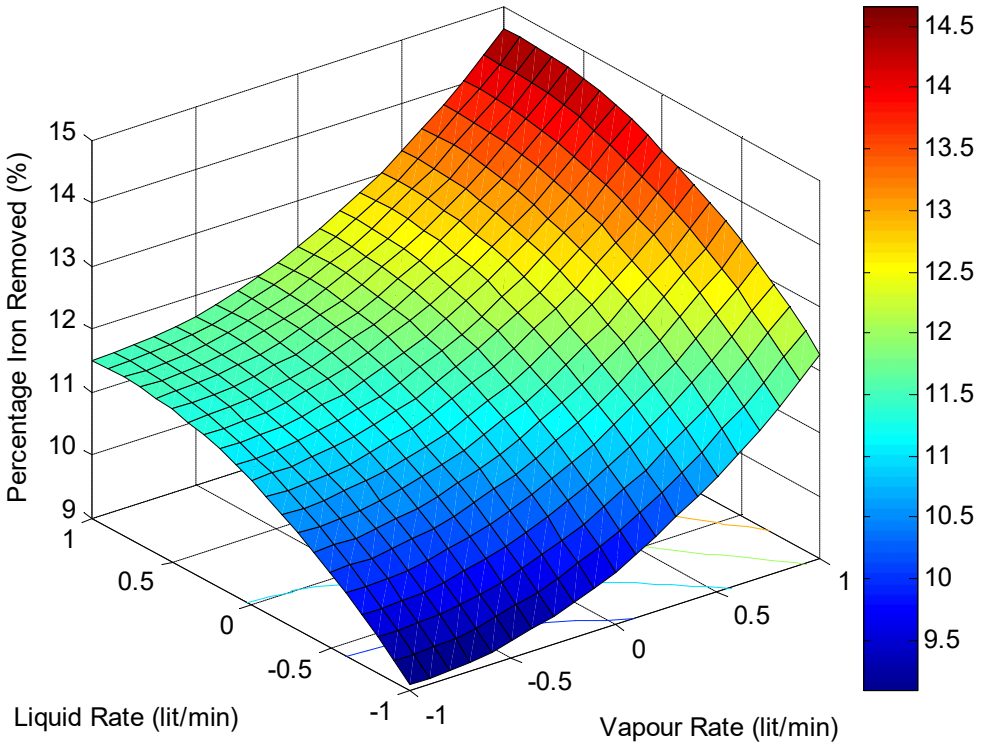

Figure 4.7: Response surface plot for model; $y = b_0+b_1x_1+b_2x_2+b_3x_3+b_4x_1^2+b_5x_2^2+b_6x_3^2$ showing the interaction effect between the liquid rate and the vapour rate with the angle of tilt held at its mid value of 10 degrees.

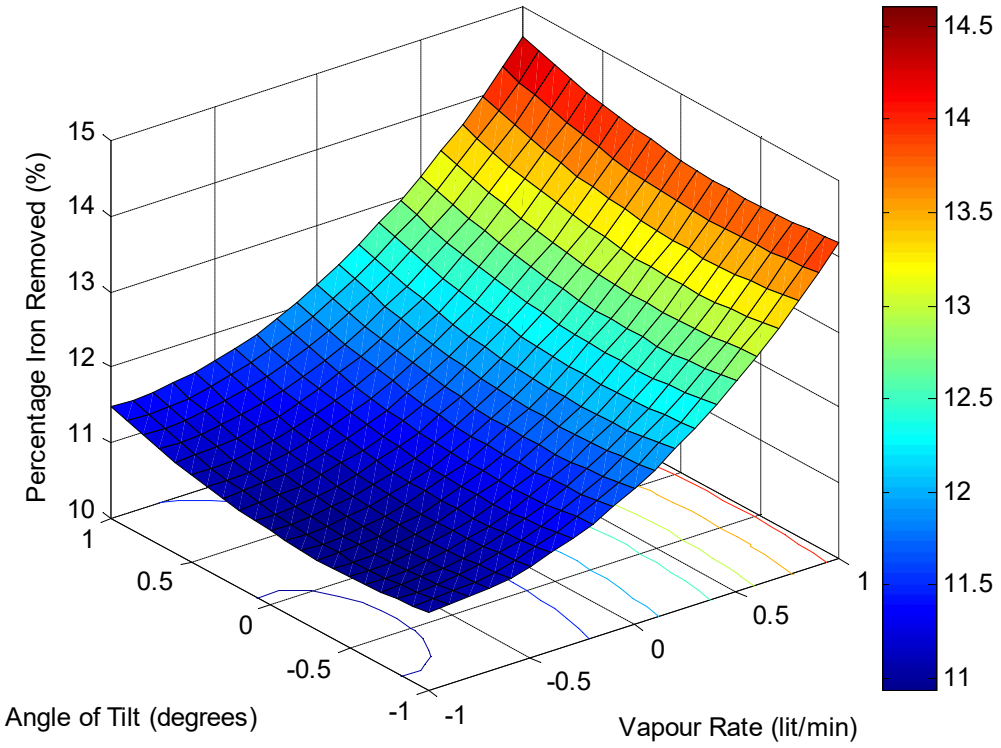

Figure 4.8: Response surface plot for model; $y = b_0+b_1x_1+b_2x_2+b_3x_3+b_4x_1^2+b_5x_2^2+b_6x_3^2$ showing the interaction effect between the angle of tilt and the vapour rate with the liquid rate held at its mid value 7 litres per minute.

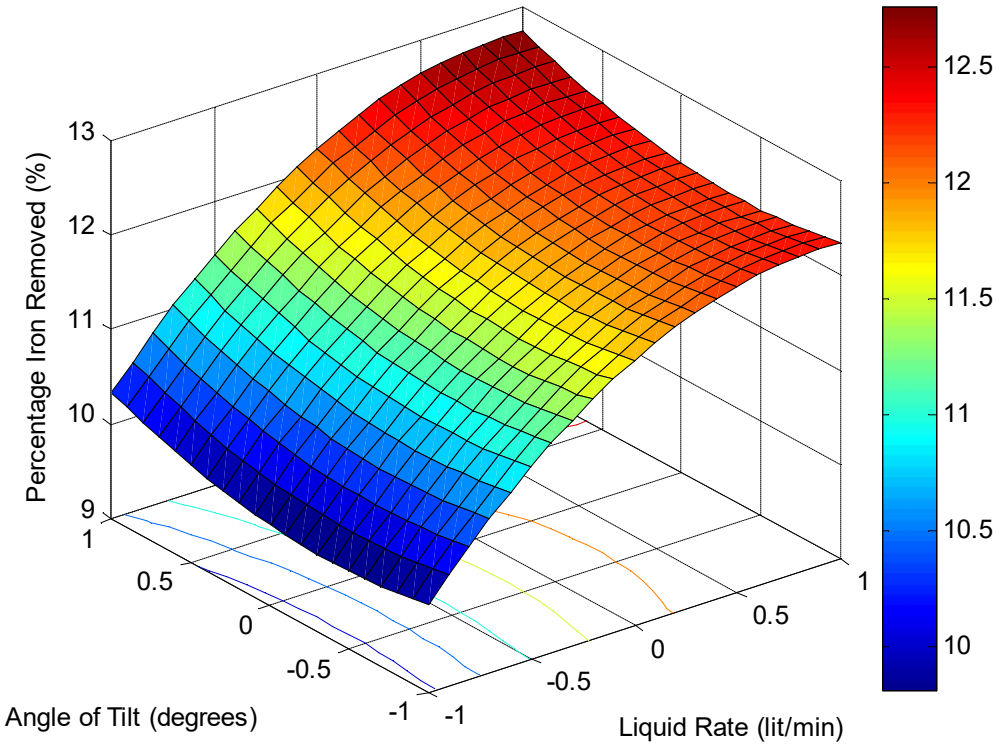

Figure 4.9: Response surface plot for model; $y = b_0+b_1x_1+b_2x_2+b_3x_3+b_4x_1^2+b_5x_2^2+b_6x_3^2$ showing the interaction effect between the angle of tilt and the liquid rate with the vapour rate held at its mid value of 2.7 litres/minute.

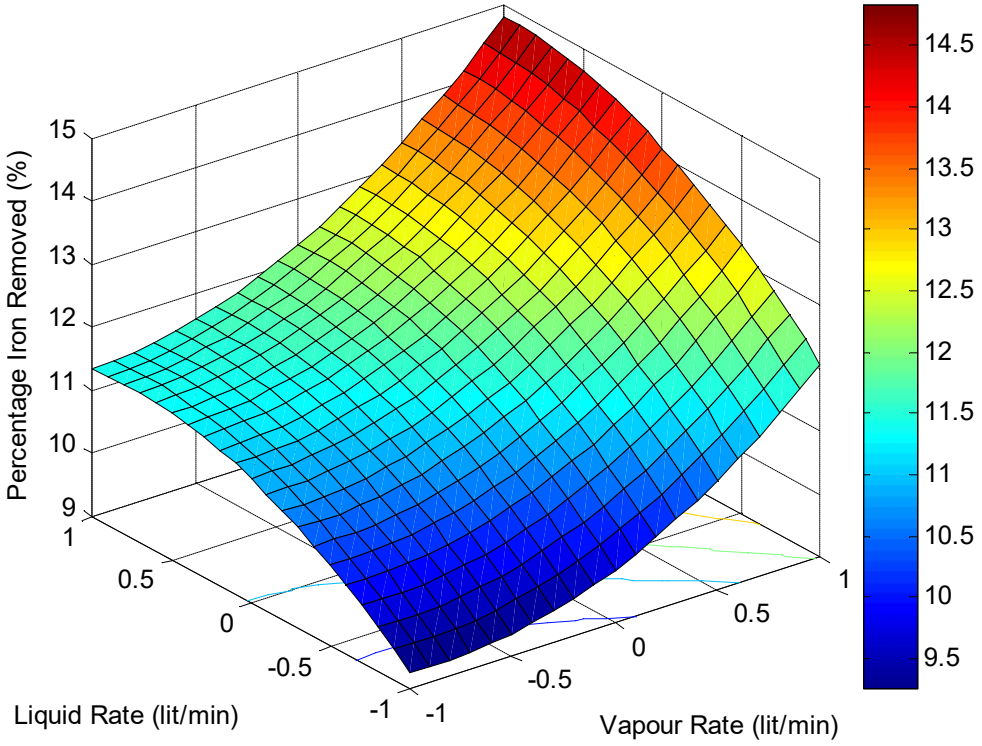

Figure 4.10: Response surface plot for model; $y = b_0+b_1x_1+b_2x_2+b_3x_3+b_4x_1x_2 +b_5x_1x_3 +b_6x_2x_3 + b_7x_1^2+b_8x_2^2+b_9x_3^2$ showing the interaction effect between the liquid rate and vapour rate with the angle of tilt held at its mid value 10 degrees.

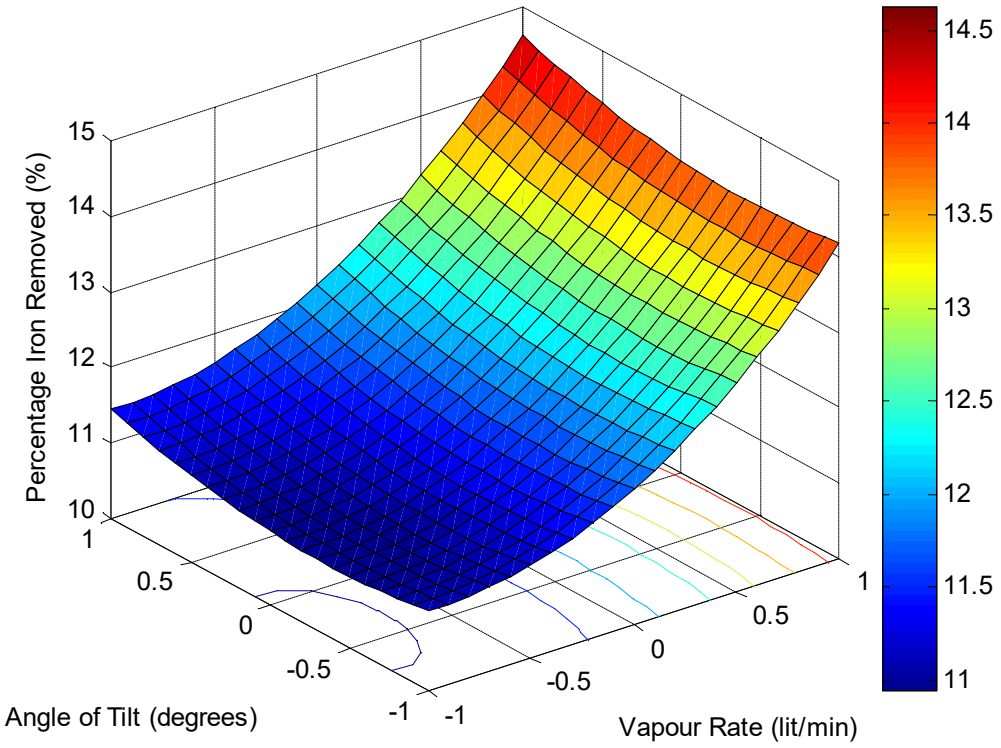

Figure 4.11: Response surface plot for model; $y = b_0+b_1x_1+b_2x_2+b_3x_3+b_4x_1x_2 +b_5x_1x_3 +b_6x_2x_3 + b_7x_1^2+b_8x_2^2+b_9x_3^2$ showing the interaction effect between the angle of tilt and vapour rate with the liquid rate held at its mid value 7 litres/minute.

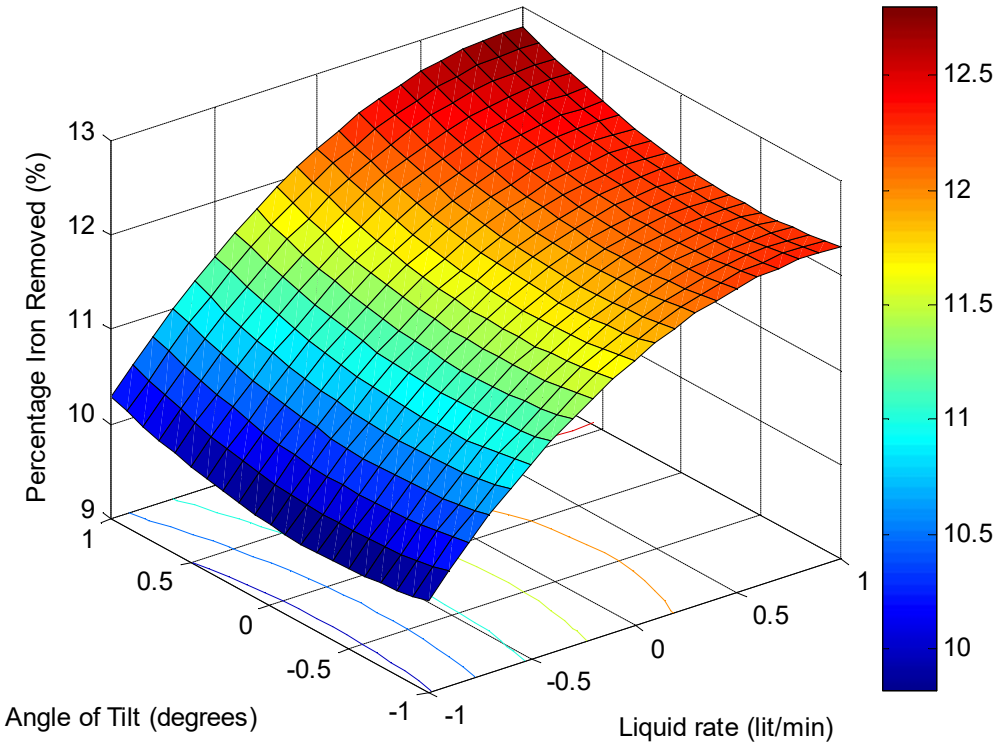

Figure 4.12: Response surface plot for model; $y = b_0+b_1x_1+b_2x_2+b_3x_3+b_4x_1x_2 +b_5x_1x_3 +b_6x_2x_3 + b_7x_1^2+b_8x_2^2+b_9x_3^2$ showing the interaction effect between the angle of tilt and the liquid rate with the vapour rate held at its mid value of 2.7 litres/minute.

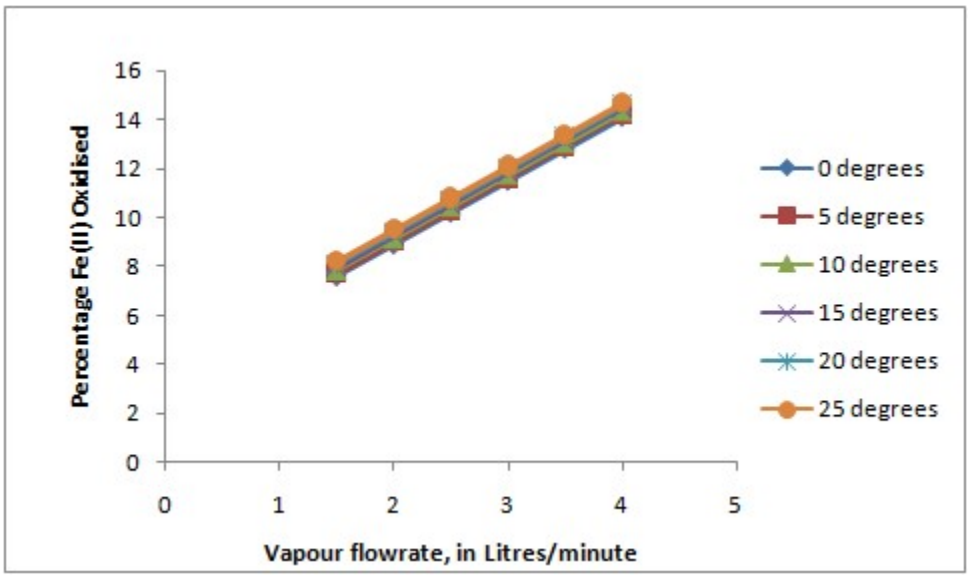

Figure 4.13: Effect of vapour flowrates and angles of tilt on percentage Fe(II) oxidised at a constant liquid flowrate of 3 litres per minute based on linear model $y=b_0 + b_1x_1 + b_2x_2 + b_3x_3$

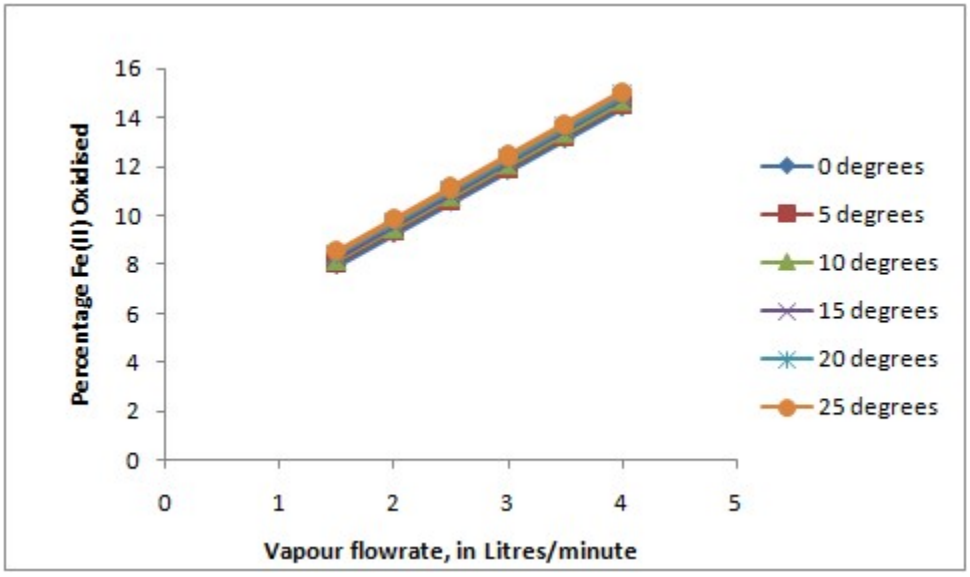

Figure 4.14: Effect of vapour flowrates and angles of tilt on percentage Fe(II) oxidised at a constant liquid flowrate of 4 litres per minute based on linear model $y=b_0 + b_1x_1 + b_2x_2 + b_3x_3$

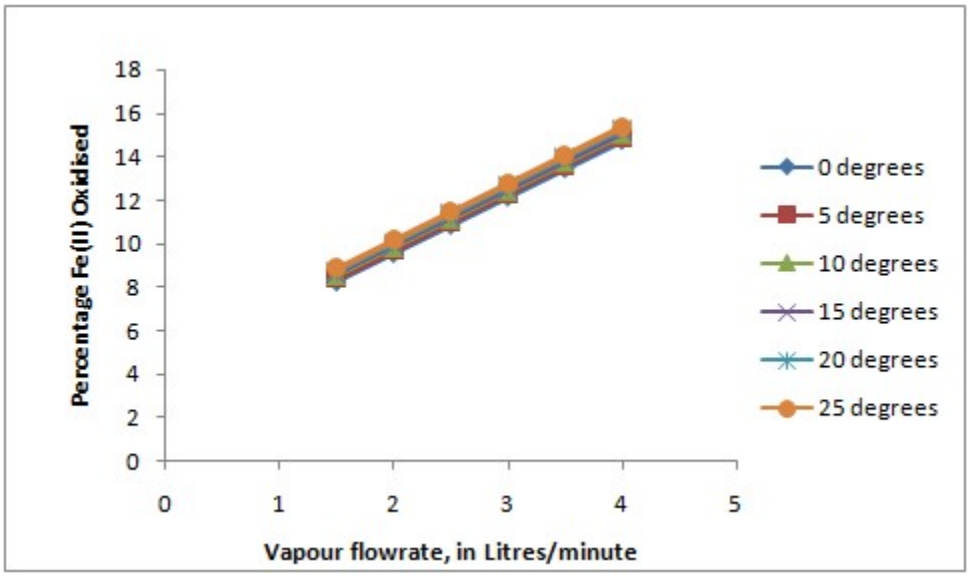

Figure 4.15: Effect of vapour flowrates and angles of tilt on percentage Fe(II) oxidised at a constant liquid flowrate of 5 litres per minute based on linear model $y=b_0 + b_1x_1 + b_2x_2 + b_3x_3$

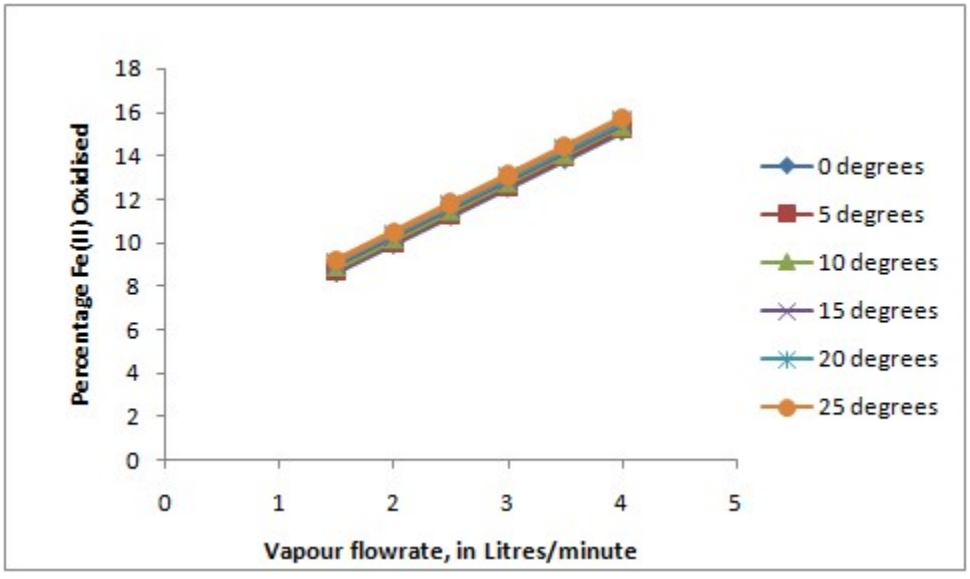

Figure 4.16: Effect of vapour flowrates and angles of tilt on percentage Fe(II) oxidised at a constant liquid flowrate of 6 litres per minute based on linear model $y=b_0 + b_1x_1 + b_2x_2 + b_3x_3$

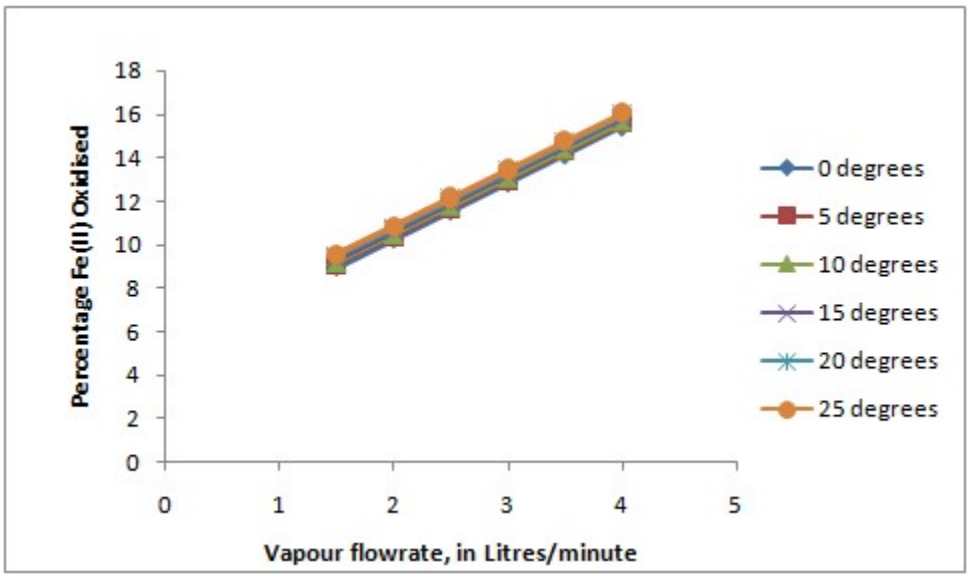

Figure 4.17: Effect of vapour flowrates and angles of tilt on percentage Fe(II) oxidised at a constant liquid flowrate of 7 litres per minute based on linear model $y=b_0 + b_1x_1 + b_2x_2 + b_3x_3$

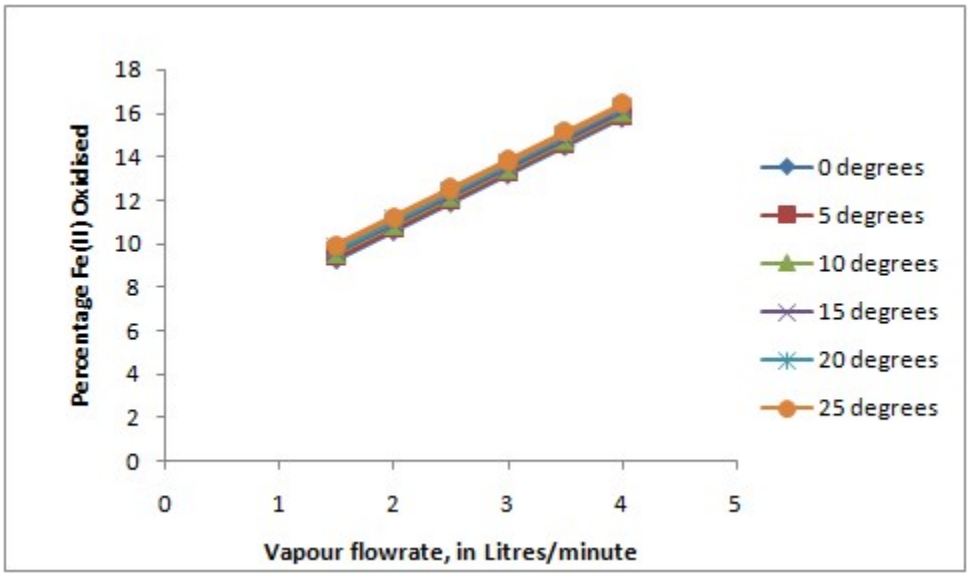

Figure 4.18: Effect of vapour flowrates and angles of tilt on percentage Fe(II) oxidised at a constant liquid flowrate of 8 litres per minute based on linear model $y=b_0 + b_1x_1 + b_2x_2 + b_3x_3$

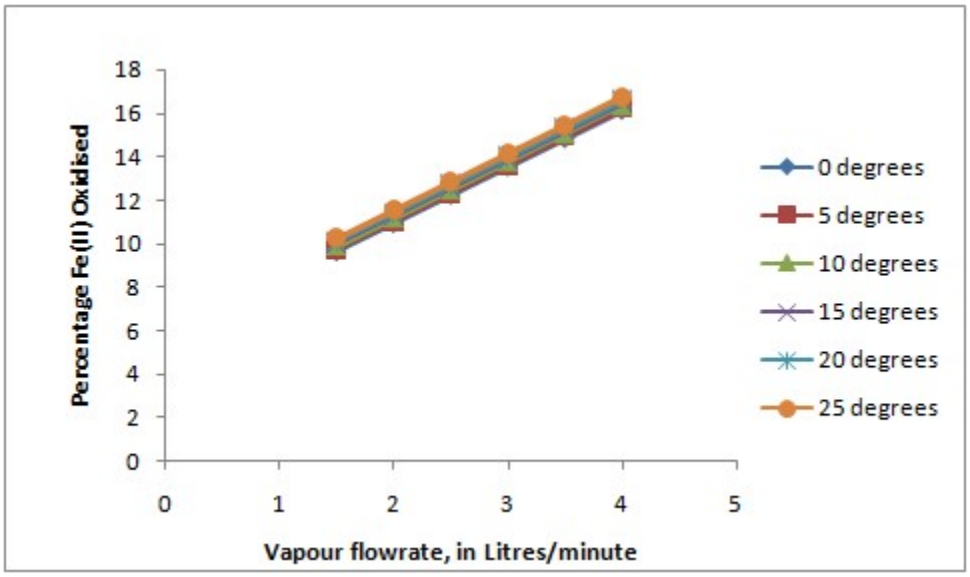

Figure 4.19: Effect of vapour flowrates and angles of tilt on percentage Fe(II) oxidised at a constant liquid flowrate of 9 litres per minute based on linear model $y=b_0 + b_1x_1 + b_2x_2 + b_3x_3$

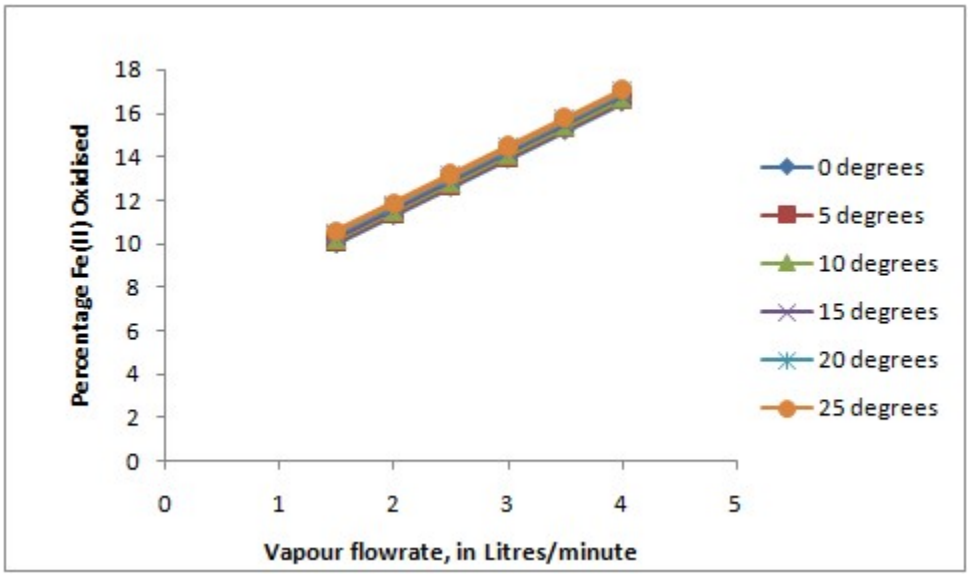

Figure 4.20: Effect of vapour flowrates and angles of tilt on percentage Fe(II) oxidised at a constant liquid flowrate of 10 litres per minute based on linear model $y=b_0 + b_1x_1 + b_2x_2 + b_3x_3$

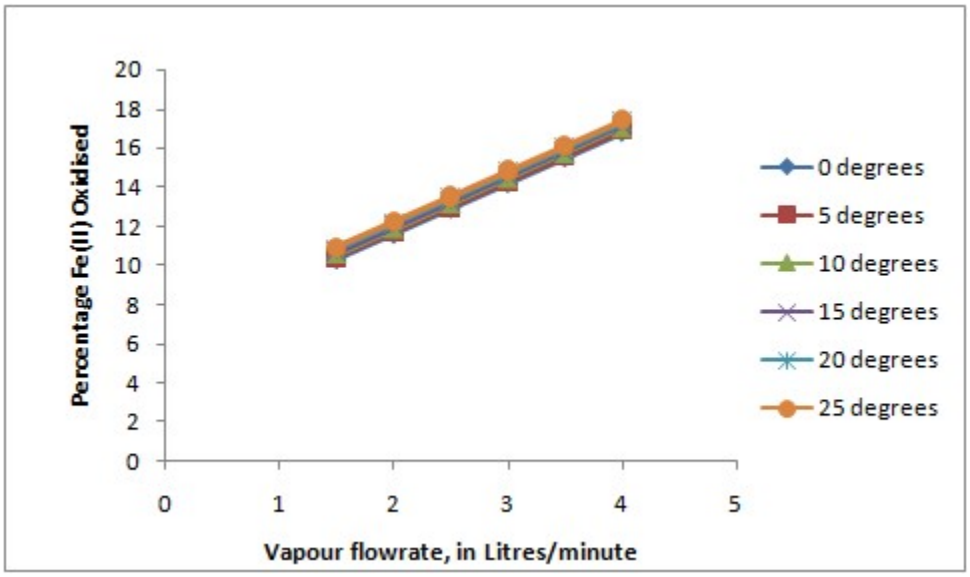

Figure 4.21: Effect of vapour flowrates and angles of tilt on percentage Fe(II) oxidised at a constant liquid flowrate of 11 litres per minute based on linear model $y=b_0 + b_1x_1 + b_2x_2 + b_3x_3$

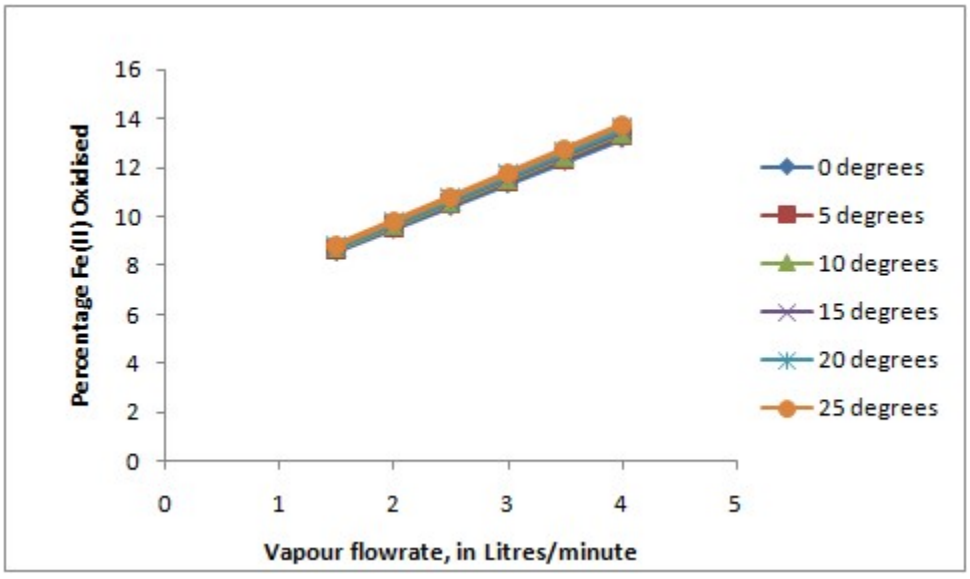

Figure 4.22: Effect of vapour flowrates and angles of tilt on percentage Fe(II) oxidised at a constant liquid flowrate of 3 litres per minute based on linear model $y=b_0 + b_1x_1 + b_2x_2 + b_3x_3 + b_4x_1x_2 + b_5x_1x_3 + b_6x_2x_3$

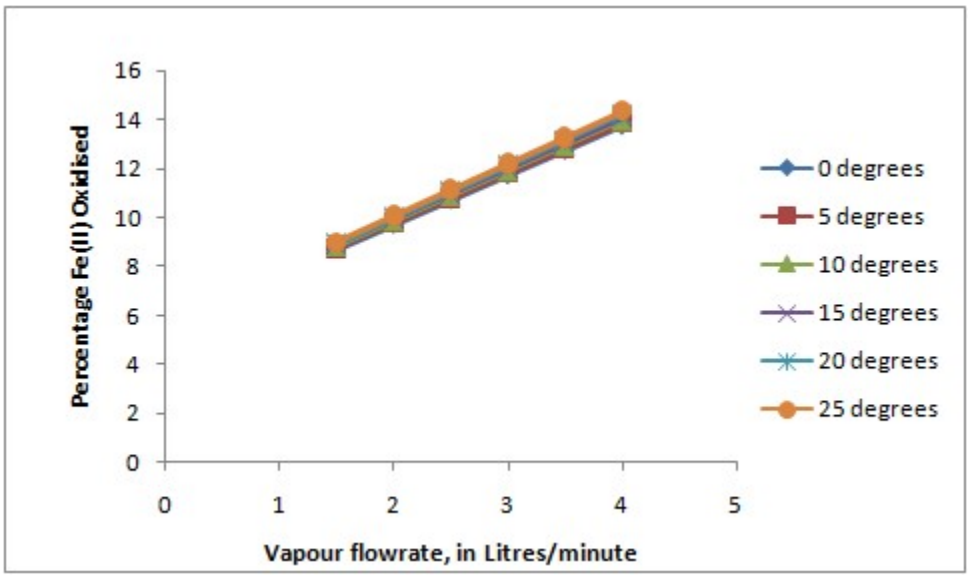

Figure 4.23: Effect of vapour flowrates and angles of tilt on percentage Fe(II) oxidised at a constant liquid flowrate of 4 litres per minute based on linear model $y=b_0 + b_1x_1 + b_2x_2 + b_3x_3 + b_4x_1x_2 + b_5x_1x_3 + b_6x_2x_3$

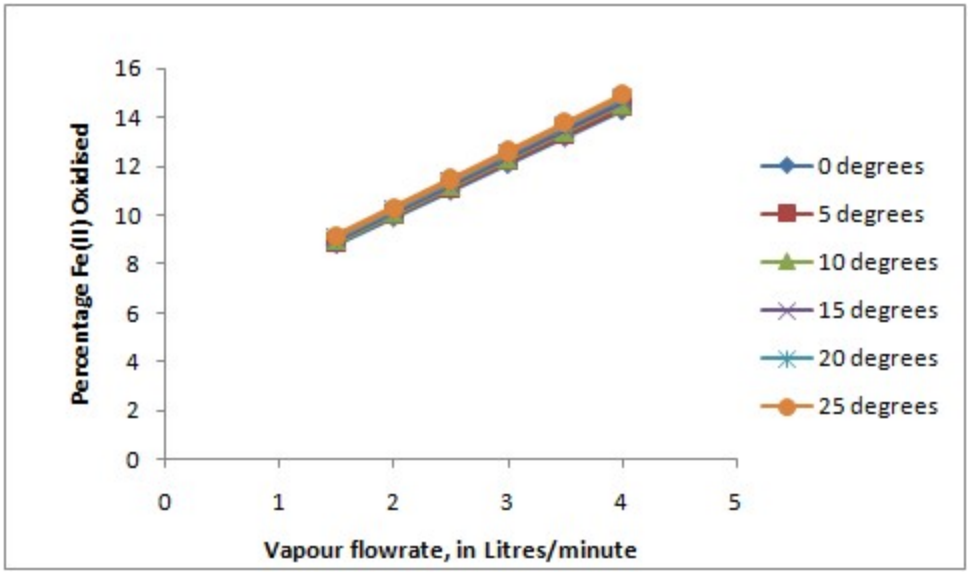

Figure 4.24: Effect of vapour flowrates and angles of tilt on percentage Fe(II) oxidised at a constant liquid flowrate of 5 litres per minute based on linear model $y=b_0 + b_1x_1 + b_2x_2 + b_3x_3 + b_4x_1x_2 + b_5x_1x_3 + b_6x_2x_3$

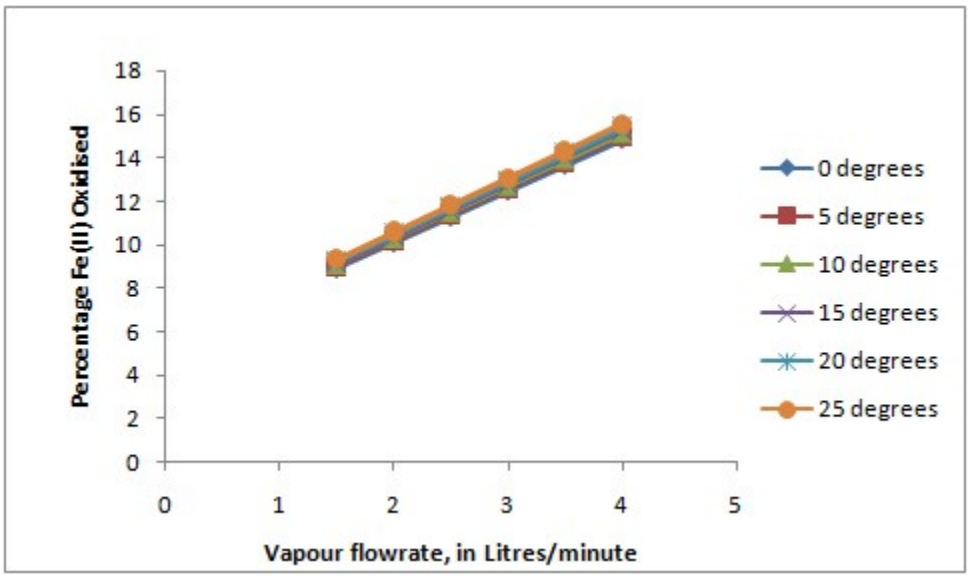

Figure 4.25: Effect of vapour flowrates and angles of tilt on percentage Fe(II) oxidised at a constant liquid flowrate of 6 litres per minute based on linear model $y=b_0 + b_1x_1 + b_2x_2 + b_3x_3 + b_4x_1x_2 + b_5x_1x_3 + b_6x_2x_3$

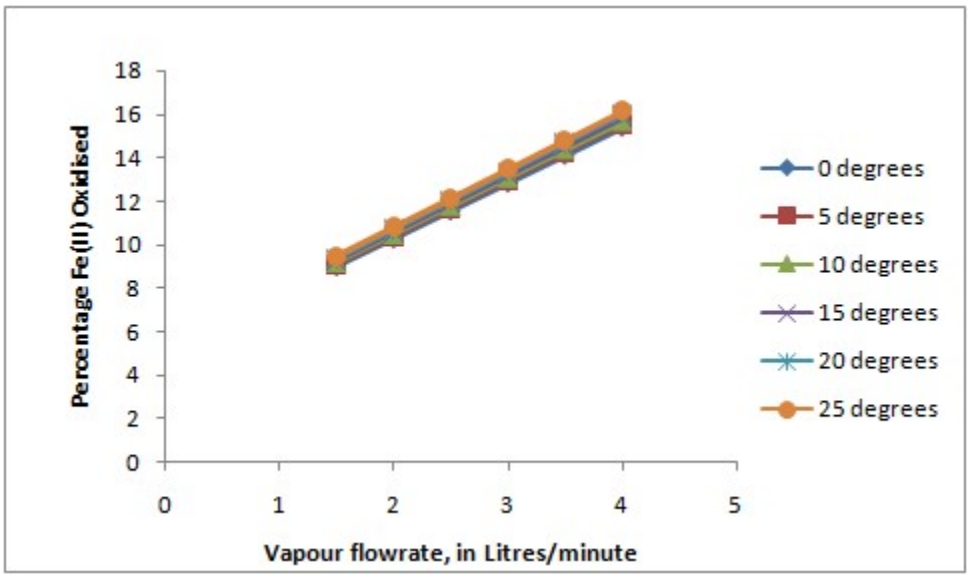

Figure 4.26: Effect of vapour flowrates and angles of tilt on percentage Fe(II) oxidised at a constant liquid flowrate of 7 litres per minute based on linear model $y=b_0 + b_1x_1 + b_2x_2 + b_3x_3 + b_4x_1x_2 + b_5x_1x_3 + b_6x_2x_3$

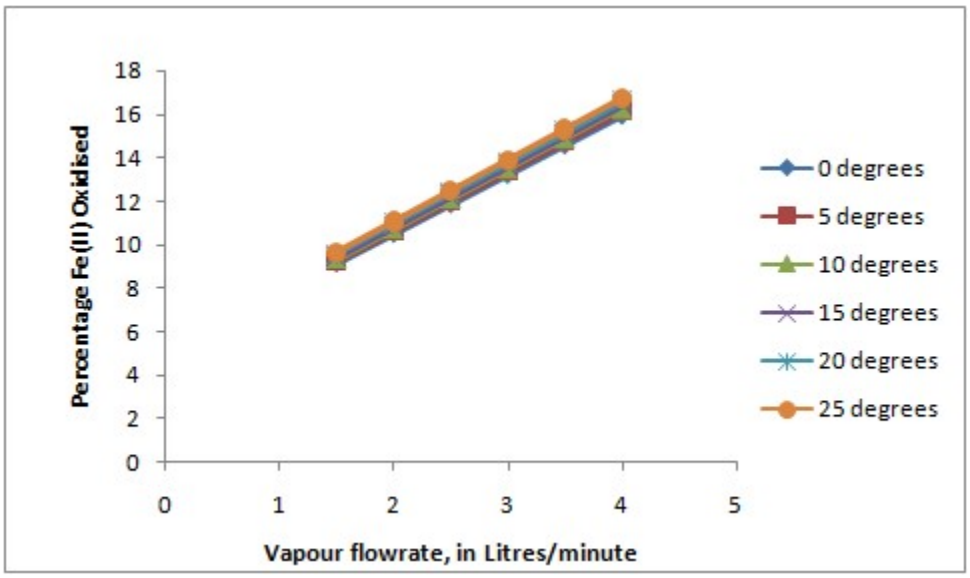

Figure 4.27: Effect of vapour flowrates and angles of tilt on percentage Fe(II) oxidised at a constant liquid flowrate of 8 litres per minute based on linear model $y=b_0 + b_1x_1 + b_2x_2 + b_3x_3 + b_4x_1x_2 + b_5x_1x_3 + b_6x_2x_3$

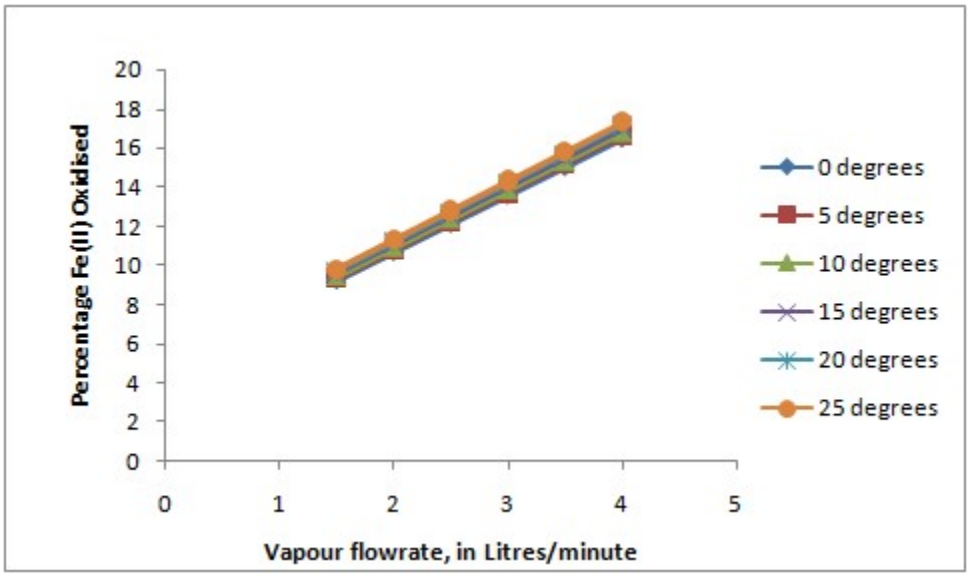

Figure 4.28: Effect of vapour flowrates and angles of tilt on percentage Fe(II) oxidised at a constant liquid flowrate of 9 litres per minute based on linear model $y=b_0 + b_1x_1 + b_2x_2 + b_3x_3 + b_4x_1x_2 + b_5x_1x_3 + b_6x_2x_3$

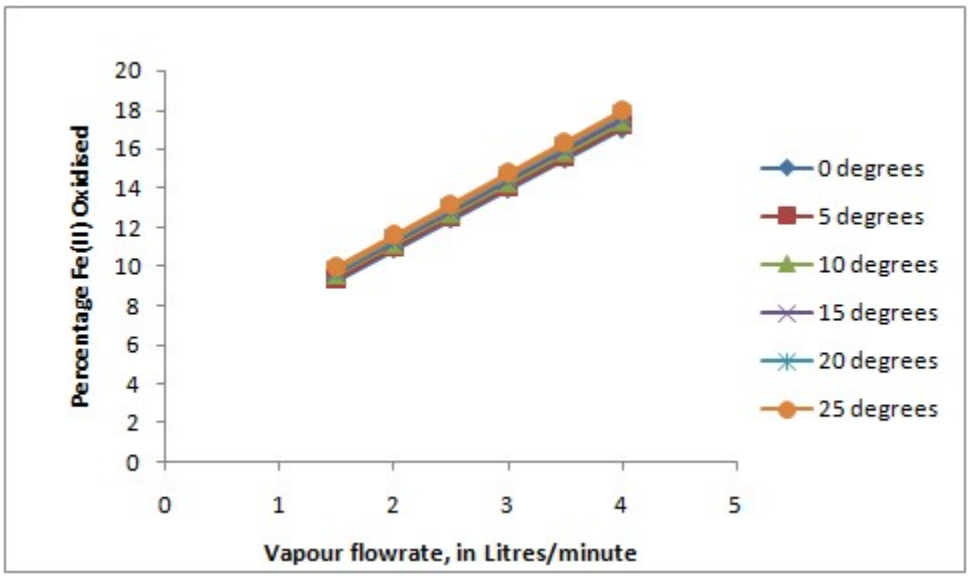

Figure 4.29: Effect of vapour flowrates and angles of tilt on percentage Fe(II) oxidised at a constant liquid flowrate of 10 litres per minute based on linear model $y=b_0 + b_1x_1 + b_2x_2 + b_3x_3 + b_4x_1x_2 + b_5x_1x_3 + b_6x_2x_3$

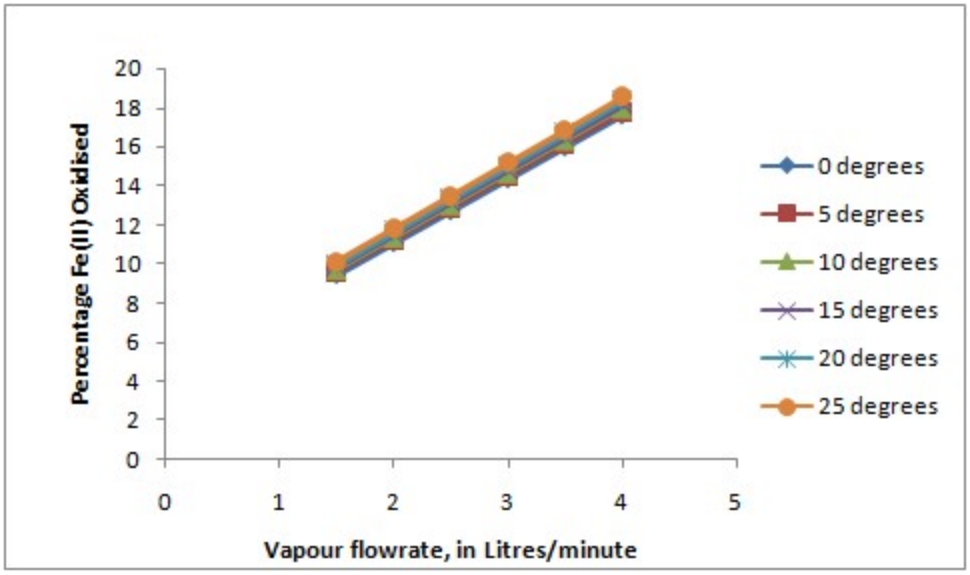

Figure 4.30: Effect of vapour flowrates and angles of tilt on percentage Fe(II) oxidised at a constant liquid flowrate of 11 litres per minute based on linear model $y=b_0 + b_1x_1 + b_2x_2 + b_3x_3 + b_4x_1x_2 + b_5x_1x_3 + b_6x_2x_3$

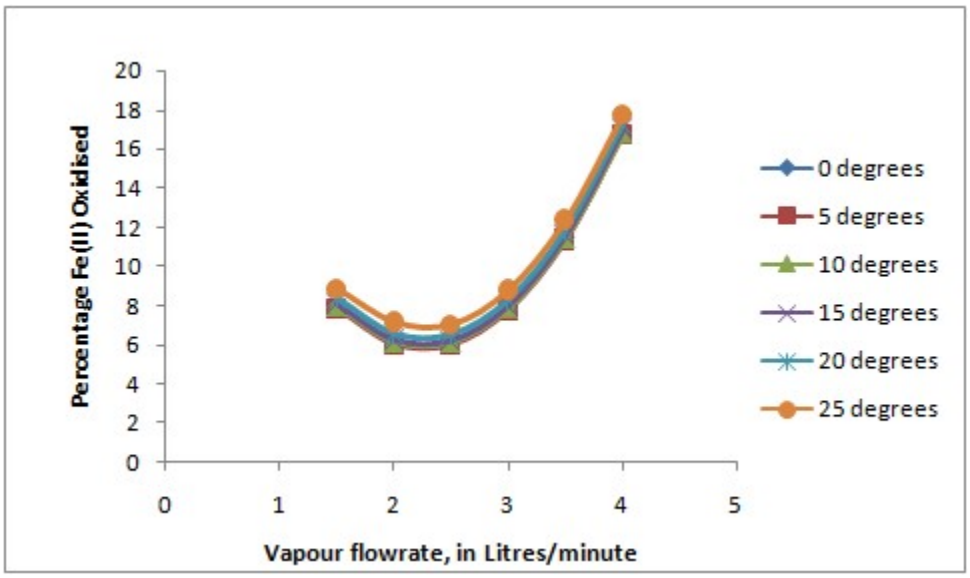

Figure 4.31: Effect of vapour flowrates and angles of tilt on percentage Fe(II) oxidised at a constant liquid flowrate of 3 litres per minute based on quadratic model $y=b_0 + b_1x_1 + b_2x_2 + b_3x_3 + b_4x_1^2 + b_5x_2^2 + b_6x_3^2$

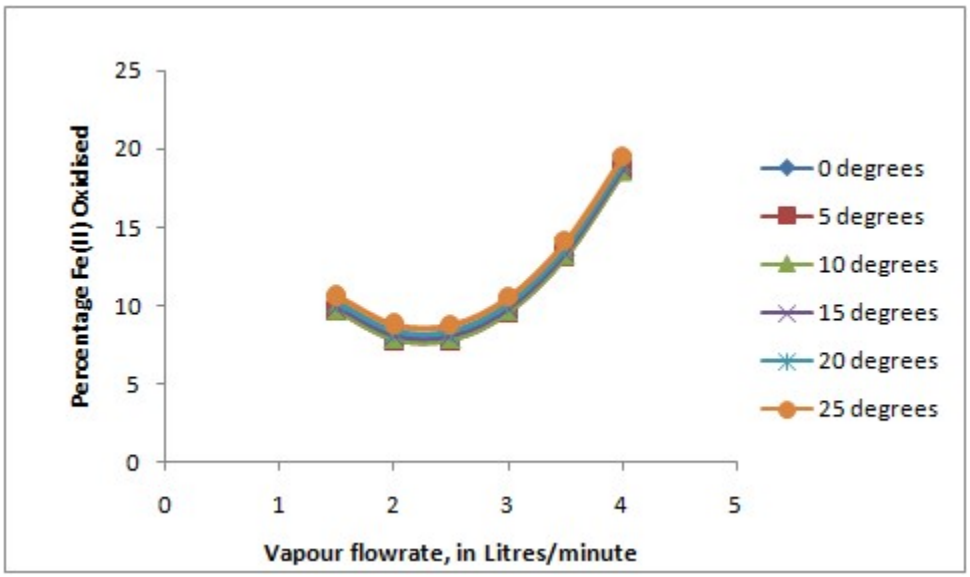

Figure 4.32: Effect of vapour flowrates and angles of tilt on percentage Fe(II) oxidised at a constant liquid flowrate of 4 litres per minute based on quadratic model $y=b_0 + b_1x_1 + b_2x_2 + b_3x_3 + b_4x_1^2 + b_5x_2^2 + b_6x_3^2$

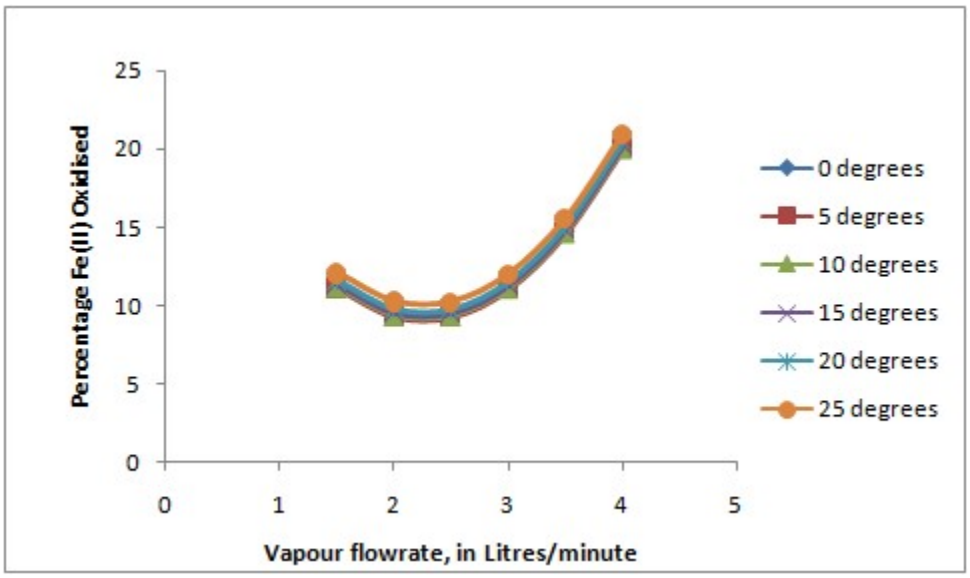

Figure 4.33: Effect of vapour flowrates and angles of tilt on percentage Fe(II) oxidised at a constant liquid flowrate of 5 litres per minute based on quadratic model $y=b_0 + b_1x_1 + b_2x_2 + b_3x_3 + b_4x_1^2 + b_5x_2^2 + b_6x_3^2$

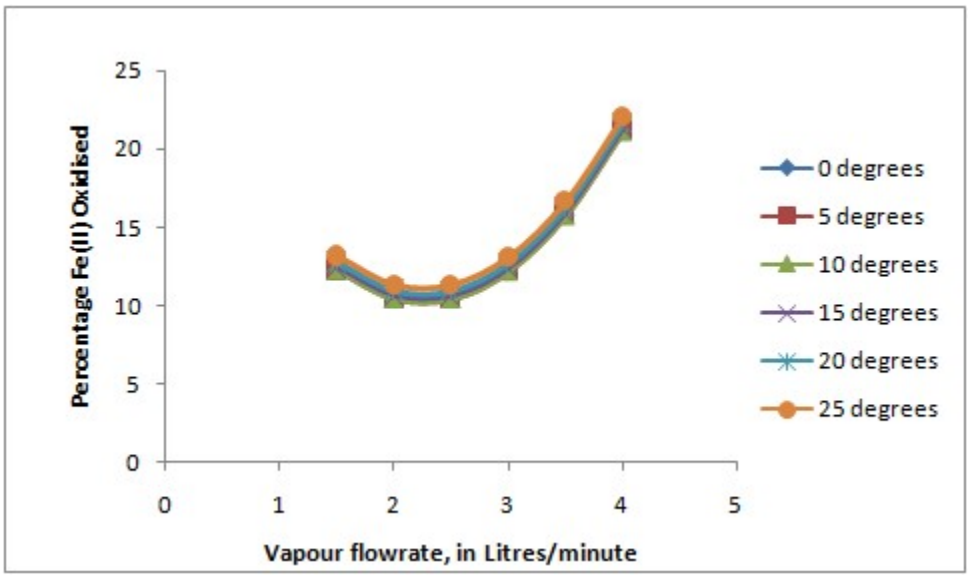

Figure 4.34: Effect of vapour flowrates and angles of tilt on percentage Fe(II) oxidised at a constant liquid flowrate of 6 litres per minute based on quadratic model $y=b_0 + b_1x_1 + b_2x_2 + b_3x_3 + b_4x_1^2 + b_5x_2^2 + b_6x_3^2$

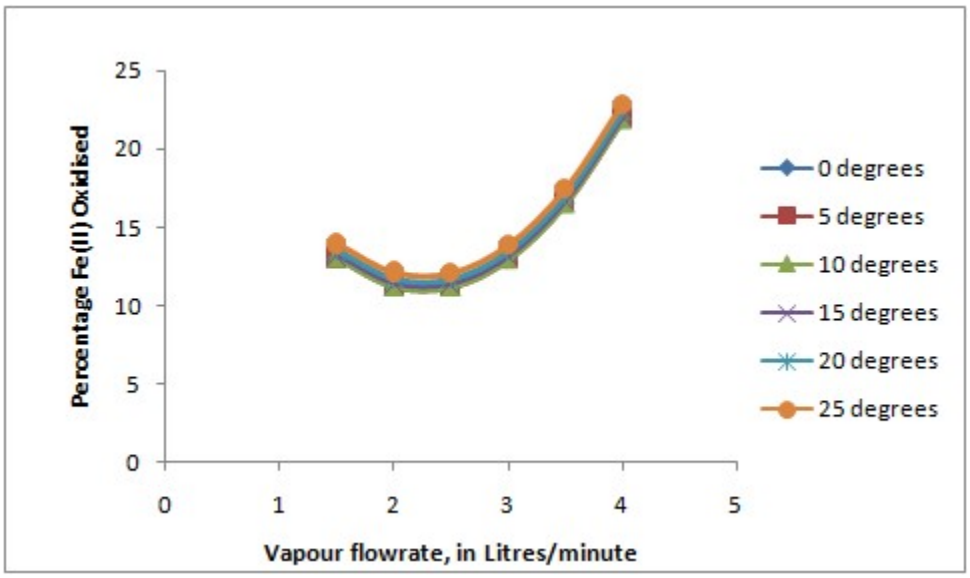

Figure 4.35: Effect of vapour flowrates and angles of tilt on percentage Fe(II) oxidised at a constant liquid flowrate of 7 litres per minute based on quadratic model $y=b_0 + b_1x_1 + b_2x_2 + b_3x_3 + b_4x_1^2 + b_5x_2^2 + b_6x_3^2$

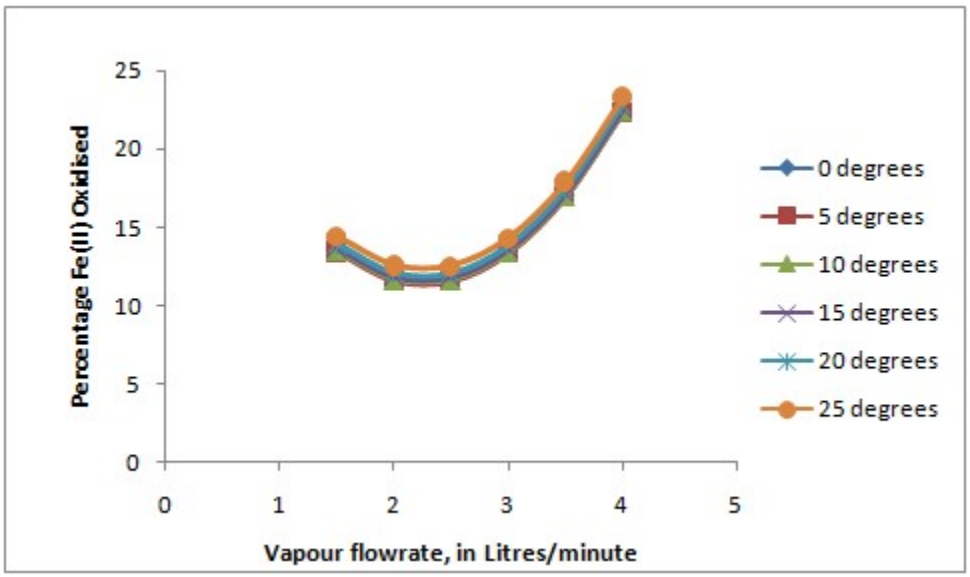

Figure 4.36: Effect of vapour flowrates and angles of tilt on percentage Fe(II) oxidised at a constant liquid flowrate of 8 litres per minute based on quadratic model $y=b_0 + b_1x_1 + b_2x_2 + b_3x_3 + b_4x_1^2 + b_5x_2^2 + b_6x_3^2$

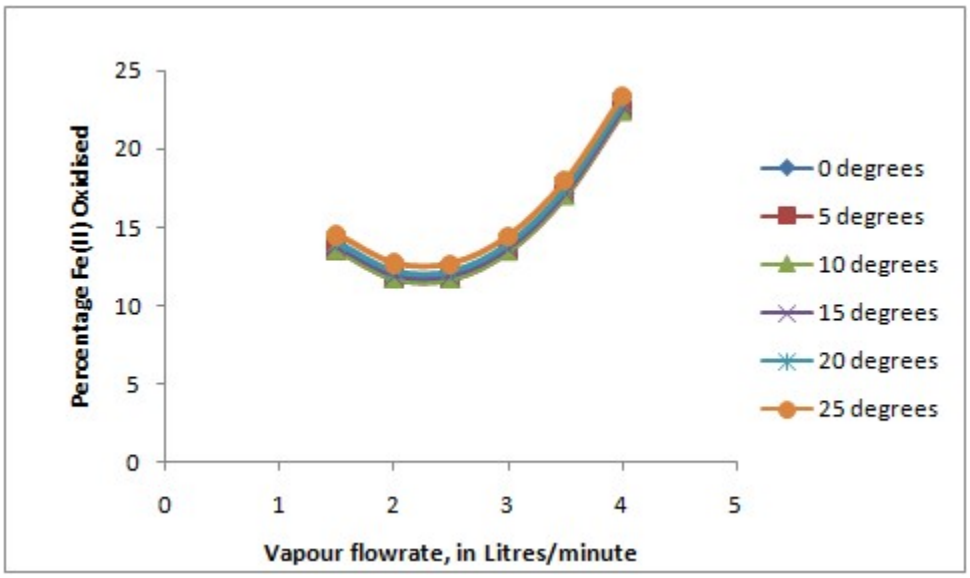

Figure 4.37: Effect of vapour flowrates and angles of tilt on percentage Fe(II) oxidised at a constant liquid flowrate of 9 litres per minute based on quadratic model $y=b_0 + b_1x_1 + b_2x_2 + b_3x_3 + b_4x_1^2 + b_5x_2^2 + b_6x_3^2$

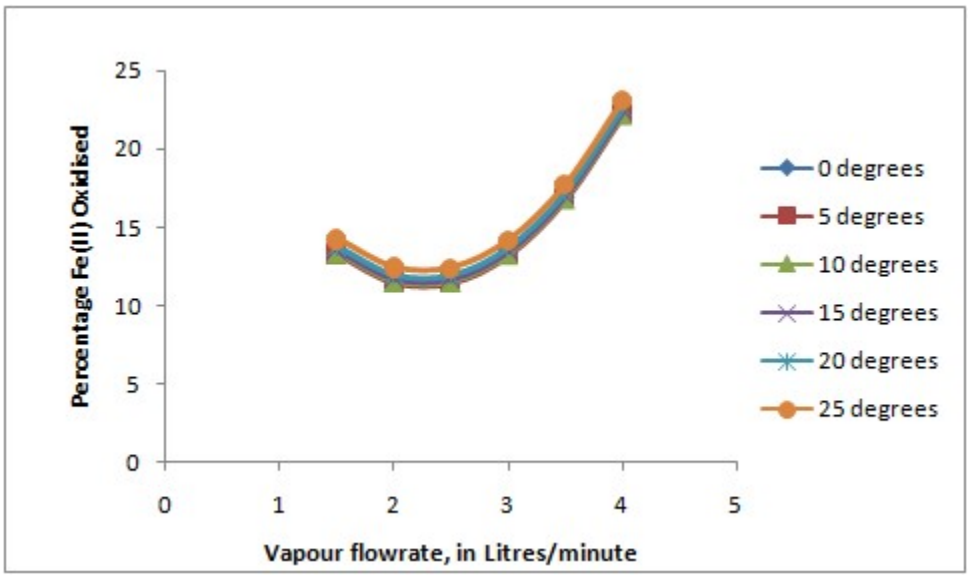

Figure 4.38: Effect of vapour flowrates and angles of tilt on percentage Fe(II) oxidised at a constant liquid flowrate of 10 litres per minute based on quadratic model $y=b_0 + b_1x_1 + b_2x_2 + b_3x_3 + b_4x_1^2 + b_5x_2^2 + b_6x_3^2$

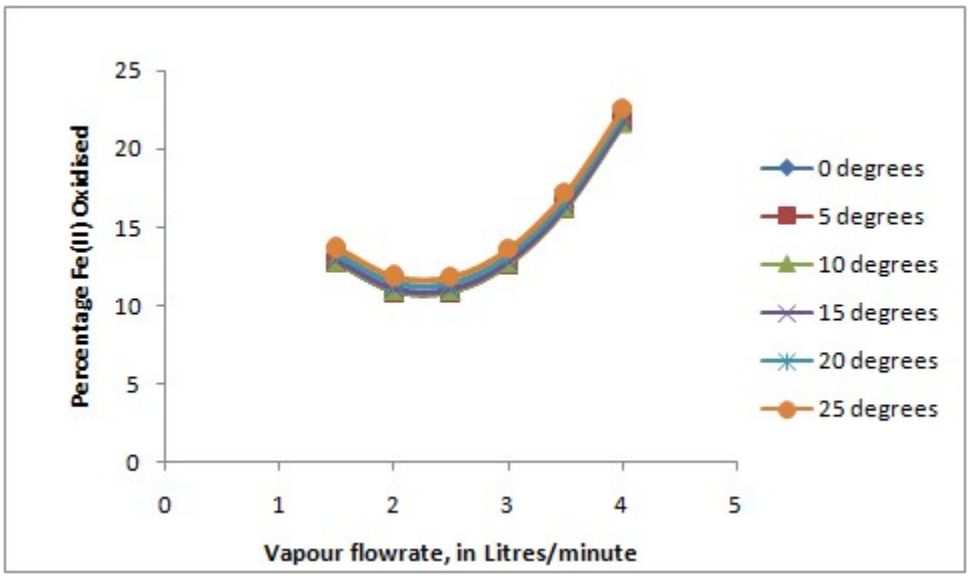

Figure 4.39: Effect of vapour flowrates and angles of tilt on percentage Fe(II) oxidised at a constant liquid flowrate of 11 litres per minute based on quadratic model $y=b_0 + b_1x_1 + b_2x_2 + b_3x_3 + b_4x_1^2 + b_5x_2^2 + b_6x_3^2$

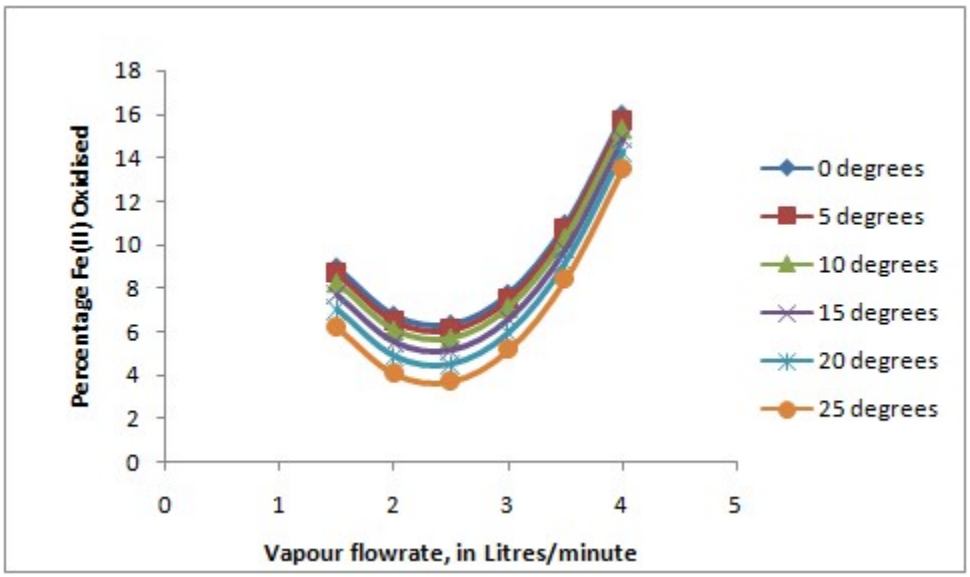

Figure 4.40: Effect of vapour flowrates and angles of tilt on percentage Fe(II) oxidised at a constant liquid flowrate of 3 litres per minute based on quadratic model $y=b_0 + b_1x_1 + b_2x_2 + b_3x_3 + b_4x_1x_2 + b_5x_1x_3 + b_6x_2x_3 + b_7x_1^2 + b_8x_2^2 + b_9x_3^2$

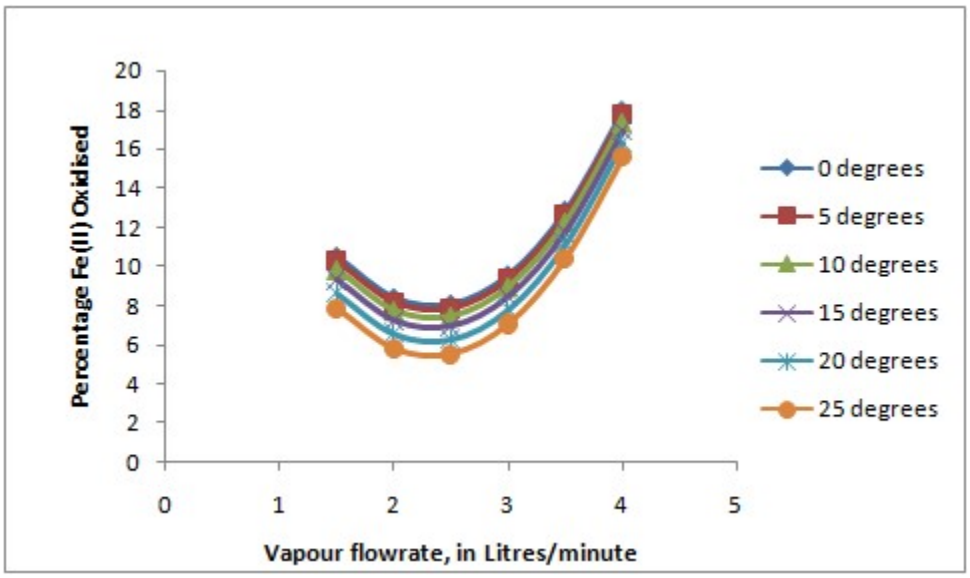

Figure 4.41: Effect of vapour flowrates and angles of tilt on percentage Fe(II) oxidised at a constant liquid flowrate of 4 litres per minute based on quadratic model $y=b_0 + b_1x_1 + b_2x_2 + b_3x_3 + b_4x_1x_2 + b_5x_1x_3 + b_6x_2x_3 + b_7x_1^2 + b_8x_2^2 + b_9x_3^2$

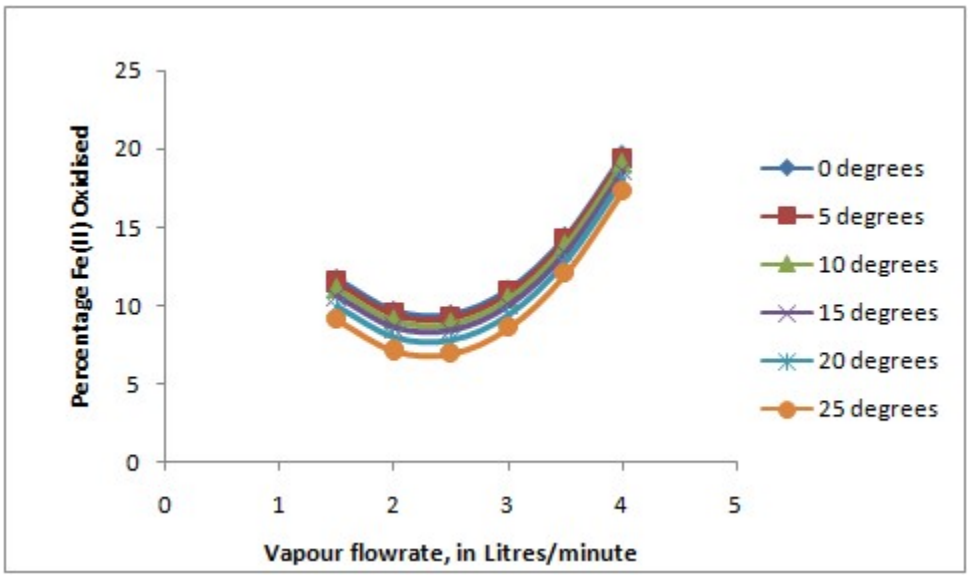

Figure 4.42: Effect of vapour flowrates and angles of tilt on percentage Fe(II) oxidised at a constant liquid flowrate of 5 litres per minute based on quadratic model $y=b_0 + b_1x_1 + b_2x_2 + b_3x_3 + b_4x_1x_2 + b_5x_1x_3 + b_6x_2x_3 + b_7x_1^2 + b_8x_2^2 + b_9x_3^2$

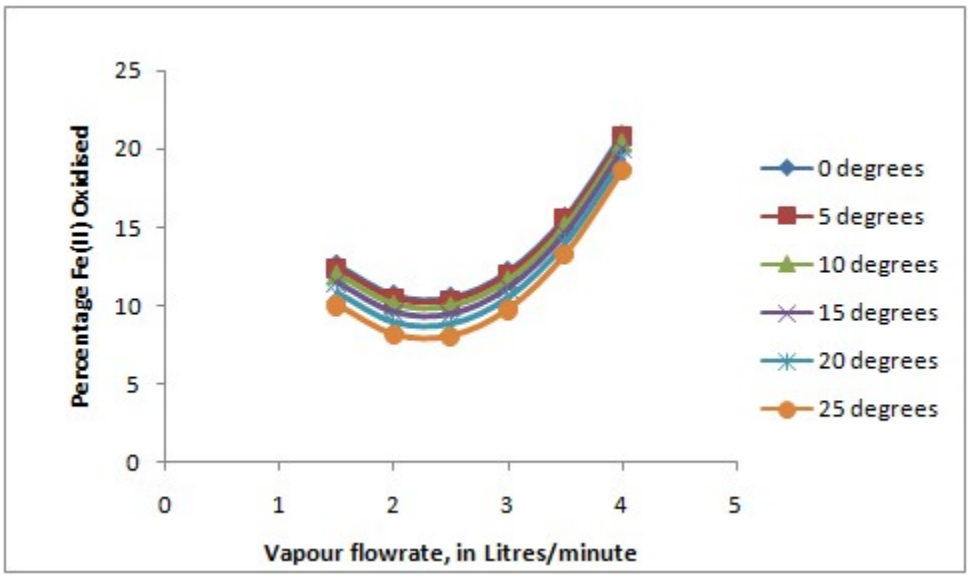

Figure 4.43: Effect of vapour flowrates and angles of tilt on percentage Fe(II) oxidised at a constant liquid flowrate of 6 litres per minute based on quadratic model $y=b_0 + b_1x_1 + b_2x_2 + b_3x_3 + b_4x_1x_2 + b_5x_1x_3 + b_6x_2x_3 + b_7x_1^2 + b_8x_2^2 + b_9x_3^2$

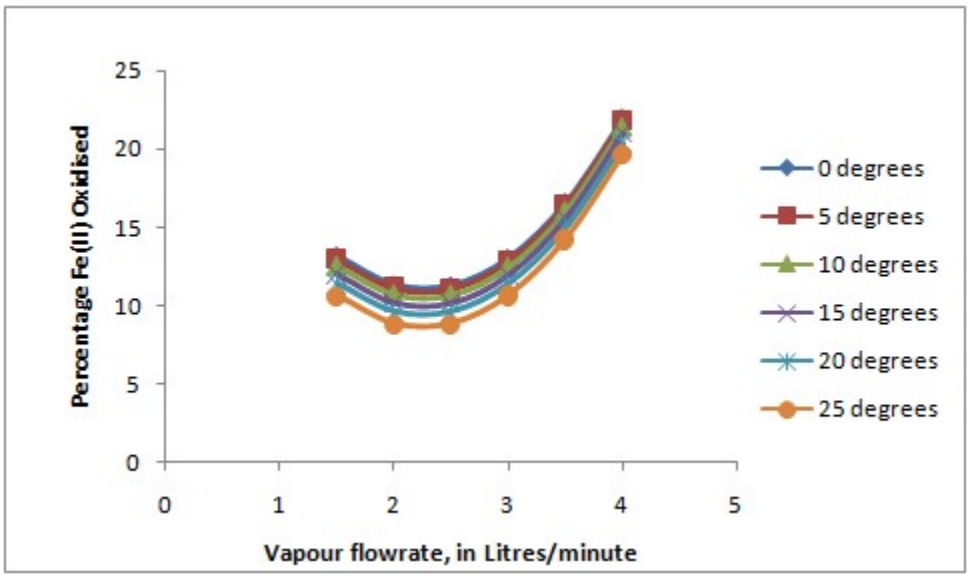

Figure 4.44: Effect of vapour flowrates and angles of tilt on percentage Fe(II) oxidised at a constant liquid flowrate of 7 litres per minute based on quadratic model $y=b_0 + b_1x_1 + b_2x_2 + b_3x_3 + b_4x_1x_2 + b_5x_1x_3 + b_6x_2x_3 + b_7x_1^2 + b_8x_2^2 + b_9x_3^2$

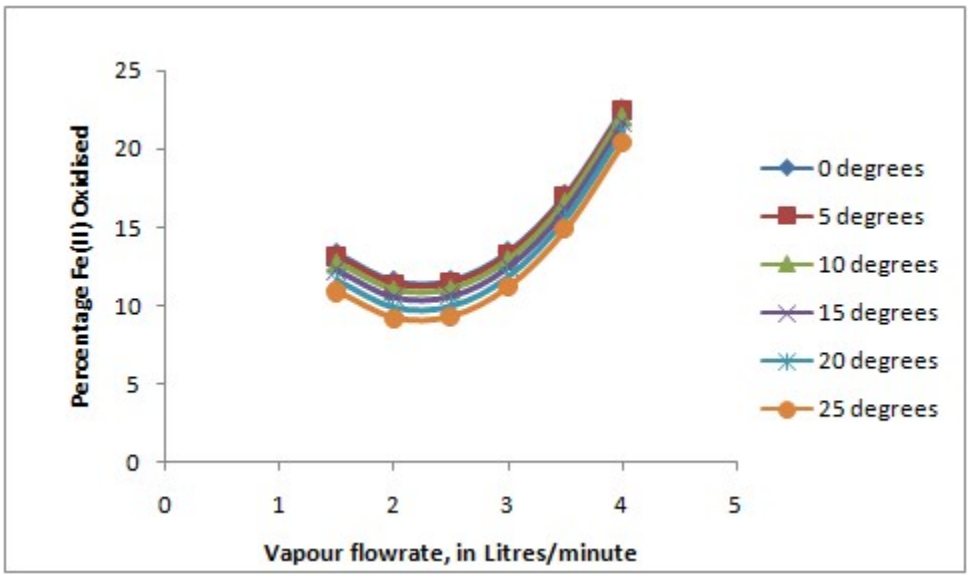

Figure 4.45: Effect of vapour flowrates and angles of tilt on percentage Fe(II) oxidised at a constant liquid flowrate of 8 litres per minute based on quadratic model $y=b_0 + b_1x_1 + b_2x_2 + b_3x_3 + b_4x_1x_2 + b_5x_1x_3 + b_6x_2x_3 + b_7x_1^2 + b_8x_2^2 + b_9x_3^2$

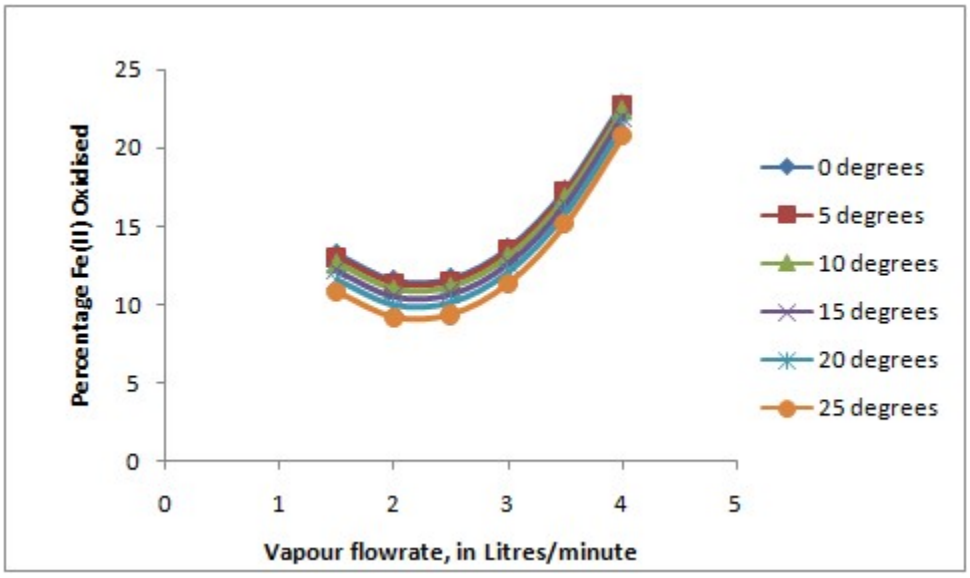

Figure 4.46: Effect of vapour flowrates and angles of tilt on percentage Fe(II) oxidised at a constant liquid flowrate of 9 litres per minute based on quadratic model $y=b_0 + b_1x_1 + b_2x_2 + b_3x_3 + b_4x_1x_2 + b_5x_1x_3 + b_6x_2x_3 + b_7x_1^2 + b_8x_2^2 + b_9x_3^2$

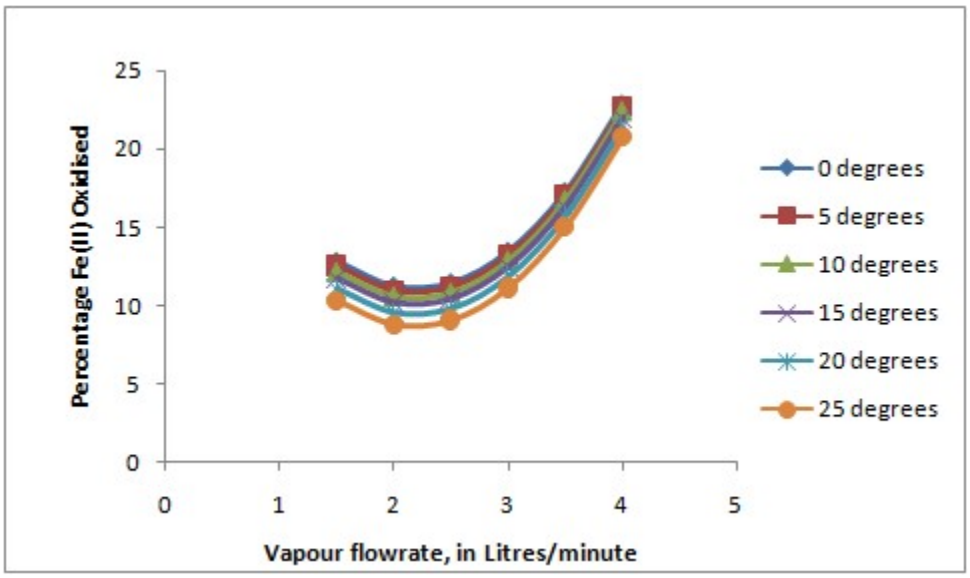

Figure 4.47: Effect of vapour flowrates and angles of tilt on percentage Fe(II) oxidised at a constant liquid flowrate of 10 litres per minute based on quadratic model $y=b_0 + b_1x_1 + b_2x_2 + b_3x_3 + b_4x_1x_2 + b_5x_1x_3 + b_6x_2x_3 + b_7x_1^2 + b_8x_2^2 + b_9x_3^2$

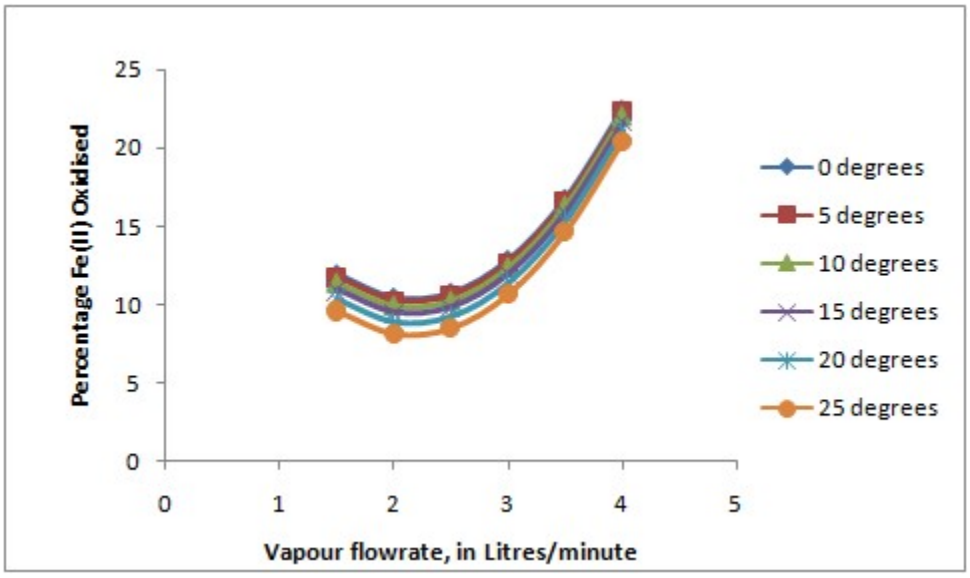

Figure 4.48: Effect of vapour flowrates and angles of tilt on percentage Fe(II) oxidised at a constant liquid flowrate of 11 litres per minute based on quadratic model $y=b_0 + b_1x_1 + b_2x_2 + b_3x_3 + b_4x_1x_2 + b_5x_1x_3 + b_6x_2x_3 + b_7x_1^2 + b_8x_2^2 + b_9x_3^2$

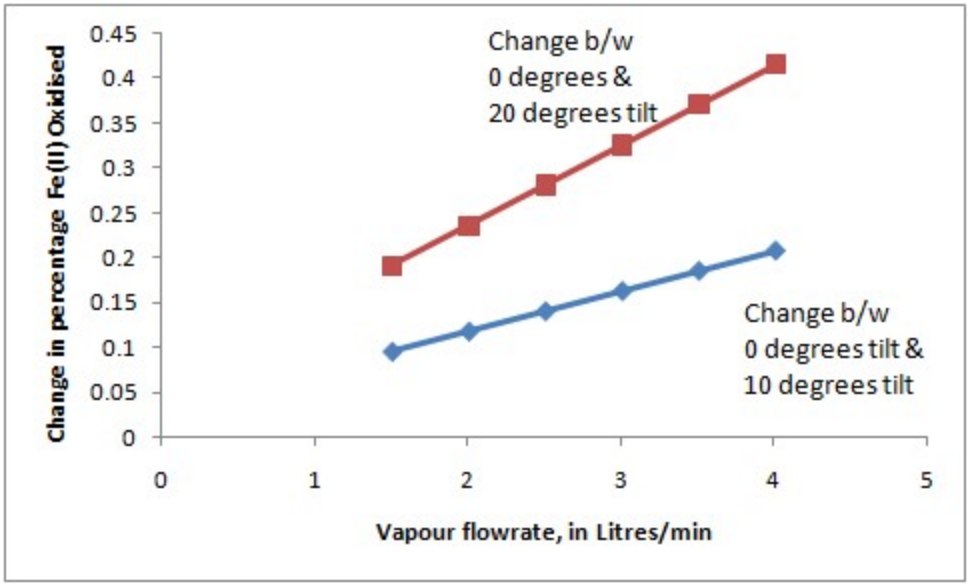

Figure 4.49: Impact of changes in angles of tilt on percentage Fe(II) oxidised at a constant liquid flowrate of 3 litres per minute based on linear model $y=b_0 + b_1x_1 + b_2x_2 + b_3x_3 + b_4x_1x_2 + b_5x_1x_3 + b_6x_2x_3$

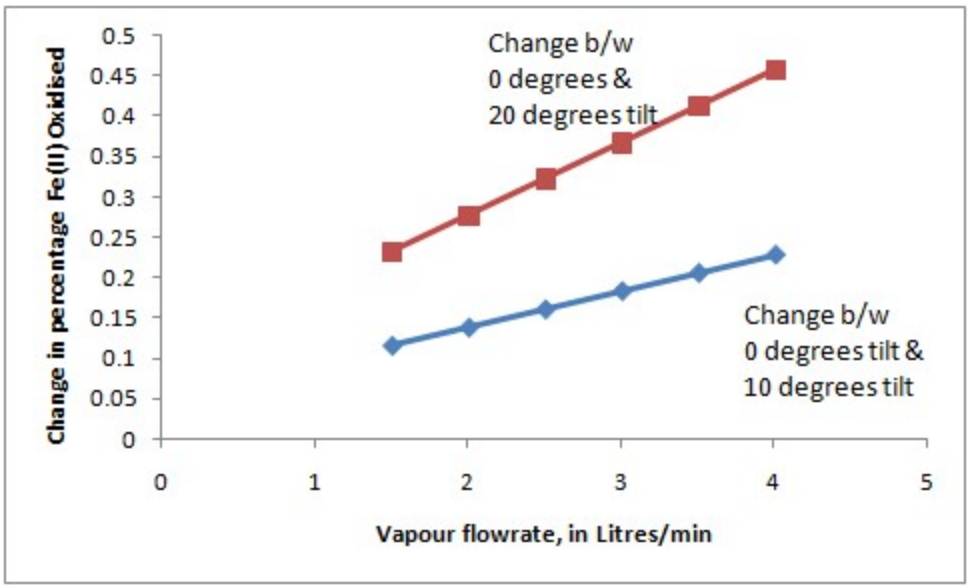

Figure 4.50: Impact of changes in angles of tilt on percentage Fe(II) oxidised at a constant liquid flowrate of 4 litres per minute based on linear model $y=b_0 + b_1x_1 + b_2x_2 + b_3x_3 + b_4x_1x_2 + b_5x_1x_3 + b_6x_2x_3$

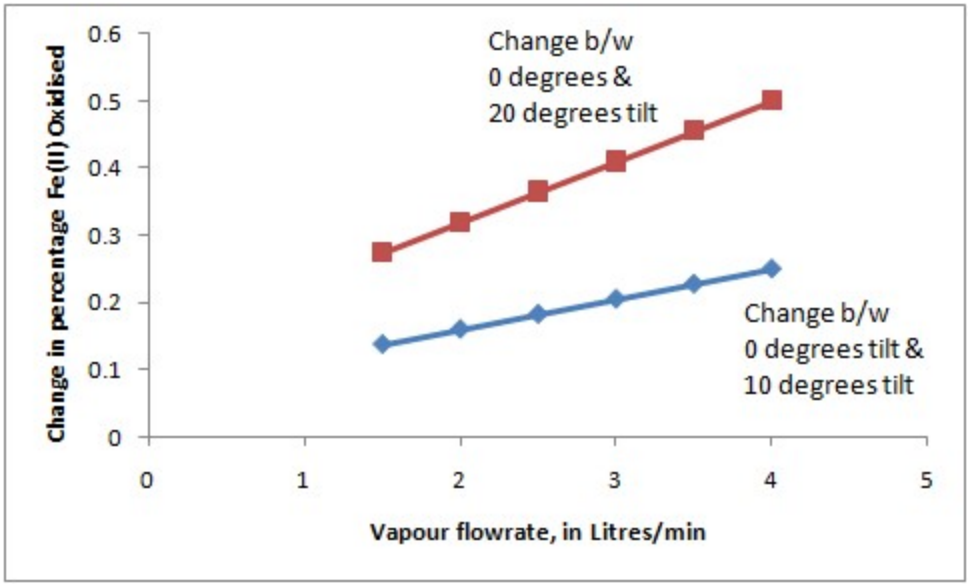

Figure 4.51: Impact of changes in angles of tilt on percentage Fe(II) oxidised at a constant liquid flowrate of 5 litres per minute based on linear model $y=b_0 + b_1x_1 + b_2x_2 + b_3x_3 + b_4x_1x_2 + b_5x_1x_3 + b_6x_2x_3$

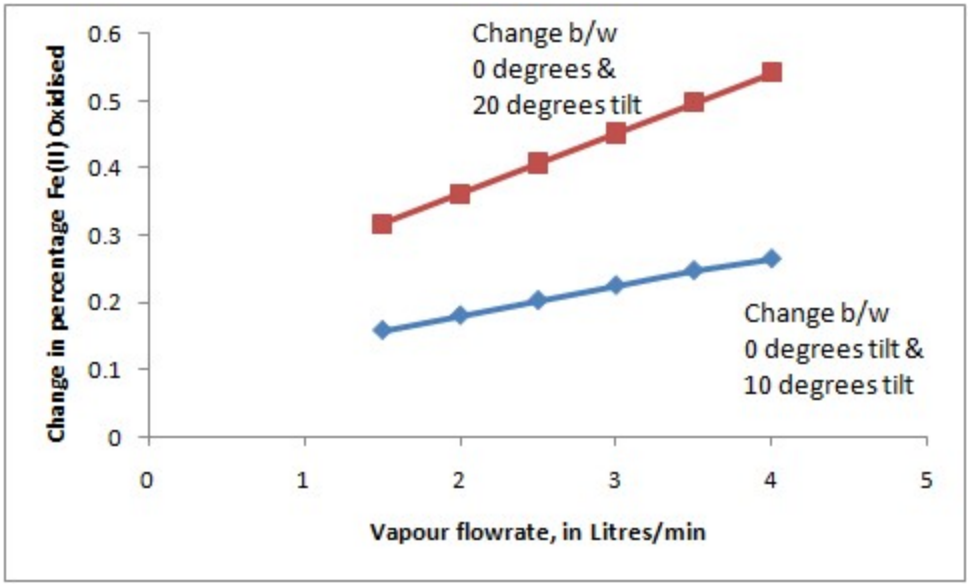

Figure 4.52: Impact of changes in angles of tilt on percentage Fe(II) oxidised at a constant liquid flowrate of 6 litres per minute based on linear model $y=b_0 + b_1x_1 + b_2x_2 + b_3x_3 + b_4x_1x_2 + b_5x_1x_3 + b_6x_2x_3$

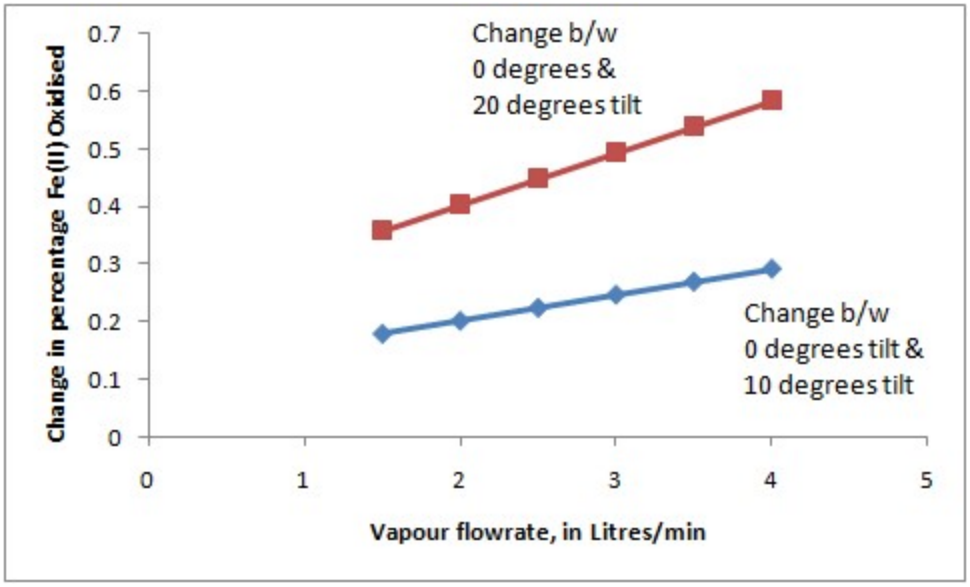

Figure 4.53: Impact of changes in angles of tilt on percentage Fe(II) oxidised at a constant liquid flowrate of 7 litres per minute based on linear model $y=b_0 + b_1x_1 + b_2x_2 + b_3x_3 + b_4x_1x_2 + b_5x_1x_3 + b_6x_2x_3$

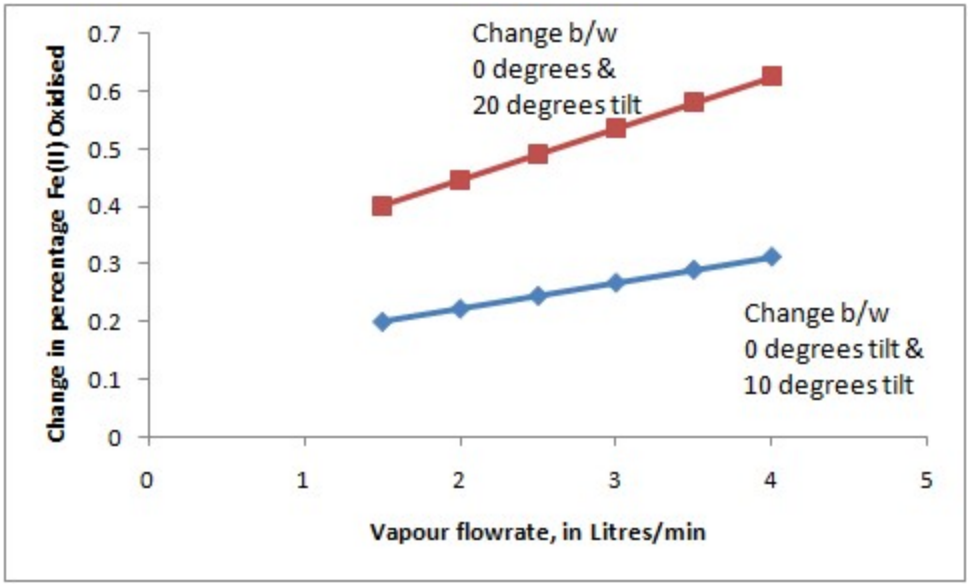

Figure 4.54: Impact of changes in angles of tilt on percentage Fe(II) oxidised at a constant liquid flowrate of 8 litres per minute based on linear model $y=b_0 + b_1x_1 + b_2x_2 + b_3x_3 + b_4x_1x_2 + b_5x_1x_3 + b_6x_2x_3$

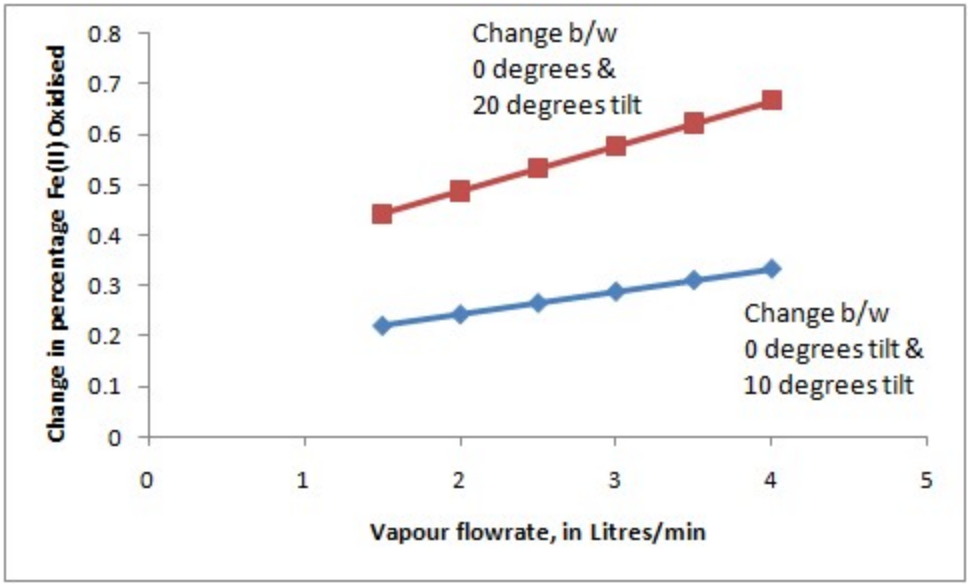

Figure 4.55: Impact of changes in angles of tilt on percentage Fe(II) oxidised at a constant liquid flowrate of 9 litres per minute based on linear model $y=b_0 + b_1x_1 + b_2x_2 + b_3x_3 + b_4x_1x_2 + b_5x_1x_3 + b_6x_2x_3$

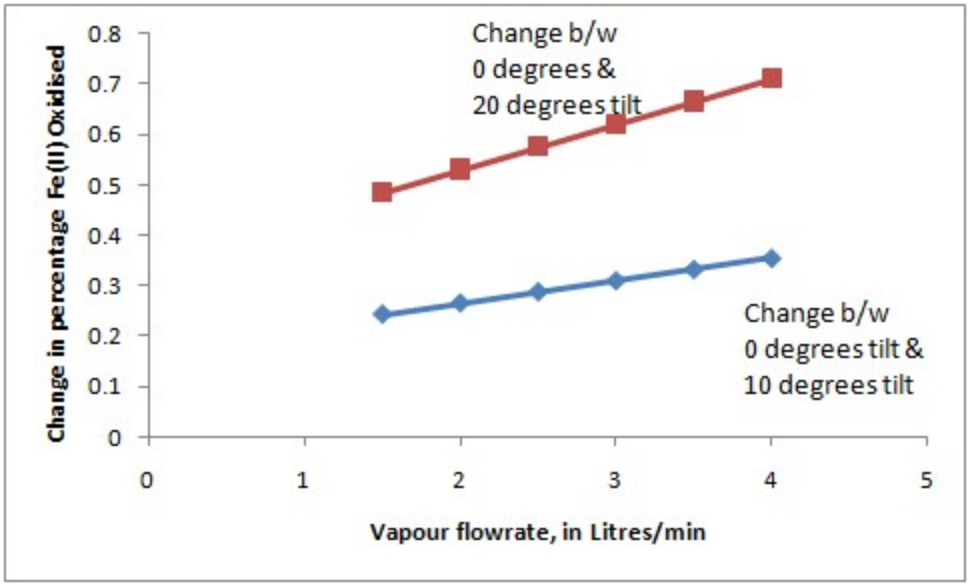

Figure 4.56: Impact of changes in angles of tilt on percentage Fe(II) oxidised at a constant liquid flowrate of 10 litres per minute based on linear model $y=b_0 + b_1x_1 + b_2x_2 + b_3x_3 + b_4x_1x_2 + b_5x_1x_3 + b_6x_2x_3$

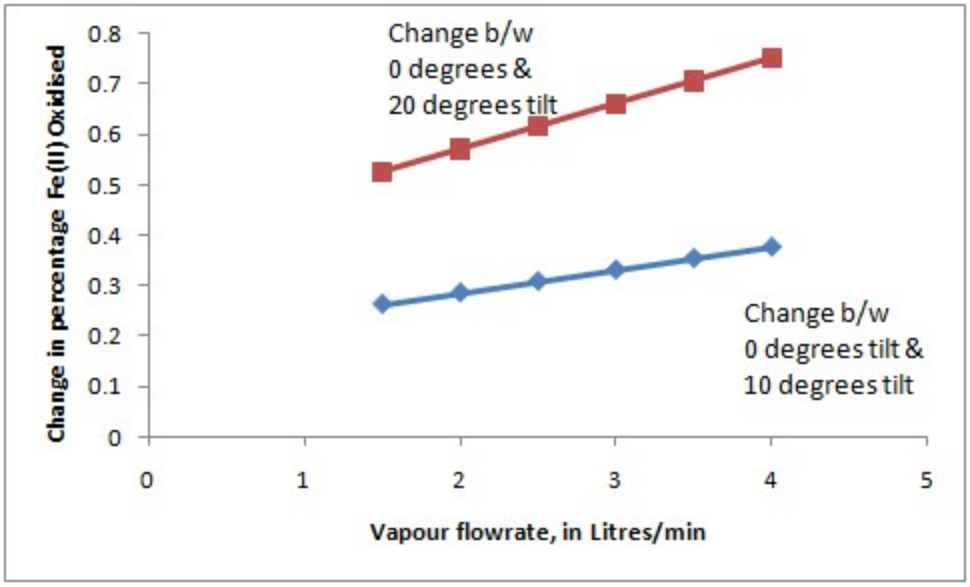

Figure 4.57: Impact of changes in angles of tilt on percentage Fe(II) oxidised at a constant liquid flowrate of 11 litres per minute based on linear model $y=b_0 + b_1x_1 + b_2x_2 + b_3x_3 + b_4x_1x_2 + b_5x_1x_3 + b_6x_2x_3$

4.1.7 VISUAL OBSERVATIONS OF THE FLUID FLOW PATTERN OF THE NOVEL TRAY COLUMN

The following flow behaviour was observed for the novel tray column during operation. The indicated values show the average observations although slight variations occurred from these mean values during operation.

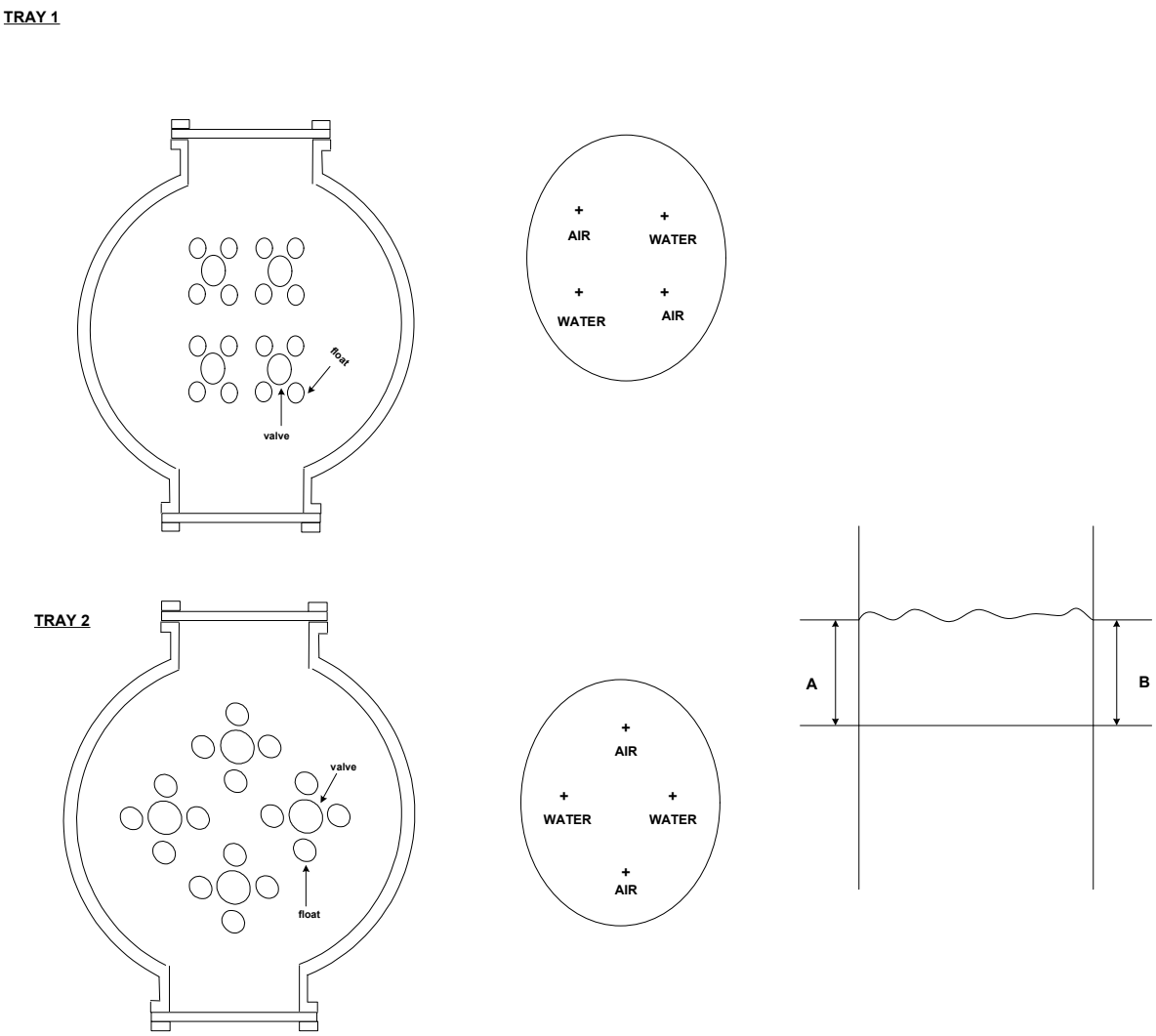

TRAY 1: A= 60mm, B = 60mm

TRAY 2: A=65mm, B= 65mm

Figure 4.58: Flow Behaviour at 0^0 Column Tilt, Liquid Rate of 5 Litres per Minute, and Vapour Rate of 3.2 Litres Per Minute.

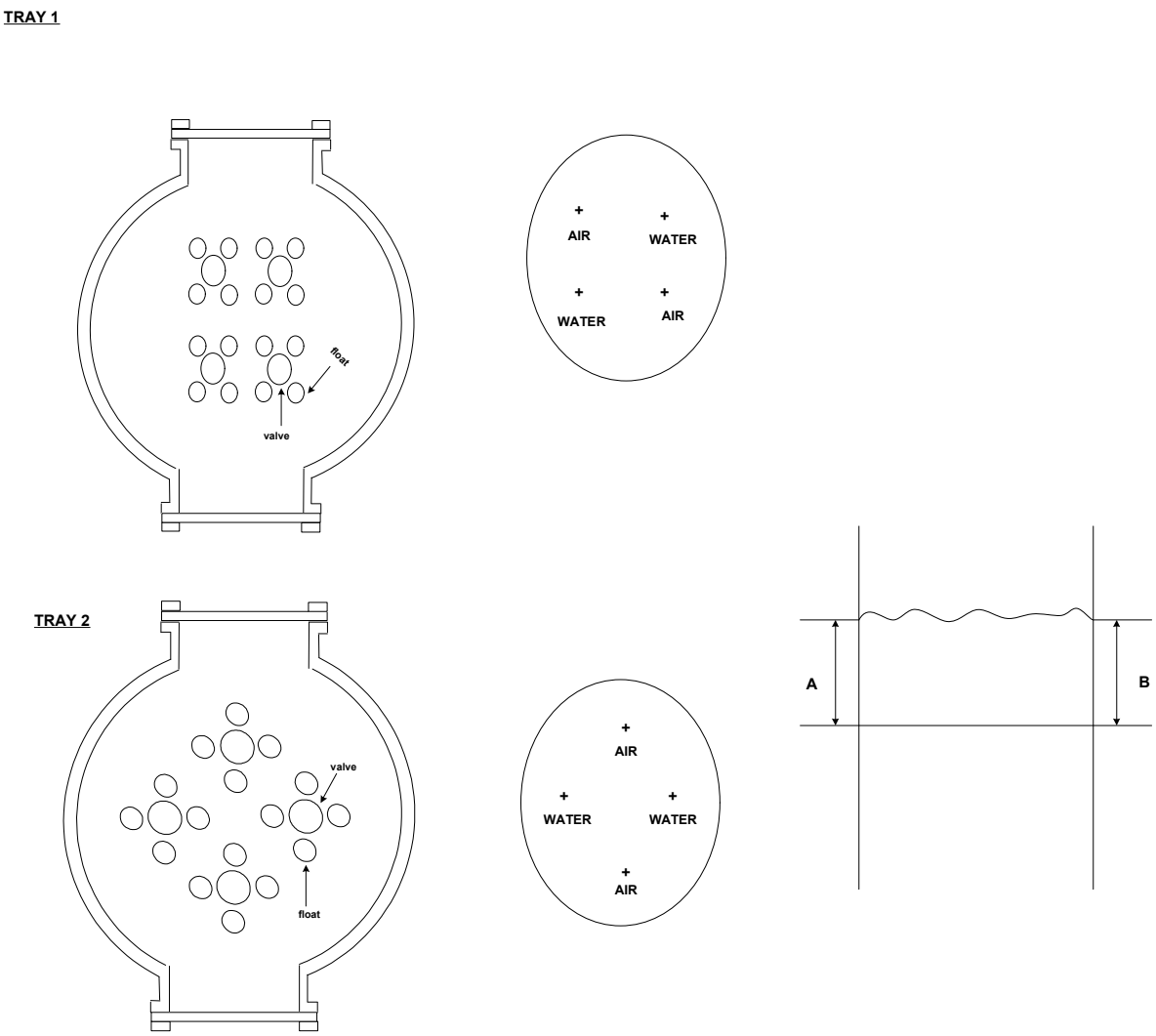

TRAY 1: A= 75mm, B = 75mm

TRAY 2: A=80mm, B= 80mm

Figure 4.59: Flow Behaviour at 0^0 Column Tilt, Liquid Rate of 9 Litres per Minute, and Vapour Rate of 3.2 Litres Per Minute.

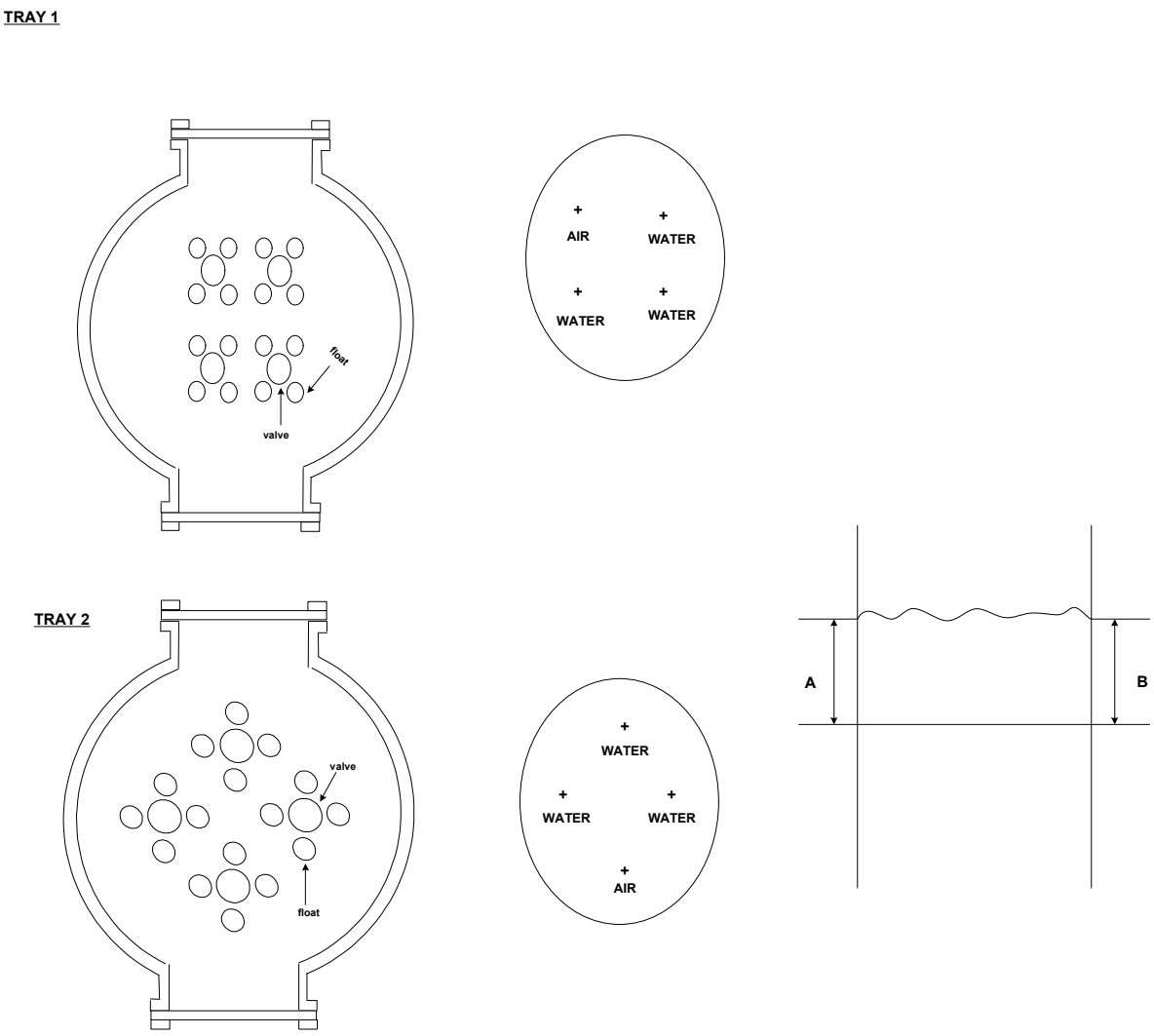

TRAY 1: A= 65mm, B = 65mm

TRAY 2: A=70mm, B= 70mm

Figure 4.60: Flow Behaviour at 0^0 Column Tilt, Liquid Rate of 9 Litres per Minute, and Vapour Rate of 2.2 Litres Per Minute.

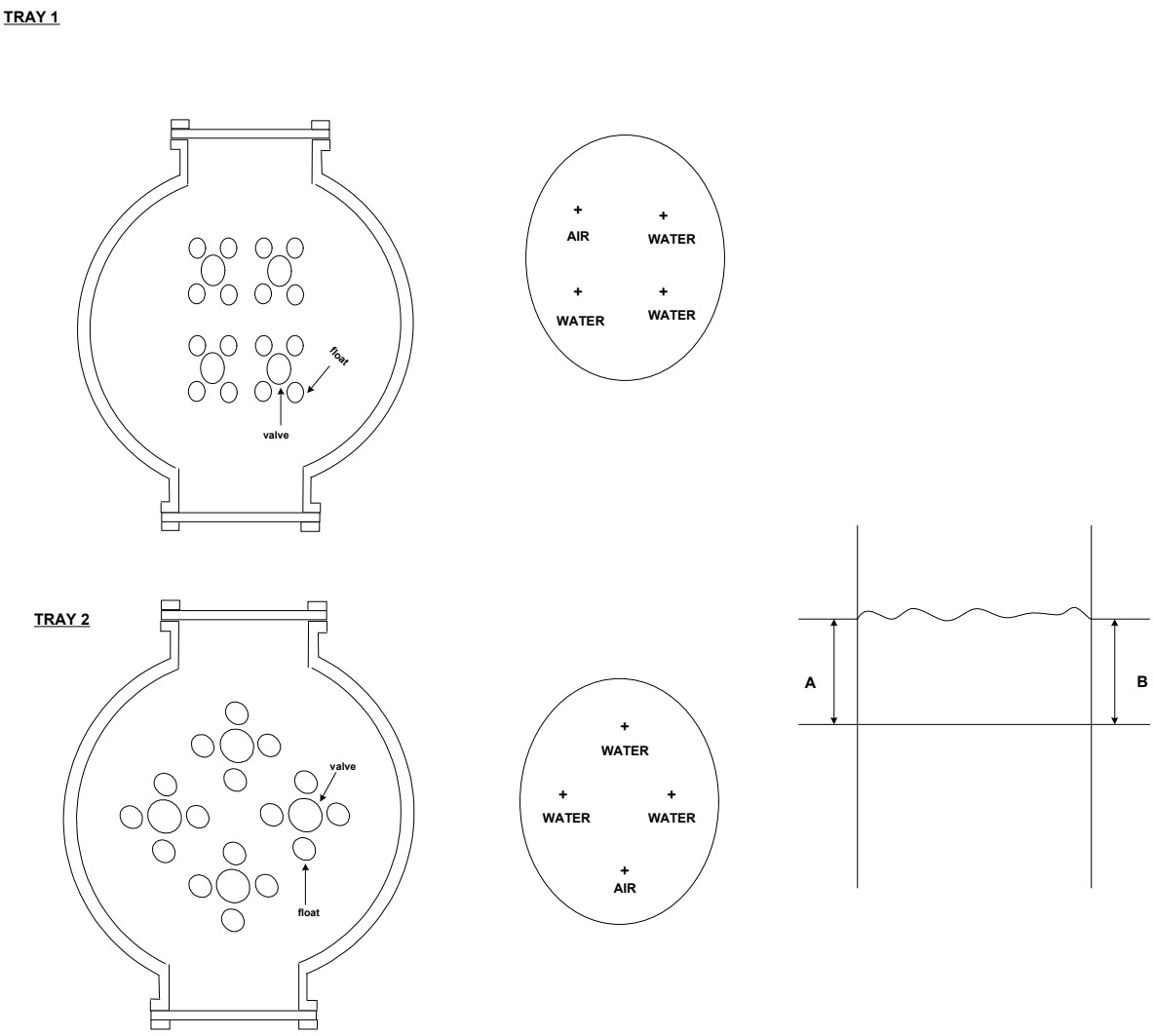

TRAY 1: A= 65mm, B = 65mm

TRAY 2: A=70mm, B= 70mm

Figure 4.61: Flow Behaviour at 0^0 Column Tilt, Liquid Rate of 5 Litres per Minute, and Vapour Rate of 2.2 Litres Per Minute.

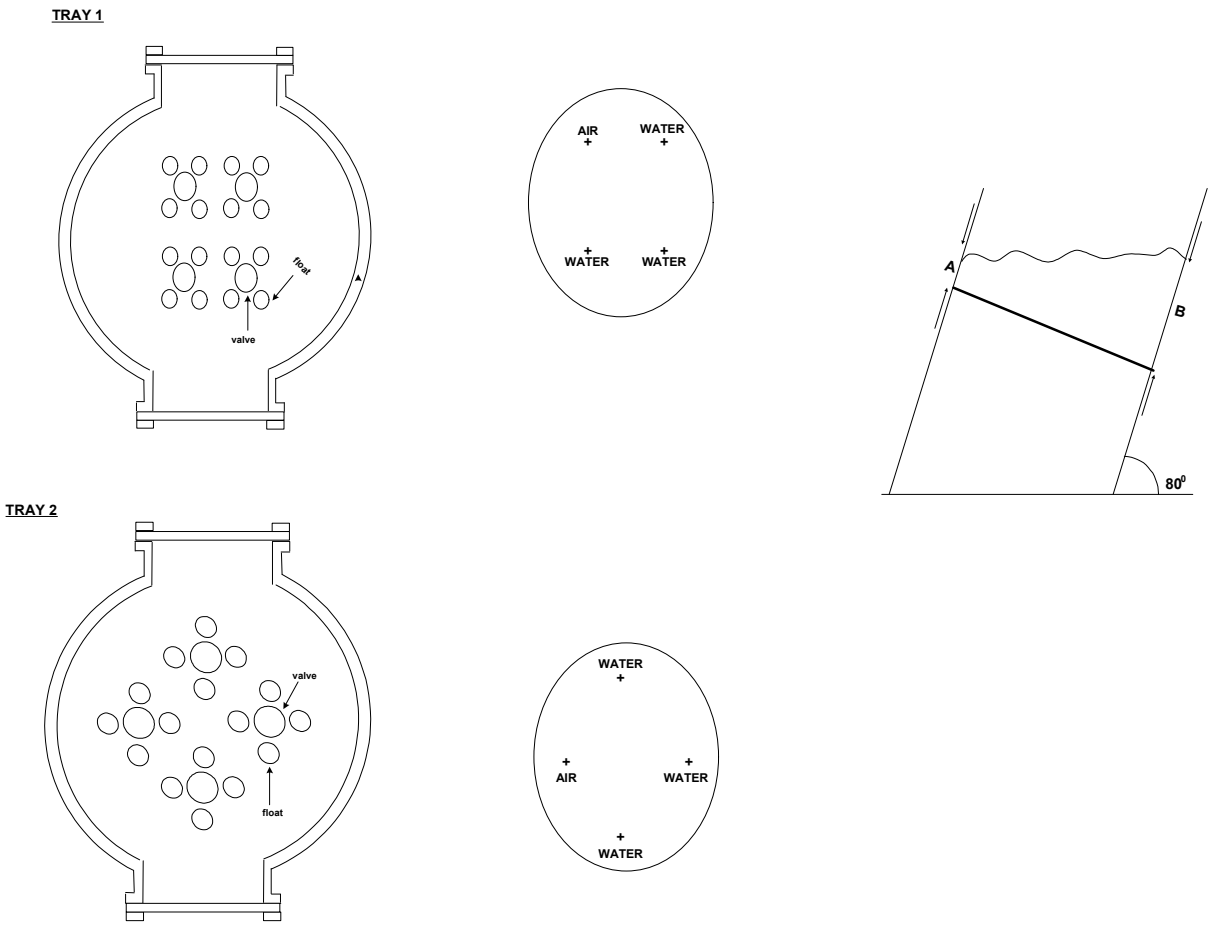

TRAY 1: A= 50mm, B = 80mm

TRAY 2: A=55mm, B= 85mm

Figure 4.62: Flow Behaviour at 10^0 Column Tilt, Liquid Rate of 7 Litres per Minute, and Vapour Rate of 1.9 Litres Per Minute.

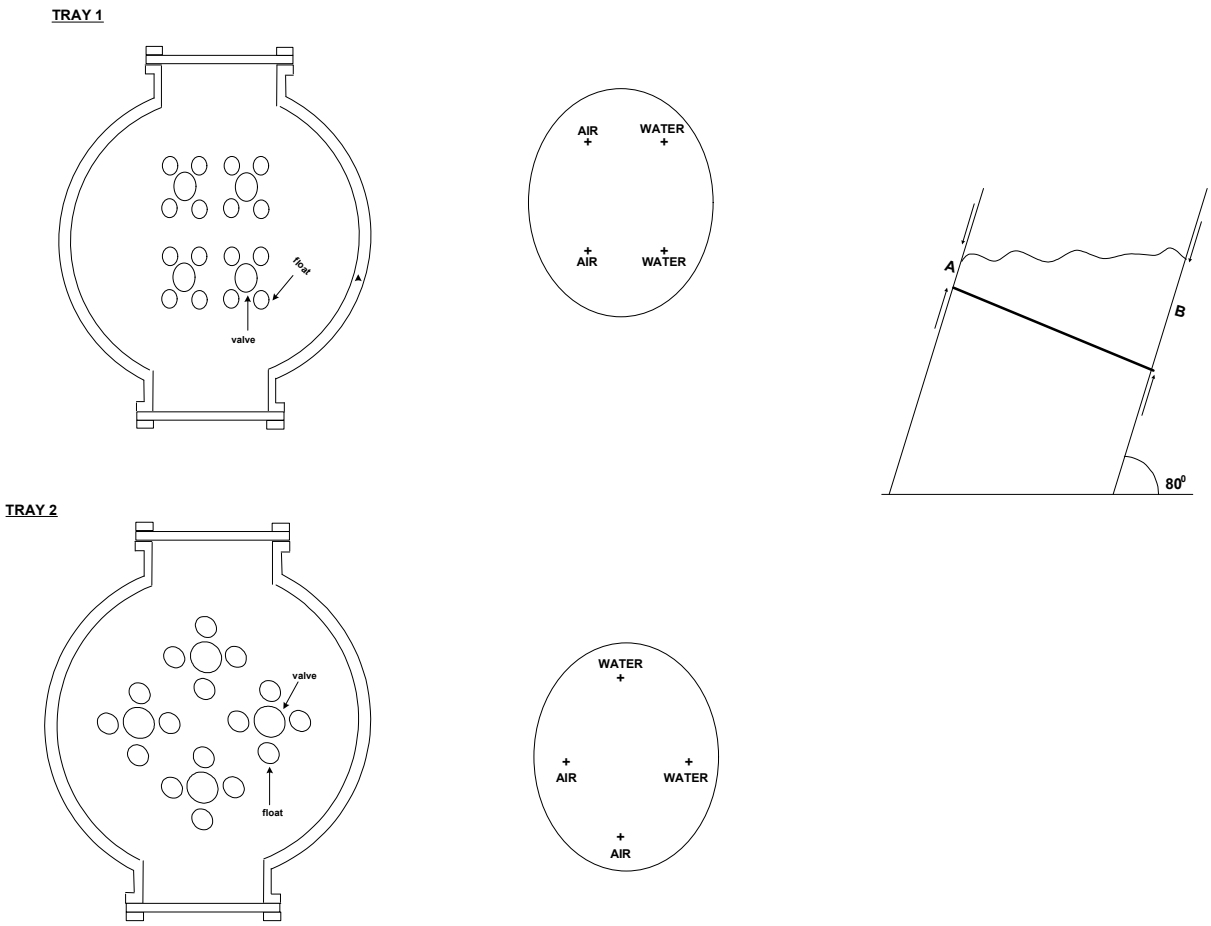

TRAY 1: A= 50mm, B = 80mm

TRAY 2: A=55mm, B= 85mm

Figure 4.63: Flow Behaviour at 10^0 Column Tilt, Liquid Rate of 7 Litres per Minute, and Vapour Rate of 3.5 Litres Per Minute.

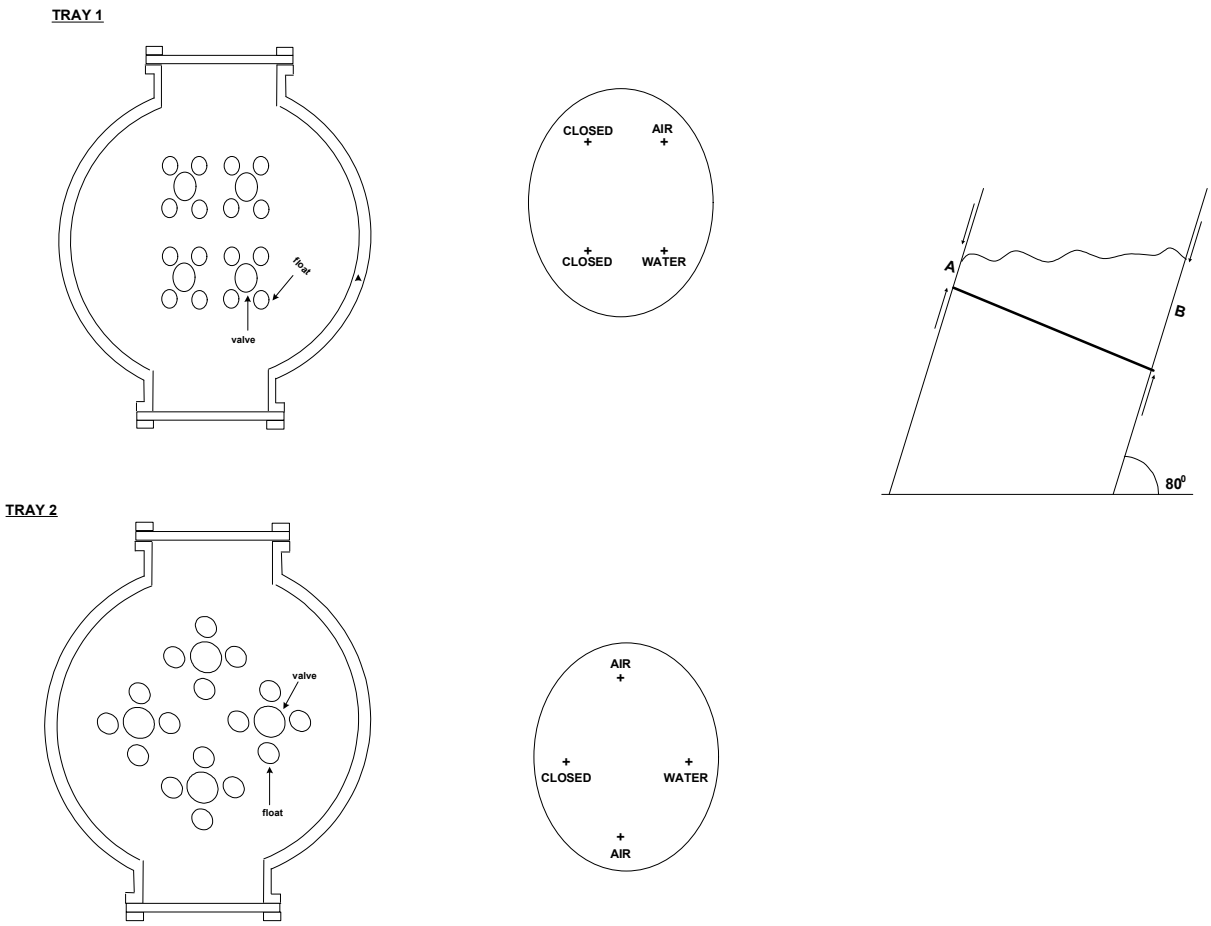

TRAY 1: A= 30mm, B = 60mm

TRAY 2: A=35mm, B= 65mm

Figure 4.64: Flow Behaviour at 10^0 Column Tilt, Liquid Rate of 3.6 Litres per Minute, and Vapour Rate of 2.7 Litres Per Minute.

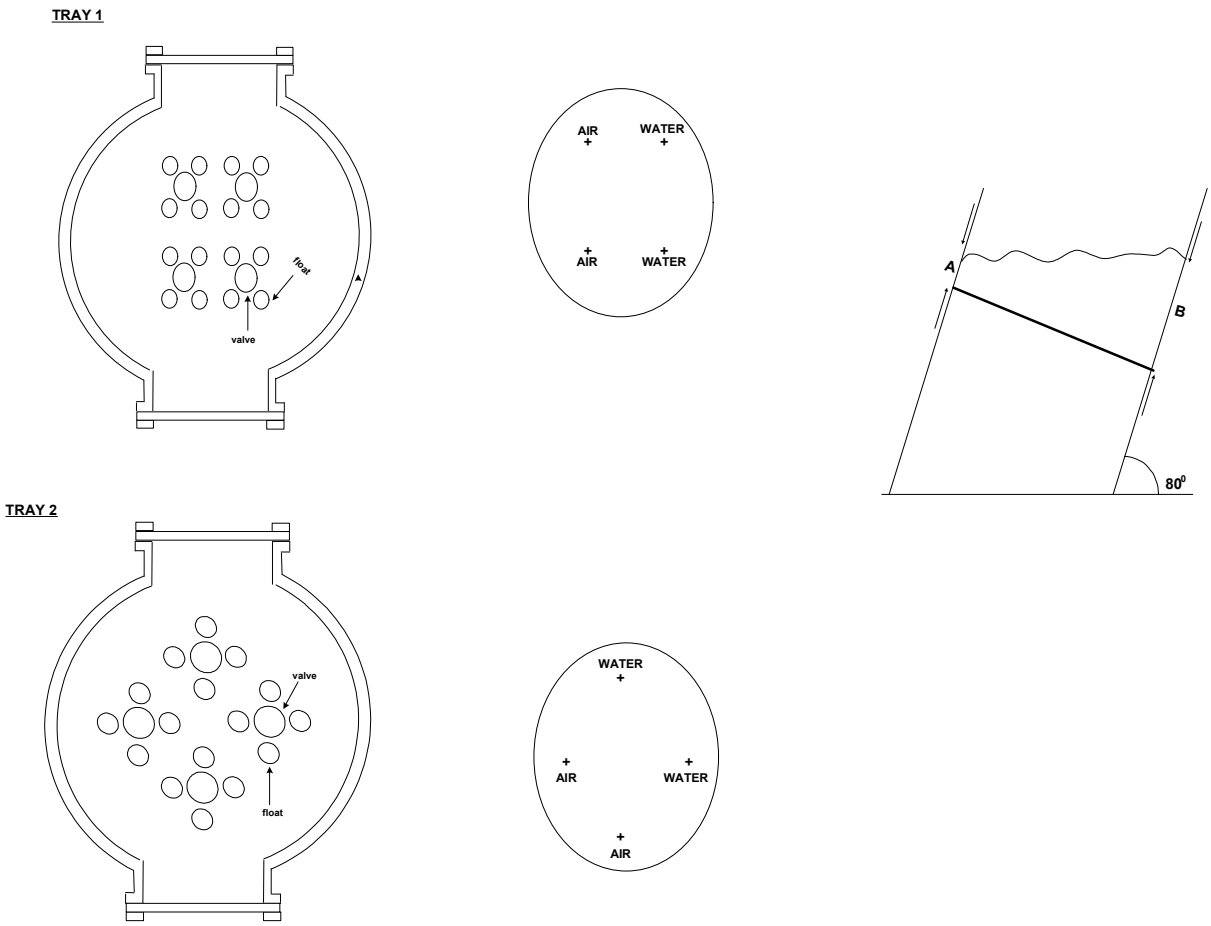

TRAY 1: A= 60mm, B = 90mm

TRAY 2: A=65mm, B= 95mm

Figure 4.65: Flow Behaviour at 10^0 Column Tilt, Liquid Rate of 10.4 Litres per Minute, and Vapour Rate of 2.7 Litres Per Minute.

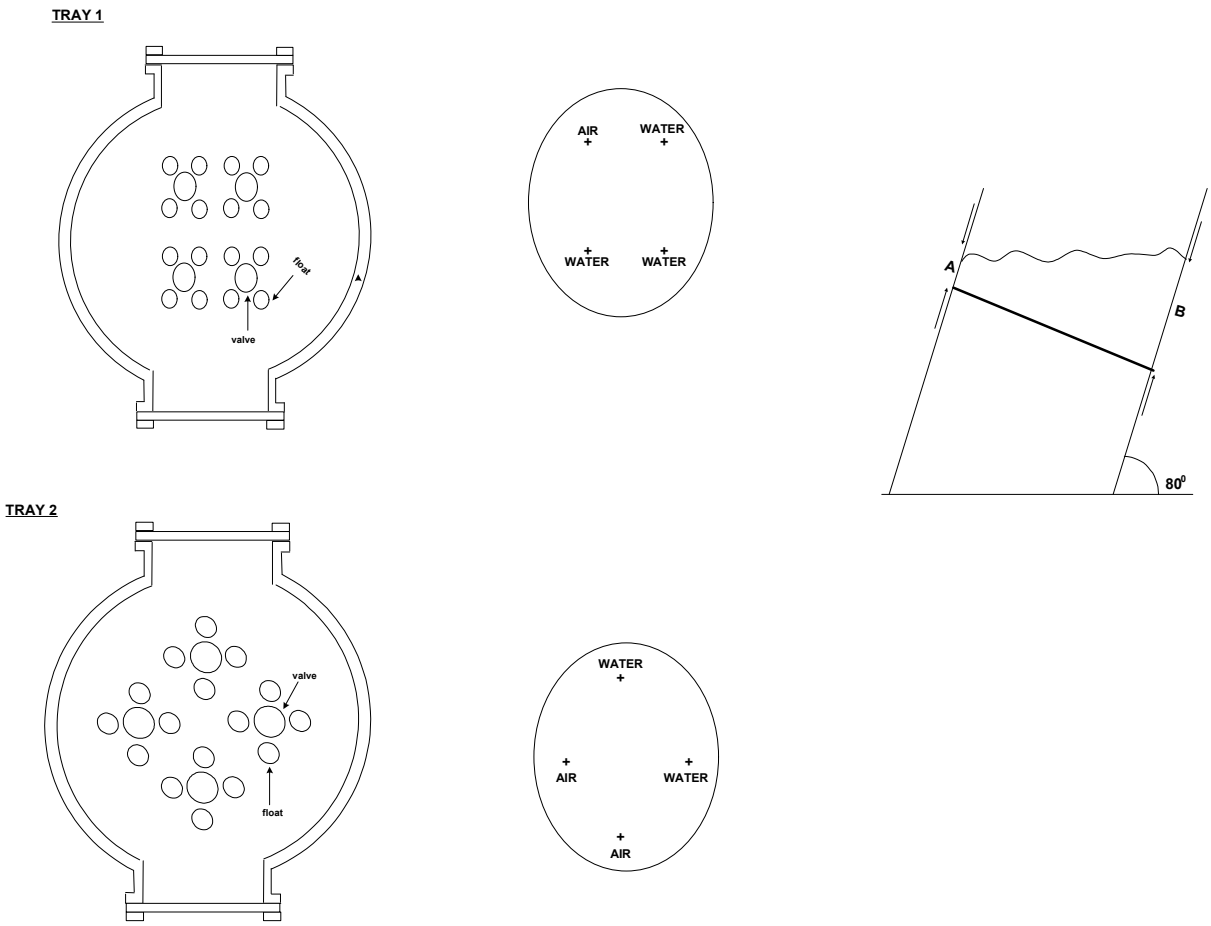

TRAY 1: A= 50mm, B = 80mm

TRAY 2: A=55mm, B= 85mm

Figure 4.66: Flow Behaviour at 10^0 Column Tilt, Liquid Rate of 7 Litres per Minute, and Vapour Rate of 2.7 Litres Per Minute.

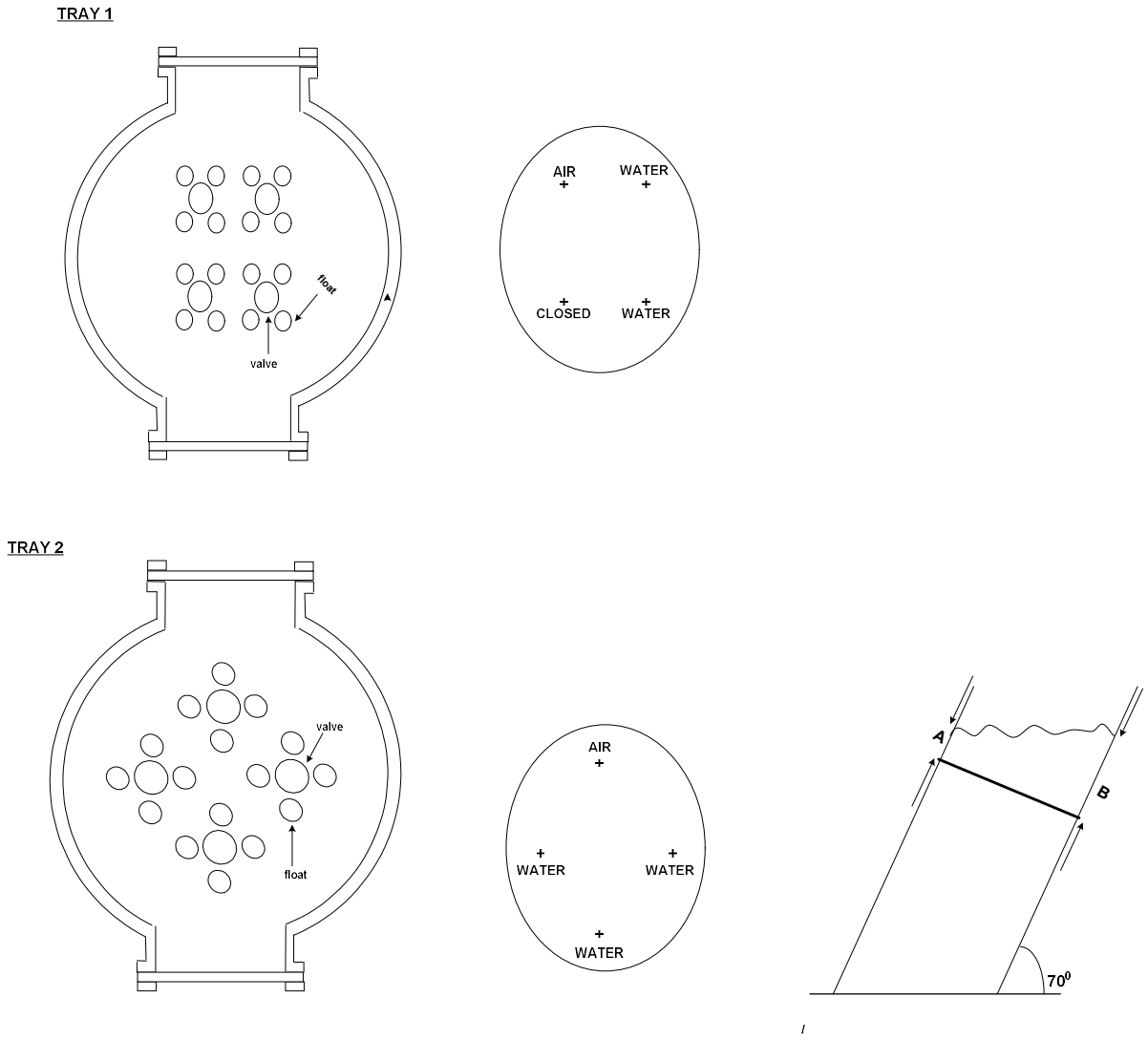

TRAY 1: A= 30mm, B = 100mm

TRAY 2: A=55mm, B= 115mm

Figure 4.67: Flow Behaviour at 20^0 Column Tilt, Liquid Rate of 9 Litres per Minute, and Vapour Rate of 3.2 Litres Per Minute.

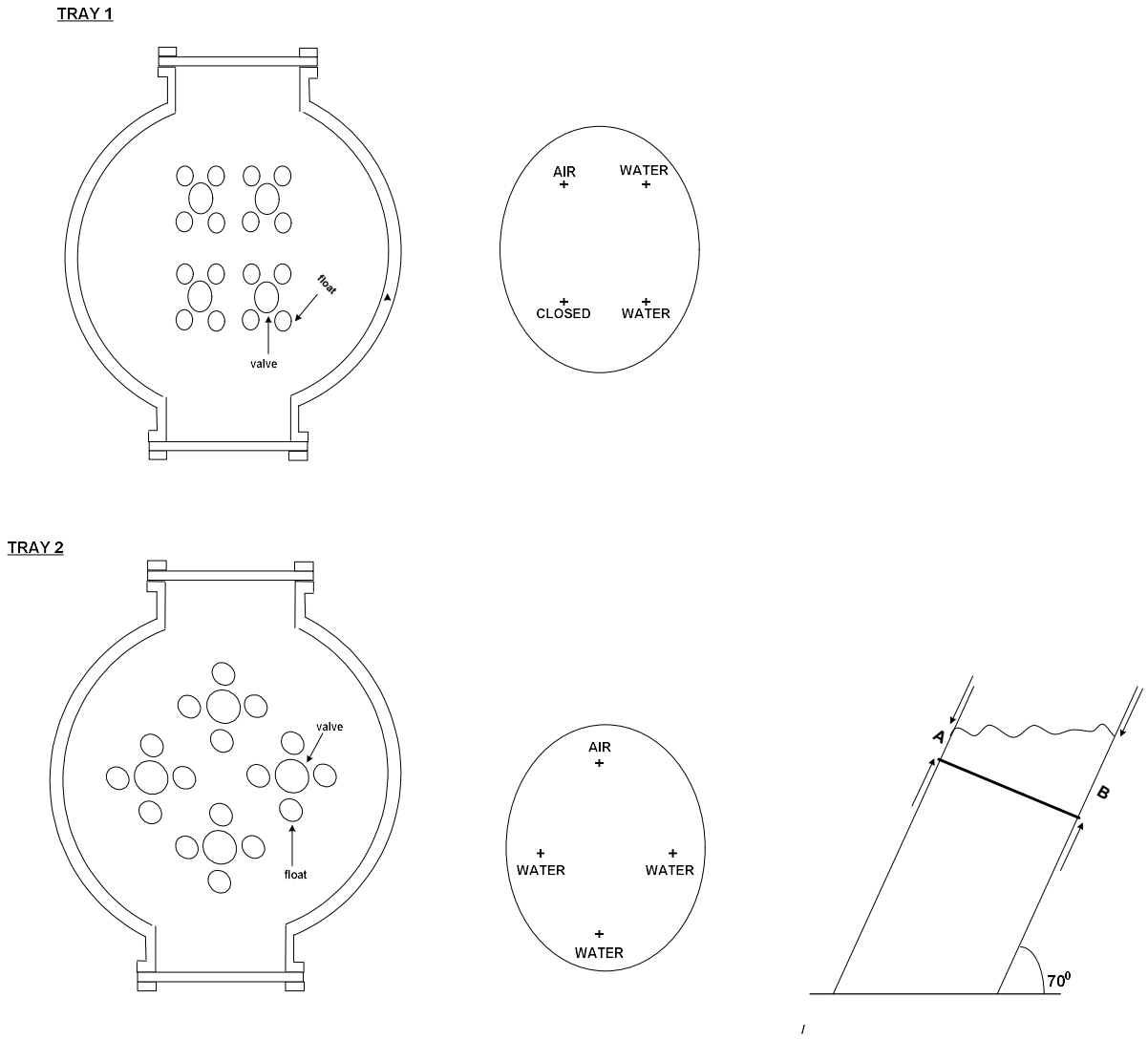

TRAY 1: A= 30mm, B = 100mm

TRAY 2: A=55mm, B= 115mm

Figure 4.68: Flow Behaviour at 20^0 Column Tilt, Liquid Rate of 9 Litres per Minute, and Vapour Rate of 2.2 Litres Per Minute.

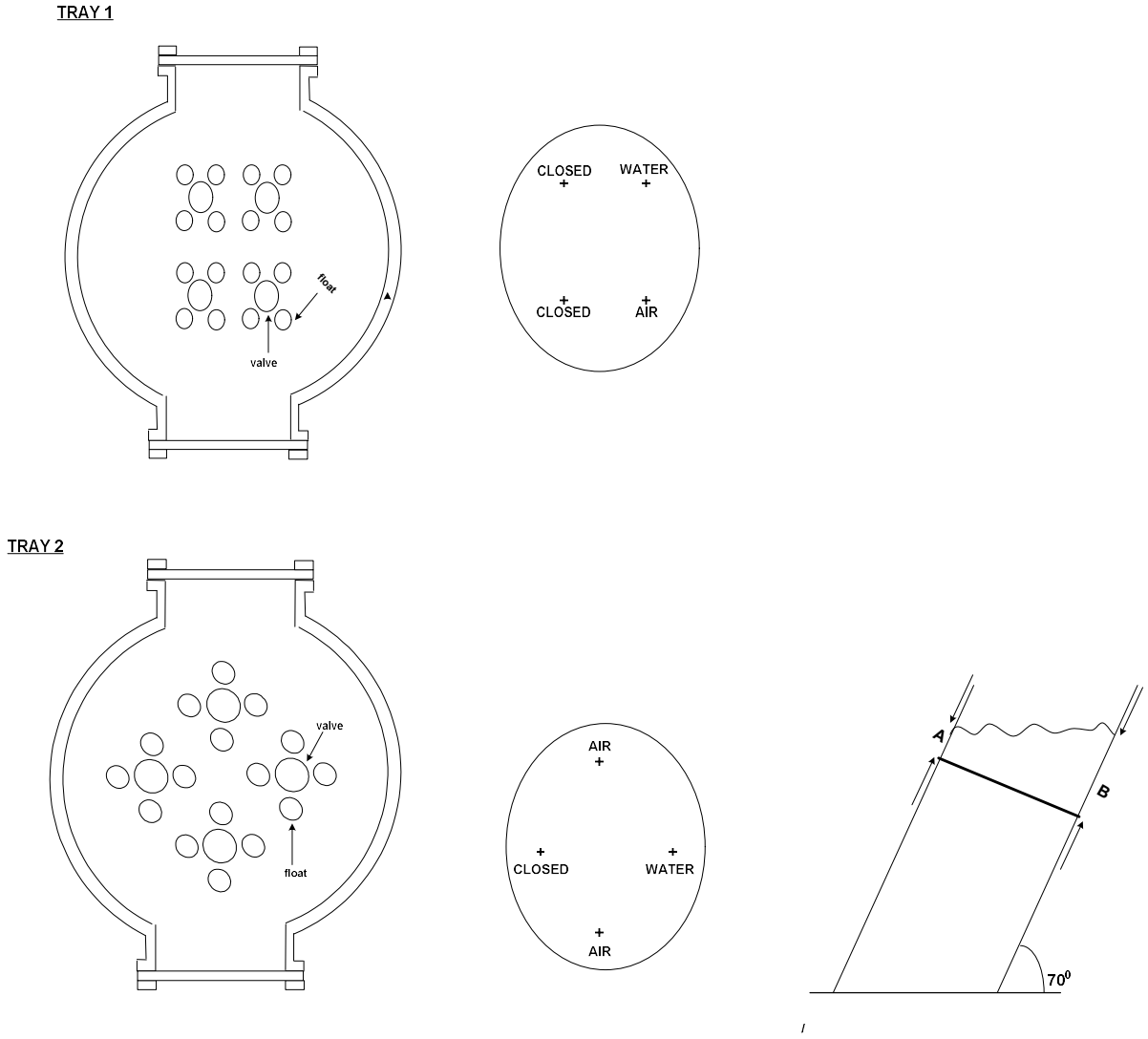

TRAY 1: A= 15mm, B = 80mm

TRAY 2: A=25mm, B= 90mm

Figure 4.69: Flow Behaviour at 20^0 Column Tilt, Liquid Rate of 5 Litres per Minute, and Vapour Rate of 3.2 Litres Per Minute.

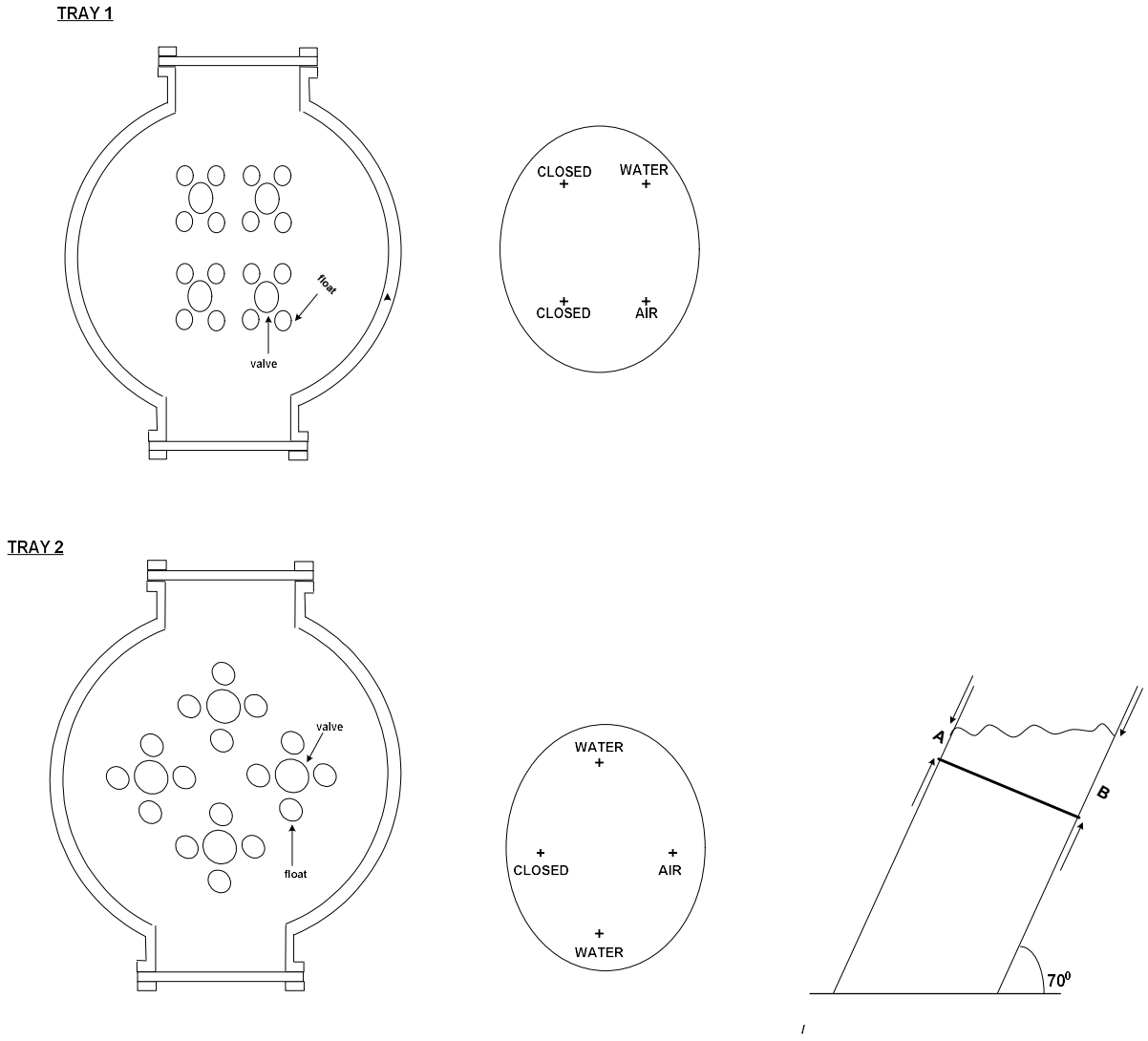

TRAY 1: A= 20mm, B = 90mm

TRAY 2: A=35mm, B= 100mm

Figure 4.70: Flow Behaviour at 20^0 Column Tilt, Liquid Rate of 5 Litres per Minute, and Vapour Rate of 2.2 Litres Per Minute.

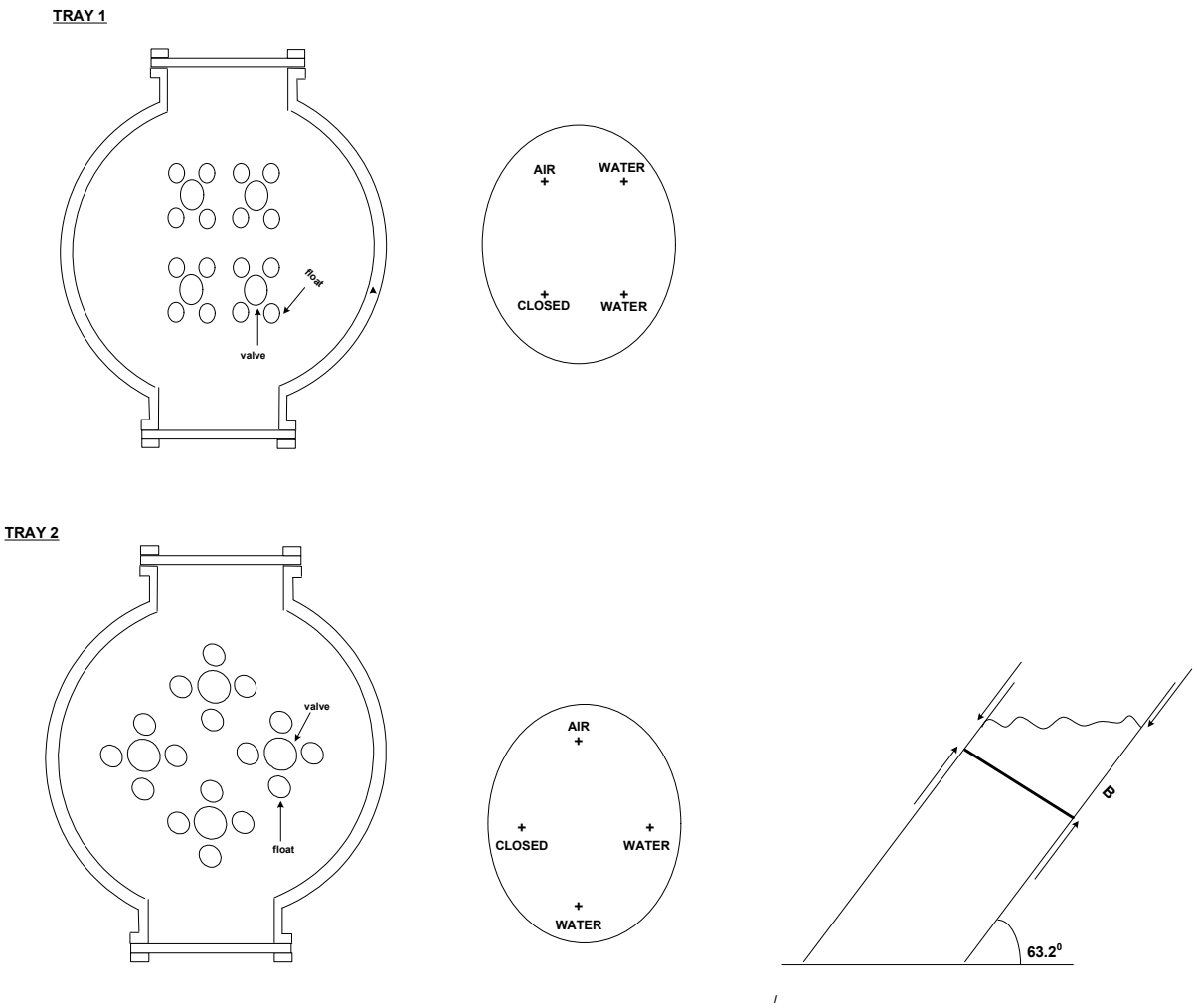

TRAY 1: A= 30mm, B = 120mm

TRAY 2: A=30mm, B= 120mm

Figure 4.71: Flow Behaviour at 26.8^0 Column Tilt, Liquid Rate of 7 Litres per Minute, and Vapour Rate of 2.7 Litres Per Minute.

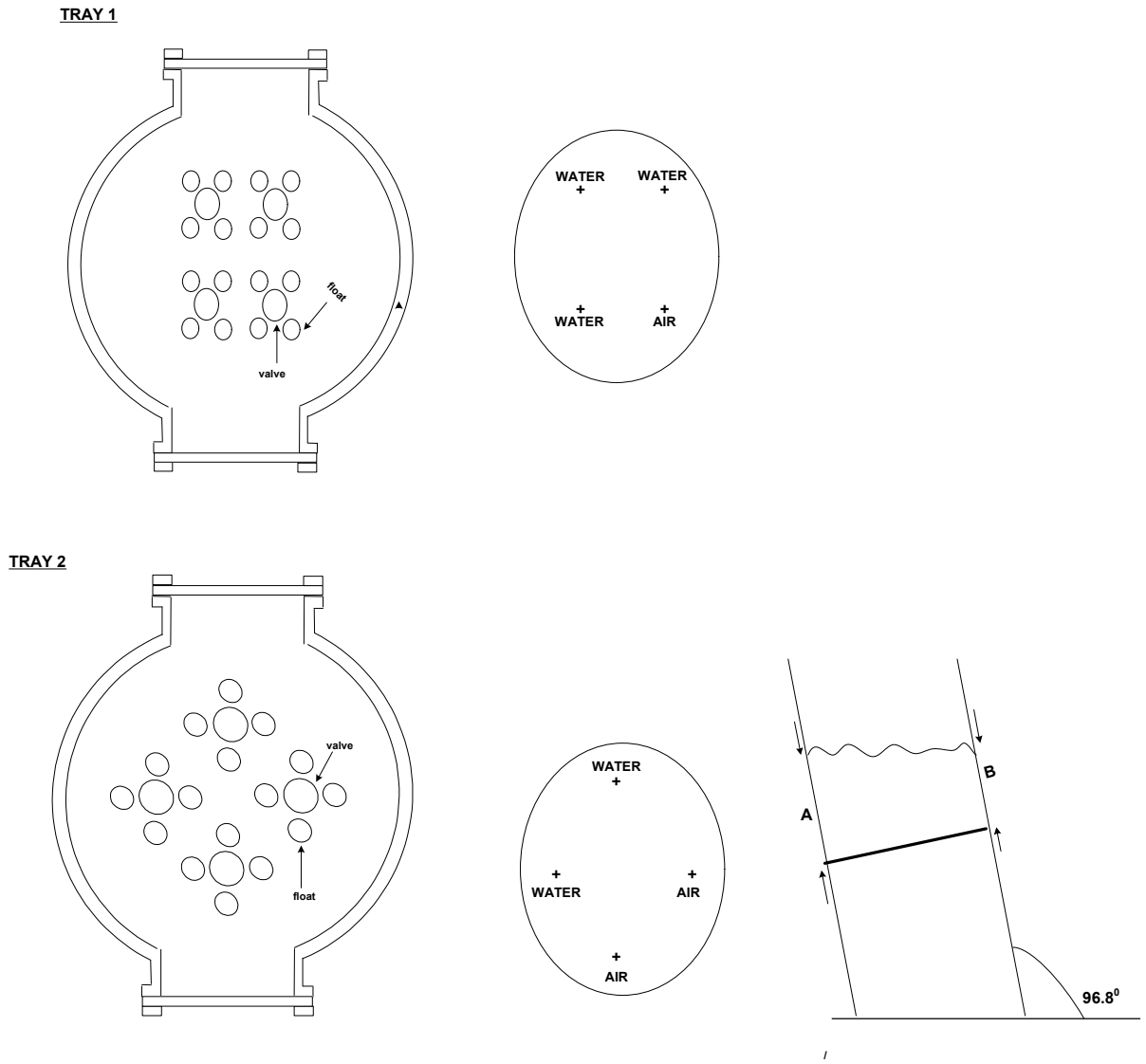

TRAY 1: A= 75mm, B = 70mm

TRAY 2: A=80mm, B= 75mm

Figure 4.72: Flow Behaviour at -6.8^0 Column Tilt, Liquid Rate of 7 Litres per Minute, and Vapour Rate of 2.7 Litres Per Minute.

4.2. DISCUSSION OF THE RESULTS

4.2.1 DISCUSSION OF THE RESULTS OF THE PURE LINEAR MODEL

Table 4.5 shows the Student's t test applied to individual coefficients in the model to test their significance. The parameters x_1 and x_2 (the vapour and liquid flow rates) are significant at 95% confidence level as their p-values are less than 0.05.

The analysis of variance (ANOVA) was used to test the significance and adequacy of the first order linear model and is shown in table 4.6 In this study, the ANOVA of the linear model demonstrates that it is significant, evident from the calculated F-value (F-model = 43.314) which exceeds the tabulated F-value ($F_{0.95,3,7}$ =4.35). The tabulated F-value is obtained from the table in appendix 1.

This significance of the model is also evident from the p-value of the model (<0.001) which is less than 0.05.

The obtained linear regression model is $y = 12.33 + 1.30x_1 + 0.68x_2 + 0.24x_3$ where x_1, x_2 and x_3 are in coded units of the variables. The fairly high R^2 value (0.9489) implies high degree of correlation between the observed and predicted values and the adjusted R^2 value is 0.9270 (a variation of 2.31%)

From the p-values of the student's t test and that of the ANOVA, we can deduce that parameters x_1 and x_2 are significant as their p-values are both much less than 0.05. However for parameter x_3 which represents the angle of tilt, the p-values

obtained from both tests are 0.114 and 0.059 respectively which are higher than 0.5. This implies that the effect of the angle of tilt is not significant.

4.2.2 DISCUSSION OF THE RESULTS OF THE LINEAR MODEL WITH INTERACTIONS

Table 4.8 shows the Student's t test applied to individual coefficients in the model to test their significance. Only parameters x_1 and x_2 (i.e. the vapour flow rate and the liquid flow rate) are significant at 95% confidence level. The angle of tilt x_3 (with p=0.18) has no significant influence on the amount of Iron II oxidized.

The analysis of variance (ANOVA) for the Fischer's F-test was used to test the significance and adequacy of the first order linear model with interactions and is shown in table 4.9. In this study, the ANOVA of the linear model with interactions shows that it is significant as evident from the calculated F-value (F-model =17.60) which exceeds the tabulated F-value ($F_{0.95,6,4}$ =6.16) and from its probability value (p = 0.008). From this test also, the model parameters x_1 and x_2 have significant influence as their calculated F-values (164.57 and 45.38 respectively) are much higher than their tabulated F-values ($F_{0.95,1,4}$ =7.71). The parameter x_3 and their interaction effects are still not significant from this test as their calculated F-values are less than their tabulated F-values of $F_{0.95,1,4}$ =7.71.

These results from the Fischer's F-test agree with that obtained from the p-value

analysis of the student's t test for parameters x_1 and x_2.

The obtained linear regression model is $y = 12.33 + 1.30x_1 + 0.68x_2 + 0.24x_3 + 0.18x_1x_2 + 0.02\ x_1x_3 + 0.04x_2x_3$ where x_1, x_2 and x_3 are in coded units of the variables. The coefficient of determination (R^2) value is 0.9635 while the adjusted determination coefficient (Adj R^2) value is 0.9088, showing a variation of 5.7%.

4.2.3 DISCUSSION OF THE RESULTS OF THE LINEAR MODEL WITH TRIPLE FACTOR INTERACTIONS

The obtained linear regression model is $y = 12.33 + 1.30x_1 + 0.68x_2 + 0.24x_3 + 0.18x_1x_2 + 0.02x_1x_3 + 0.04x_2x_3 + 0.09x_1x_2x_3$ where x_1, x_2 and x_3 are in coded units of the variables. The coefficient of determination (R^2) value is 0.9665 while the adjusted determination coefficient (Adj R^2) value is 0.890, showing a variation of 8%. From the p-value analysis shown in table 4.10, the parameter $x_1x_2x_3$ which is the only difference between this and the previous linear model is not significant at 95% confidence level as its p-value is >0.05.

The first linear model with interactions $y = 12.33 + 1.30x_1 + 0.68x_2 + 0.24x_3 + 0.18x_1x_2 + 0.02\ x_1x_3 + 0.04x_2x_3$ is preferred to the second one with triple interaction effect $y = 12.33 + 1.30x_1 + 0.68x_2 + 0.24x_3 + 0.18x_1x_2 + 0.02x_1x_3 + 0.04x_2x_3 + 0.09x_1x_2x_3$ for the following reason;

1. The model is simpler and generally the simplest possible model that best represents a system is normally used to analyse its behaviour (Ruzicka,

2013).

2. There is no significant difference between the Coefficient of Determination values of the 2 models (96.4 % and 96.7%); hence they both correlate the data equally.
3. The adjusted R^2 value of the first model differs from the R^2 value by 5.7% while the variation for the second model is 8.0%. This makes the first model superior to the second one.
4. The added triple effect factor is not significant hence the model does not offer any advantage.

Quadratic models based on the Box-Wilson design were next evaluated to ascertain if they would give a better fit.

4.2.4 DISCUSSION OF THE RESULTS OF THE PURE QUADRATIC MODEL FIT

From table 4.12 the obtained quadratic model without effects of interaction is $y = 11.73 + 1.57x_1 + 1.21x_2 + 0.21x_3 + 0.82x_1^2 - 0.67x_2^2 + 0.28x_3^2$ where x_1, x_2 and x_3 are in coded units of the variables. The lower R^2 value (0.8812) implies a not so good degree of correlation between the observed and predicted values. The adjusted R^2 value is 0.8264, showing a variation of 6.22% from the R^2 value.

Table 4.13 shows the Student's t test applied to individual coefficients in the model

to test their significance. Only parameters x_1 and x_2, and their square products x_1^2 and x_2^2 are significant at 95% confidence level. The angle of tilt x_3 (with p=0.392) and its square x_3^2 (with p=0.248) have no significant influence on the amount of Iron II oxidized.

The analysis of variance (ANOVA) for the Fischer's F-test was used to test the significance and adequacy of this quadratic model and is shown in table 4.14. In this study, the ANOVA of this quadratic model shows that it is significant as evident from the calculated F-value (F-model = 16.072) which exceeds the tabulated F-value several times ($F_{0.95,6,10}$ =3.22) and from its probability value ($p < 0.001$). From this test also, parameters x_1 (with $F_{calculated}$ =111.24) and tabulated F-value ($F_{0.95,3,10}$ =3.71), x_2 (with $F_{calculated}$ =93.24) and tabulated F-value ($F_{0.95,3,10}$ =3.71) are also significant at 95% confidence level. This finding is further validated by their p-values which are all less than 0.05. From this analysis, the angle of tilt parameter x_3 is not significant at 95% confidence level. These results agree with those obtained from the p-values of the student's t-test.

4.2.5 DISCUSSION OF THE RESULTS OF QUADRATIC MODEL WITH INTERACTION

Table 4.15 shows the predicted responses and coefficient of determination of the quadratic model with effects of interaction the obtained equation is y = 11.73 +

$1.57x_1 + 1.21x_2 + 0.21x_3 + 0.18x_1x_2 + 0.02\ x_1x_3 + 0.04x_2x_3 + 0.82x_1^2 - 0.67x_2^2 + 0.28x_3^2$, where x_1, x_2 and x_3 are in coded units of the variables. The coefficient of determination (R^2) value is 0.8845 while the adjusted determination coefficient (Adj R^2) value is 0.7805, showing a variation of 11.8%. The R^2 value of 0.8845 indicates that the fit is not so good.

Table 4.16 also shows the Student's t test applied to individual coefficients in the model to test their significance. Only parameters x_1 and x_2 (i.e. the vapour flow rate and the liquid flow rate) and their square products are significant at 95% confidence level. The angle of tilt x_3 (with p=0.449), its cross products x_1x_3 (with p=0.95) and x_2x_3 (with p=0.905) and its square x_3^2 (with p=0.307) have no significant influence on the amount of Iron II oxidized.

The analysis of variance (ANOVA) for the Fischer's F-test was used to test the significance and adequacy of the quadratic model with interaction effects and is shown in table 4.17. In this study, the ANOVA of the quadratic model with interactions shows that it is significant as evident from the calculated F-value (F-model = 8.505) which exceeds the tabulated F-value ($F_{0.95,9,7}$ =3.68) and from its probability value (p = 0.001). From this test also, parameters x_1 (with $F_{calculated}$ =11.24) and tabulated F-value ($F_{0.95,3,7}$ =4.35), x_2 (with $F_{calculated}$ =93.24) and tabulated F-value ($F_{0.95,3,7}$ =4.35) are highly significant at 95% confidence level. This finding is further validated by their p-values (<0.001) which are both less than

0.05. From this analysis, the angle of tilt parameter x_3 and its interaction effects x_1x_3 and x_2x_3 are not significant at 95% confidence level. These results agree with those obtained from the p-values of the student's t-test.

4.2.6 DISCUSSION OF THE RESULTS OF THE GRAPHICAL ANALYSIS

In the analysis of surface plots, the impact of any parameter on system response is indicated by the slope of that parameter. The less the slope, the less the impact of the corresponding parameter on the response. It is seen from all the 12 plots (figures 4.1 to 4.12) that the slopes of the axis of the "angle of tilt" is the least in all and is even almost zero in figure 4.5 where the liquid rate is held at its mid value for the linear model with interactions.

Figures 4.13 to 4.48 are the x-y scatter plots showing the variation in percentage Fe (II) oxidised at constant liquid flowrates and various degrees of column tilt for the different models. For all the liquid flowrates, the % Fe (II) oxidised increased with increasing vapour flowrates for the linear models. The impact of the angles of tilt was observed to be minimal as the graphs are clustered with no clearly discernable variations attributable to the angles of tilt. This observation is further emphasized by figures 4.49 to 4.57 which show the impact of changes in angle of tilt on change in percentage Fe(II) oxidised at various vapour flowrates for the linear model with interaction $y=b_0 + b_1x_1 + b_2x_2 + b_3x_3 + b_4x_1x_2 + b_5x_1x_3 + b_6x_2x_3$. For all the liquid

flowrates within the range of our experiments, the change in the percentage Fe (II) oxidised between 0 degrees to 10 degrees column tilt and between 0 degrees to 20 degrees column tilt is seen to be less than 1% at constant vapour flow rates.

4.2.7 DISCUSSION OF THE VISUAL OBSERVATIONS OF THE FLUID FLOW PATTERN OF THE TRAY COLUMN

Figures 4.58 to 4.72 show the observed fluid flow pattern of the tray column during operation. It was observed that each valve was either passing air or water at any time and not the two fluids simultaneously. This observation agrees with the findings of Weiland (2001) on the operation of Dual flow trays. At the higher vapour flow rates of 3.2 and 3.5 Litres per minute and for all liquid flow rates used, 2 out of the 4 trays passed water while the other 2 passed air for 0 degrees column tilt. At the lower vapour flow rates of 1.9 and 2.2 Litres per minute and for all liquid rates used, 3 out of the 4 valves passed water while the remaining one passed air. When the column was operated in tilted conditions, the air preferentially passed through the portions of the tray having lower levels of liquid while water passed through the others. Also when the column was operated in tilted conditions, the valves closed in portions of the tray with liquid levels lower than that required to lift the floats and open the valves. This action forced the air to go through the portions of the tray having liquid thereby ensuring proper contact of the phases.

4.2.8 SUMMARY OF THE DISCUSSION OF THE RESULTS

From the preceding discussion of results, the linear model with interaction $y = 12.33 + 1.30x_1 + 0.68x_2 + 0.24x_3 + 0.18x_1x_2 + 0.02\ x_1x_3 + 0.04x_2x_3$ is the best representation of the effects of the liquid rate, the vapour rate and angle of tilt on the performance of the novel tray column when used for the oxidation of Iron II to Iron III. This model best represents the data with R^2 value of 0.9635 and the analysis previously enumerated indicates that the angle of tilt (represented by parameter x_3) and its interaction effects do not have any significant impact on the model and hence the operation of the column within the range of the experimental investigation will not be affected by the angle of column tilt.

CHAPTER FIVE

CONCLUSION AND RECOMMENDATIONS

5.1 CONCLUSION

Conventional dual flow trays are characterised by low efficiency and unstable fluid flow patterns. According to Weiland (2001), liquid tends to rain through several clusters of openings and these clusters meander randomly across the tray surface with vapour rising through the remaining areas of the tray even when the trays are perfectly level. When dual flow trays are out of level *(as expected in this design)*, liquid raining through one part of the tray tends to be associated with raining from another collection of holes in the same lateral position on the tray below. Similarly, vapour rising from one part of the tray tends to induce vapour flow through a similar portion of the tray above. This kind of maldistribution can propagate through many if not all the trays in both directions, resulting in the vapour and liquid passing through separate diametrically opposite sections of the column.

With dual flow trays fitted with the novel float valves presented in this thesis, this kind of maldistribution will be curtailed because the valve operation will guide the liquid and vapour flow patterns. Vapour will not therefore be restricted to portions of the tray with lower liquid levels as these portions will be partially or totally shut by the valves. Analysis of the experimental data indicates that the linear model with interaction $y = 12.33 + 1.30x_1 + 0.68x_2 + 0.24x_3 + 0.18x_1x_2 + 0.02x_1x_3 +$

$0.04x_2x_3$ is a good representation of the effects of the liquid rate, the vapour rate and angle of tilt on the performance of the novel tray column when used for the oxidation of Iron II to Iron III. This model best represents the data with R^2 value of 0.9635 and the analysis previously enumerated indicates that the angle of tilt (represented by parameter x_3) and its interaction effects do not have any significant impact on the model; hence the operation of the novel tray column is encouraged within the range of the experimental investigation. This finding validates our earlier hypothesis that a liquid operated and controlled valve tray (such as the Plunger Cap Multifloat Valve Tray presented in this thesis) will provide solution to the problems of liquid maldistribution and efficiency collapse occasioned by tray column tilt and motion during operation.

5.2 CONTRIBUTION TO KNOWLEDGE

The significant contributions to knowledge of this research are as follows;

1. This research work has added a new type of valve tray to the already existing ones.
2. This research work has provided a solution to the challenges encountered by plate contacting columns when operated on mobile platforms.
3. The results of this research when applied will greatly increase the

energy supply available to man by enhancing the harnessing and conversion of gaseous fuels to much needed liquid fuels.

5.3 RECOMMENDATIONS

The following are the recommendations arising from this work.

1. It is recommended that funding should be made available for scale up of this design.
2. It is recommended that this scaled up design be extensively tested to enable us derive empirical relationships for general design of this valve tray type. The empirical relationships to be obtained will be used for determination of the tray operating range, tray spacings, allowable tray pressure drop, turn down ratio, tray pitch, valve spacings, etc.
3. It is also recommended that this valve tray type should be used for other VLE operations such as distillation, absorption, stripping, etc to fully exploit its operational advantages.
4. It is recommended that modifications of this valve tray type be investigated for possible improvement on the design for better operational efficiency.

REFERENCES

ASANO, K.,**2006**, *"Mass Transfer: From Fundamentals to Modern Industrial Applications"*, WILEY-VCH Verlag GmbH & Co., Weinheim, p XIII.

ATKINSON,A.C. AND DONEV, A.N.,**1992**, *"Optimum Experimental Designs"*, Clarendon Press Oxford, pp. 24 - 31.

BAEHR, H.D., AND STEPHAN, K., **2006**, *"Heat and Mass Transfer"*, 2nd Edition, Springer-Verlag Berlin Heidelberg, p. 94.

BAKER, S. A. AND WALDIE, B.,**1996**, *"A Novel Redistributor Concept for Packed Columns"*, Chemical Engineering Research and Design, 74(A1),106-112.

BANDYOPADHYAY, A., AND BISWAS, M.N., **2011**, *"Determination of Interfacial Area in a Tapered Bubble Column"*, Journal of Chemical Technology and Biotechnology, 86(9),1211-1225.

BENITEZ, J., **2009**, *"Principles and Modern Applications of Mass Transfer Operations"* Wiley Book Company, New York.

BILLET, R., **2001**, *"Separation Trays without Downcomers"*, Chemical Engineering and Technology, 24(11), 1103-1112.

BOLLES, W.L. **1963**. *"Tray Hydraulics: Bubble-cap Trays"*, in: SMITH, B.D., *"Design of Equilibrium Stage Processes"*, McGraw-Hill Book Co. New York, p.474.

DOMINGUES, T.L., SECCHI, A.R., MENDES, T.F., **2010**, *"Overall Efficiency of Commercial Distillation Columns with Valve and Dualflow Trays"*, AIChE Journal, 56(9), 2323-2330.

EDGAR, T. F. AND HIMMELBLAU, D.M., **1988**, *"Optimisation of Chemical Processes"*, McGraw-Hill Book Co. New York, pp. 4 - 60

FARD, H.H., ZIVDAR, M., RAHIMI, R., ESTAHANI, N.N., AFACAN, A., NANDAKUMAR, K., CHUANG, K.T., **2007**, *"CFD Simulation of Mass Transfer Efficiency and Pressure Drop in a Structured Packed Distillation Column"*, Chemical Engineering and Technology, 30(30), 854-861.

FAIR, J. R. **1963**. *"Tray Hydraulics: Bubble-cap Trays"*, in: SMITH, B.D., *"Design of Equilibrium Stage Processes"*, McGraw-Hill Book Co. New York p. 566.

GOLDSTONE, P.G.,TIJM,P.J.A.,MILLER,D.,**1998**, *"The Safe and Efficient Provision of Oxygen for Remote Offshore Conversion of Natural Gas"*, paper presented at the "Remote and Stranded Gas Reserves" Conference, Marble Arch Marriot Hotel, London.

GUTIERREZ-OPPE, E.E., SALVAGNINI, W.M., TAQUEDA, M.E.S., **2013**, *"Comparison between the Design of Experiments and Simulation in the Three-phase Distillation in a Sieve Tray Column for Glycerine Dehydration",* Chemical Engineering Research and Design, In Press accepted Manuscript, available online

February 7, 2013. (Articles “In Press” are accepted peer reviewed articles that are not yet assigned to an issue, but are citable).

HANLEY, B., **2012**, *“On Packed Columns Hydraulics”*, AIChE Journal, 58(6), 1671-1682.

HOON, C.Y., LING, A.L., JAYA, A., **2011**, *“Distillation Column Selection and Sizing: Engineering Design Guidelines”*, a KLM Technology Group Publication, p. 11, [viewed February 12, 2013] available at www.kolmetz.com/pdf/EDG/Engineering_Design_Guidelines-distillation_column-Rev03web.pdf.

LAZIC, Z.R. ,**2004**, “*Design of Experiments in Chemical Engineering, A Practical Guide”*, WILEY-VCH verlag GmbH & Co., Weinheim,. pp. 157 -348.

LIU, Y., GAO, H., SUN, J., WANG, Y., WU, P., LIU, Y., JI, Y., **2011**, *“Novel Packing-Enhanced Distillation Separation of Isoamyl Alcohol Isomer:Experimental and Pilot Scale Study”*, AIChE Journal, 57(11), 3037-3041.

LOCKETT, M. J. & BILLINGHAM, J. F., **2002**, *“A Simple Method to Assess the Sensitivity of Packed Distillation Columns to Maldistribution”*, Chemical Engineering Research and Design, 80, 373-382.

LOCKETT, M. J. & BILLINGHAM, J. F., **2003**, *“The Effect of Maldistribution on Separation in Packed Columns”*, Chemical Engineering Research and Design, 81,131-135.

LUDWIG, E.E. ,**1997**, "*Applied Processes Design for Chemical and Petrochemical Plants"*, Vol.2. 3rd Edn. Gulf Publishing Company, Houston Texas. pp. 122-133, 187-192.

LYE, J.,BROWN,D.,PATEL,M.,**2007**, *"Optimization of Floating Production, Storage and Offloading Platforms"*, Exploration and Production: The Oil & Gas Review, Issue II. [viewed January 2009] available at www.touchoilandgas.com/optimization-floating-production-storage-a77II-1.html.

NAZIRI, N., ZADGHAFFARI, R., NAZIRI, H., **2012**, *"CFD Simulation and Experimental Study of New Developed Centrifugal Trays"*, International Journal of Chemical Engineering and Applications, 3(3), 201-205.

NEGREA, P. SIDEA, F., NEGREA, A., LUPA, L., CIOPEC, M., MUNTEAN, C., **2008**, *"Studies regarding the Benzene, Toluene and o-Xylene Removal from Waste Water"*, Chem. Bull. "POLITEHNICA" Univ.(Timisoara), 53(67), 144-147.

NNOLIM, B. N.,**1993**, *"Worked Examples in Mass Transfer"* CECTA Nigeria Ltd., p 43.

PERRY, R.H. AND GREEN, D.W. (eds), **1997**, "*Perry's Chemical Engineering Handbook*" 7th Edn. McGraw-Hill Book Company, New York. Pp. 14-23 - 14-26.

REMESAT, D., CHUANG, K., SVRCEK, W., **2005**, *"The Evaluation of Out-of-Level Trays for the Improvement of Industry Guidelines"*, Chemical Engineering

Research and Design, 83(5), 505-514.

RICHARDSON, J.F. AND HARKER, J.H., **2002**, *"Coulson and Richardson's Chemical Engineering", Volume 2*, 5th Edition, Reed Elsevier India, pp. 702-707.

RUZICKA, M.C., **2013**, *"On Stability of a Bubble Column"*, Chemical Engineering Research and Design, 91(2), 191-203.

SMITH, B.D.**, 1963** "*Design of equilibrium stage processes*", McGraw-Hill Book Co. New York. pp. 570.

SINNOT, R.K., **1993** *"Coulson and Richardsons Chemical Engineering" Volume 6*, Pergramon press Ltd. pp.421, 523 .

SULTANA, R.S., ARIFIN, B.M.S., ISLAM, M.M., AND KUMAR, A., **2010**, *"Demonstration of Mass Transfer using Aeration of Water"*, Journal of Chemical Engineering, CHE 25(1), 56-60.

TANNER, R. K., BAKER, S. A., MILLAR, M. K., WALDIE, B.,**1996**, *"Modelling the Performance of a Packed Column Subjected to tilt"*, Chemical Engineering Research and Design, 74(A1),177-182 .

TREYBAL, R.E. **1980**, *"Mass Transfer Operations"*, 3rd Edn., McGraw-Hill Book Co. New York. Pp. 138, 177.

WALDIE, B.,**1996**, *"A New High Intensity Contactor for Deoxygenation of Water"*, Chemical Engineering Research and Design, 74(A1),183-189.

WALDIE, B., **2002**, *"Effects of Tilt and Motion on LNG and GTL Process Equipment for Floating Production",*[viewed July 2004] available at www.gasprocessors.com/GlobalDocuments/E02Sept_10.pdf.

WEILAND,R. H. ,**2001**, *"Hydraulic Stability of Dualflow Trays",* paper prepared for presentation at the AIChE Spring National Meeting, Houston, TX on New Frontiers in High Capacity Tray Technology.

WIJN, F.,**1998**, *"Recently Development Trays",* [viewed October 2002], available at http:// www.Euronet. Nl/~wijnef.

WIKIPEDIA, **2013**, *"Null Hypothesis, from Wikipedia the free encyclopedia",*[viewed April, 2013] , available at http://www.en.wikipedia.org/wiki/Null_hypothesis.

XU, Z.P., AFACAN, A., CHUANG, K.T.,**1994**, *"Efficiency of Dualflow Trays in Distillation"*, The Canadian Journal of Chemical Engineering, 72(4), 607-613.

ZHANG, L., LIU, X., LI, H., SUI, H., LI, X., ZHANG, J., YANG, Z., TIAN, C., GAO, G., **2012**, *"Hydrodynamic and Mass Transfer Performance of a New SiC Foam Column Tray"*, Chemical Engineering and Technology, 35(12), 2075-2083.

APPENDIX 1;

Table A1.1: Table for obtaining tabulated F-values for comparison with the calculated F-values for regression diagnostics. (source, www4.uwsp.edu/psych/stat/F.htm)

F Table

Critical values for alpha equals .05. (95% confidence level)

df_W	df_B																		
	1	**2**	**3**	**4**	**5**	**6**	**7**	**8**	**9**	**10**	**12**	**15**	**20**	**24**	**30**	**40**	**60**	**120**	∞
1	161.4	199.5	215.7	224.6	230.2	234.0	236.8	238.9	240.5	241.9	243.9	245.9	248.0	249.1	250.1	251.1	252.2	253.3	254.3
2	18.51	19.00	19.16	19.25	19.30	19.33	19.35	19.37	19.38	19.40	19.41	19.43	19.45	19.45	19.46	19.47	19.48	19.49	19.50
3	10.13	9.55	9.28	9.12	9.01	8.94	8.89	8.85	8.81	8.79	8.74	8.70	8.66	8.64	8.62	8.59	8.57	8.55	8.53
4	7.71	6.94	6.59	6.39	6.26	6.16	6.09	6.04	6.00	5.96	5.91	5.86	5.80	5.77	5.75	5.72	5.69	5.66	5.63
5	6.61	5.79	5.41	5.19	5.05	4.95	4.88	4.82	4.77	4.74	4.68	4.62	4.56	4.53	4.50	4.46	4.43	4.40	4.36
6	5.99	5.14	4.76	4.53	4.39	4.28	4.21	4.15	4.10	4.06	4.00	3.94	3.87	3.84	3.81	3.77	3.74	3.70	3.67
7	5.59	4.74	4.35	4.12	3.97	3.87	3.79	3.73	3.68	3.64	3.57	3.51	3.44	3.41	3.38	3.34	3.30	3.27	3.23
8	5.32	4.46	4.07	3.84	3.69	3.58	3.50	3.44	3.39	3.35	3.28	3.22	3.15	3.12	3.08	3.04	3.01	2.97	2.93
9	5.12	4.26	3.86	3.63	3.48	3.37	3.29	3.23	3.18	3.14	3.07	3.01	2.94	2.90	2.86	2.83	2.79	2.75	2.71
10	4.96	4.10	3.71	3.48	3.33	3.22	3.14	3.07	3.02	2.98	2.91	2.85	2.77	2.74	2.70	2.66	2.62	2.58	2.54
11	4.84	3.98	3.59	3.36	3.20	3.09	3.01	2.95	2.90	2.85	2.79	2.72	2.65	2.61	2.57	2.53	2.49	2.45	2.40
12	4.75	3.89	3.49	3.26	3.11	3.00	2.91	2.85	2.80	2.75	2.69	2.62	2.54	2.51	2.47	2.43	2.38	2.34	2.30
13	4.67	3.81	3.41	3.18	3.03	2.92	2.83	2.77	2.71	2.67	2.60	2.53	2.46	2.42	2.38	2.34	2.30	2.25	2.21

14	4.60	3.74	3.34	3.11	2.96	2.85	2.76	2.70	2.65	2.60	2.53	2.46	2.39	2.35	2.31	2.27	2.22	2.18	2.13
15	4.54	3.68	3.29	3.06	2.90	2.79	2.71	2.64	2.59	2.54	2.48	2.40	2.33	2.29	2.25	2.20	2.16	2.11	2.07
16	4.49	3.63	3.24	3.01	2.85	2.74	2.66	2.59	2.54	2.49	2.42	2.35	2.28	2.24	2.19	2.15	2.11	2.06	2.01
17	4.45	3.59	3.20	2.96	2.81	2.70	2.61	2.55	2.49	2.45	2.38	2.31	2.23	2.19	2.15	2.10	2.06	2.01	1.96
18	4.41	3.55	3.16	2.93	2.77	2.66	2.58	2.51	2.46	2.41	2.34	2.27	2.19	2.15	2.11	2.06	2.02	1.97	1.92
19	4.38	3.52	3.13	2.90	2.74	2.63	2.54	2.48	2.42	2.38	2.31	2.23	2.16	2.11	2.07	2.03	1.98	1.93	1.88
20	4.35	3.49	3.10	2.87	2.71	2.60	2.51	2.45	2.39	2.35	2.28	2.20	2.12	2.08	2.04	1.99	1.95	1.90	1.84
21	4.32	3.47	3.07	2.84	2.68	2.57	2.49	2.42	2.37	2.32	2.25	2.18	2.10	2.05	2.01	1.96	1.92	1.87	1.81
22	4.30	3.44	3.05	2.82	2.66	2.55	2.46	2.40	2.34	2.30	2.23	2.15	2.07	2.03	1.98	1.94	1.89	1.84	1.78
23	4.28	3.42	3.03	2.80	2.64	2.53	2.44	2.37	2.32	2.27	2.20	2.13	2.05	2.01	1.96	1.91	1.86	1.81	1.76
24	4.26	3.40	3.01	2.78	2.62	2.51	2.42	2.36	2.30	2.25	2.18	2.11	2.03	1.98	1.94	1.89	1.84	1.79	1.73
25	4.24	3.39	2.99	2.76	2.60	2.49	2.40	2.34	2.28	2.24	2.16	2.09	2.01	1.96	1.92	1.87	1.82	1.77	1.71
26	4.23	3.37	2.98	2.74	2.59	2.47	2.39	2.32	2.27	2.22	2.15	2.07	1.99	1.95	1.90	1.85	1.80	1.75	1.69
27	4.21	3.35	2.96	2.73	2.57	2.46	2.37	2.31	2.25	2.20	2.13	2.06	1.97	1.93	1.88	1.84	1.79	1.73	1.67
28	4.20	3.34	2.95	2.71	2.56	2.45	2.36	2.29	2.24	2.19	2.12	2.04	1.96	1.91	1.87	1.82	1.77	1.71	1.65
29	4.18	3.33	2.93	2.70	2.55	2.43	2.35	2.28	2.22	2.18	2.10	2.03	1.94	1.90	1.85	1.81	1.75	1.70	1.64
30	4.17	3.32	2.92	2.69	2.53	2.42	2.33	2.27	2.21	2.16	2.09	2.01	1.93	1.89	1.84	1.79	1.74	1.68	1.62
40	4.08	3.23	2.84	2.61	2.45	2.34	2.25	2.18	2.12	2.08	2.00	1.92	1.84	1.79	1.74	1.69	1.64	1.58	1.51
60	4.00	3.15	2.76	2.53	2.37	2.25	2.17	2.10	2.04	1.99	1.92	1.84	1.75	1.70	1.65	1.59	1.53	1.47	1.39
120	3.92	3.07	2.68	2.45	2.29	2.17	2.09	2.02	1.96	1.91	1.83	1.75	1.66	1.61	1.55	1.50	1.43	1.35	1.25
∞	3.84	3.00	2.60	2.37	2.21	2.10	2.01	1.94	1.88	1.83	1.75	1.67	1.57	1.52	1.46	1.39	1.32	1.22	1.00

Only some Degrees are freedom are shown. If you want an intermediate value, use the next lowest in the table.

Df_B = Degree of freedom between groups = k -1

Df_W = Degree of freedom within groups = N – k

Total Degree of freedom = N -1

N = Total number of samples

k = Total number of groups

APPENDIX 2:
TABLES SHOWING VARIATIONS IN PERCENTAGE OF IRON (II) OXIDISED AS OBTAINED FROM THE VARIOUS MODELS

Table A2.1: Variations in percentage Fe(II) oxidised at a constant liquid flowrate of 3 litres per minute and various angles of tilt based on linear model $y=b_0 + b_1x_1 + b_2x_2 + b_3x_3$

Vapour rate	**Liquid rate**	**Y, % Fe(II) oxidised at various angles of tilt**					
		0^0	5^0	10^0	15^0	20^0	25^0
1.5	3	7.6297	7.7472	7.8647	7.9822	8.0997	8.2172
2.0	3	8.9247	9.0422	9.1597	9.2772	9.3947	9.5122
2.5	3	10.2197	10.3372	10.4547	10.5722	10.6897	10.8072
3.0	3	11.5147	11.6322	11.7497	11.8672	11.9847	12.1022
3.5	3	12.8097	12.9272	13.0447	13.1622	13.2797	13.3972
4.0	3	14.1047	14.2222	14.3397	14.4572	14.5747	14.6922

Table A2.2: Variations in percentage Fe(II) oxidised at a constant liquid flowrate of 4 litres per minute and various angles of tilt based on linear model $y=b_0 + b_1x_1 + b_2x_2 + b_3x_3$

Vapour rate	**Liquid rate**	**Y, % Fe(II) oxidised at various angles of tilt**					
		0^0	5^0	10^0	15^0	20^0	25^0
1.5	4	7.9697	8.0847	8.2047	8.3222	8.4397	8.5572
2.0	4	9.2647	9.3822	9.4997	9.6172	9.7347	9.8522
2.5	4	10.5597	10.6772	10.7947	10.9122	11.0297	11.1472
3.0	4	11.8547	11.9722	12.0897	12.2072	12.3247	12.4422
3.5	4	13.1497	13.2672	13.3847	13.5022	13.6197	13.7372
4.0	4	14.4447	14.5622	14.6797	14.7972	14.9147	15.0322

Table A2.3: Variations in percentage Fe(II) oxidised at a constant liquid flowrate of 5 litres per minute and various angles of tilt based on linear model $y=b_0 + b_1x_1 + b_2x_2 + b_3x_3$

Vapour rate	Liquid rate	Y, % Fe(II) oxidised at various angles of tilt					
		0^0	5^0	10^0	15^0	20^0	25^0
1.5	5	8.3097	8.4272	8.5447	8.6622	8.7797	8.8972
2.0	5	9.6047	9.7222	9.8397	9.9572	10.0747	10.1922
2.5	5	10.8997	11.0172	11.1347	11.2522	11.3697	11.4872
3.0	5	12.1947	12.3122	12.4297	12.5472	12.6647	12.7822
3.5	5	13.4897	13.6072	13.7247	13.8422	13.9597	14.0722
4.0	5	14.7847	14.9022	15.0197	15.1372	15.2547	15.3722

Table A2.4: Variations in percentage Fe(II) oxidised at a constant liquid flowrate of 6 litres per minute and various angles of tilt based on linear model $y=b_0 + b_1x_1 + b_2x_2 + b_3x_3$

Vapour rate	Liquid rate	Y, % Fe(II) oxidised at various angles of tilt					
		0^0	5^0	10^0	15^0	20^0	25^0
1.5	6	8.6497	8.7672	8.8847	9.0022	9.1197	9.2372
2.0	6	9.9447	10.0622	10.1797	10.2972	10.4147	10.5322
2.5	6	11.2397	11.3572	11.4747	11.5922	11.7097	11.8272
3.0	6	12.5347	12.6522	12.7697	12.8872	13.0047	13.1222
3.5	6	13.8297	13.9472	14.0647	14.1822	14.2997	14.4172
4.0	6	15.1247	15.2422	15.3597	15.4772	15.5947	15.7122

Table A2.5: Variations in percentage Fe(II) oxidised at a constant liquid flowrate of 7 litres per minute and various angles of tilt based on linear model $y=b_0 + b_1x_1 + b_2x_2 + b_3x_3$

Vapour rate	**Liquid rate**	**Y, % Fe(II) oxidised at various angles of tilt**					
		0^0	5^0	10^0	15^0	20^0	25^0
1.5	7	8.9897	9.1072	9.2247	9.3422	9.4597	9.5772
2.0	7	10.2847	10.4022	10.5197	10.6372	10.7547	10.8722
2.5	7	11.5797	11.6972	11.8147	11.9322	12.0497	12.1672
3.0	7	12.8747	12.9922	13.1097	13.2272	13.3447	13.4622
3.5	7	14.1697	14.2872	14.4047	14.5222	14.6397	14.7572
4.0	7	15.4647	15.5822	15.6997	15.8172	15.9347	16.0522

Table A2.6: Variations in percentage Fe(II) oxidised at a constant liquid flowrate of 8 litres per minute and various angles of tilt based on linear model $y=b_0 + b_1x_1 + b_2x_2 + b_3x_3$

Vapour rate	**Liquid rate**	**Y, % Fe(II) oxidised at various angles of tilt**					
		0^0	5^0	10^0	15^0	20^0	25^0
1.5	8	9.3297	9.4472	9.5647	9.6822	9.7997	9.9172
2.0	8	10.6247	10.7422	10.8597	10.9772	11.0947	11.2122
2.5	8	11.9197	12.0372	12.1547	12.2722	12.3897	12.5072
3.0	8	13.2147	13.3322	13.4497	13.5672	13.6847	13.8022
3.5	8	14.5097	14.6272	14.7447	14.8622	14.9797	15.0972
4.0	8	15.8047	15.9222	16.0397	16.1572	16.2747	16.3922

Table A2.7: Variations in percentage Fe(II) oxidised at a constant liquid flowrate of 9 litres per minute and various angles of tilt based on linear model $y=b_0 + b_1x_1 + b_2x_2 + b_3x_3$

Vapour rate	Liquid rate	Y, % Fe(II) oxidised at various angles of tilt					
		0^0	5^0	10^0	15^0	20^0	25^0
1.5	9	9.6697	9.7872	9.9047	10.0222	10.1397	10.2572
2.0	9	10.9647	11.0822	11.1997	11.3172	11.4347	11.552
2.5	9	12.2597	12.3772	12.4947	12.6122	12.7297	12.8472
3.0	9	13.5547	13.6722	13.7897	13.9072	14.0247	14.1422
3.5	9	14.8497	14.9672	15.0847	15.2022	15.3197	15.4372
4.0	9	16.1447	16.2622	16.3797	16.4972	16.6147	16.7322

Table A2.8: Variations in percentage Fe(II) oxidised at a constant liquid flowrate of 10 litres per minute and various angles of tilt based on linear model $y=b_0 + b_1x_1 + b_2x_2 + b_3x_3$

Vapour rate	Liquid rate	Y, % Fe(II) oxidised at various angles of tilt					
		0^0	5^0	10^0	15^0	20^0	25^0
1.5	10	10.0097	10.1272	10.2447	10.3622	10.4797	10.5972
2.0	10	11.3047	11.4222	11.5397	11.6572	11.7747	11.8922
2.5	10	12.5997	12.7172	12.8347	12.9552	13.0697	13.1872
3.0	10	13.8947	14.0122	14.1297	14.2472	14.3647	14.4822
3.5	10	15.1897	15.3072	15.4247	15.5422	15.6597	15.7772
4.0	10	16.4847	16.6022	16.7197	16.8372	16.9547	17.0722

Table A2.9: Variations in percentage Fe(II) oxidised at a constant liquid flowrate of 11 litres per minute and various angles of tilt based on linear model $y=b_0 + b_1x_1 + b_2x_2 + b_3x_3$

Vapour rate	Liquid rate	Y, % Fe(II) oxidised at various angles of tilt					
		0^0	5^0	10^0	15^0	20^0	25^0
1.5	11	10.3497	10.4672	10.5847	10.7022	10.8197	10.9372
2.0	11	11.6447	11.7622	11.8797	11.9972	12.1147	12.2322
2.5	11	12.9397	13.0572	13.1747	13.2922	13.4097	13.5272
3.0	11	14.2347	14.3522	14.4697	14.5872	14.7047	14.8222
3.5	11	15.5297	15.6472	15.7647	15.8822	15.9997	16.1172
4.0	11	16.8247	16.9422	17.0597	17.1772	17.2947	17.4122

Table A2.10: Variations in percentage Fe(II) oxidised at a constant liquid flowrate of 3 litres per minute and various angles of tilt based on linear model $y=b_0 + b_1x_1 + b_2x_2 + b_3x_3 + b_4x_1x_2 + b_5x_1x_3 + b_6x_2x_3$

Vapour rate	Liquid rate	Y, % Fe(II) oxidised at various angles of tilt					
		0^0	5^0	10^0	15^0	20^0	25^0
1.5	3	8.6207	8.6685	8.7162	8.7640	8.8117	8.8595
2.0	3	9.5382	9.5972	9.6562	9.7152	9.7742	9.8332
2.5	3	10.4557	10.5260	10.5962	10.6665	10.7367	10.8070
3.0	3	11.3732	11.4547	11.5362	11.6177	11.6992	11.7807
3.5	3	12.2907	12.3835	12.4762	12.5690	12.6617	12.7545
4.0	3	13.2082	13.3122	13.4162	13.5202	13.6242	13.7282

Table A2.11: Variations in percentage Fe(II) oxidised at a constant liquid flowrate of 4 litres per minute and various angles of tilt based on linear model $y=b_0 + b_1x_1 + b_2x_2 + b_3x_3 + b_4x_1x_2 + b_5x_1x_3 + b_6x_2x_3$

Vapour rate	**Liquid rate**	**Y, % Fe(II) oxidised at various angles of tilt**					
		0^0	5^0	10^0	15^0	20^0	25^0
1.5	4	8.7265	8.7847	8.8430	8.9012	8.9595	9.0177
2.0	4	9.7327	9.8022	9.8717	9.9412	10.0107	10.0802
2.5	4	10.7390	10.8197	10.9005	10.9812	11.0620	11.1427
3.0	4	11.7452	11.8372	11.9292	12.0212	12.1132	12.2052
3.5	4	12.7515	12.8547	12.9580	13.0612	13.1645	13.2677
4.0	4	13.7577	13.8722	13.9867	14.1012	14.2157	14.3302

Table A2.12: Variations in percentage Fe(II) oxidised at a constant liquid flowrate of 5 litres per minute and various angles of tilt based on linear model $y=b_0 + b_1x_1 + b_2x_2 + b_3x_3 + b_4x_1x_2 + b_5x_1x_3 + b_6x_2x_3$

Vapour rate	**Liquid rate**	**Y, % Fe(II) oxidised at various angles of tilt**					
		0^0	5^0	10^0	15^0	20^0	25^0
1.5	5	8.8322	8.9010	8.9697	9.0385	9.1072	9.1760
2.0	5	9.9272	10.0072	10.0872	10.1672	10.2472	10.3272
2.5	5	11.0222	11.1135	11.2047	11.2960	11.3872	11.4785
3.0	5	12.1172	12.2197	12.3222	12.4247	12.5272	12.6297
3.5	5	13.2122	13.3260	13.4397	13.5535	13.6672	13.7810
4.0	5	14.3072	14.4322	14.5572	14.6822	14.8072	14.9322

Table A2.13: Variations in percentage Fe(II) oxidised at a constant liquid flowrate of 6 litres per minute and various angles of tilt based on linear model $y=b_0 + b_1x_1 + b_2x_2 + b_3x_3 + b_4x_1x_2 + b_5x_1x_3 + b_6x_2x_3$

Vapour rate	**Liquid rate**	**Y, % Fe(II) oxidised at various angles of tilt**					
		0^0	5^0	10^0	15^0	20^0	25^0
1.5	6	8.9380	9.0172	9.0965	9.1757	9.2550	9.3342
2.0	6	10.1217	10.2122	10.3027	10.3932	10.4837	10.5742
2.5	6	11.3055	11.4072	11.5090	11.6107	11.7125	11.8142
3.0	6	12.4892	12.6022	12.7152	12.8282	12.9412	13.0542
3.5	6	13.6730	13.7972	13.9215	14.0457	14.1700	14.2942
4.0	6	14.8567	14.9922	15.1277	15.2632	15.3987	15.5342

Table A2.14: Variations in percentage Fe(II) oxidised at a constant liquid flowrate of 7 litres per minute and various angles of tilt based on linear model $y=b_0 + b_1x_1 + b_2x_2 + b_3x_3 + b_4x_1x_2 + b_5x_1x_3 + b_6x_2x_3$

Vapour rate	**Liquid rate**	**Y, % Fe(II) oxidised at various angles of tilt**					
		0^0	5^0	10^0	15^0	20^0	25^0
1.5	7	9.0437	9.1335	9.2232	9.3130	9.4027	9.4925
2.0	7	10.3162	10.4172	10.5182	10.6192	10.7202	10.8212
2.5	7	11.5887	11.7010	11.8132	11.9255	12.0377	12.1500
3.0	7	12.8612	12.9847	13.1082	13.2317	13.3552	13.4787
3.5	7	14.1337	14.2685	14.4032	14.5380	14.6727	14.8075
4.0	7	15.4062	15.5522	15.6982	15.8442	15.9902	16.1362

Table A2.15: Variations in percentage Fe(II) oxidised at a constant liquid flowrate of 8 litres per minute and various angles of tilt based on linear model $y=b_0 + b_1x_1 + b_2x_2 + b_3x_3 + b_4x_1x_2 + b_5x_1x_3 + b_6x_2x_3$

Vapour rate	**Liquid rate**	**Y, % Fe(II) oxidised at various angles of tilt**					
		0^0	5^0	10^0	15^0	20^0	25^0
1.5	8	9.1495	9.2497	9.3500	9.4502	9.5505	9.6507
2.0	8	10.5107	10.6222	10.7337	10.8452	10.9567	11.0682
2.5	8	11.8720	11.9947	12.1175	12.2402	12.3630	12.4857
3.0	8	13.2332	13.3672	13.5012	13.6352	13.7692	13.9032
3.5	8	14.5945	14.7397	14.8850	15.0302	15.1755	15.3207
4.0	8	15.9557	16.1122	16.2687	16.4252	16.5817	16.7382

Table A2.16: Variations in percentage Fe(II) oxidised at a constant liquid flowrate of 9 litres per minute and various angles of tilt based on linear model $y=b_0 + b_1x_1 + b_2x_2 + b_3x_3 + b_4x_1x_2 + b_5x_1x_3 + b_6x_2x_3$

Vapour rate	**Liquid rate**	**Y, % Fe(II) oxidised at various angles of tilt**					
		0^0	5^0	10^0	15^0	20^0	25^0
1.5	9	9.2552	9.3660	9.4767	9.5875	9.6982	9.8090
2.0	9	10.7052	10.8272	10.9492	11.0712	11.1932	11.3152
2.5	9	12.1552	12.2885	12.4217	12.5550	12.6882	12.8215
3.0	9	13.6052	13.7497	13.8942	14.0387	14.1832	14.3277
3.5	9	15.0552	15.2110	15.3667	15.5225	15.6782	15.8340
4.0	9	16.5052	16.6722	16.8392	17.0062	17.1732	17.3402

Table A2.17: Variations in percentage Fe(II) oxidised at a constant liquid flowrate of 10 litres per minute and various angles of tilt based on linear model $y=b_0 + b_1x_1 + b_2x_2 + b_3x_3 + b_4x_1x_2 + b_5x_1x_3 + b_6x_2x_3$

Vapour rate	**Liquid rate**	**Y, % Fe(II) oxidised at various angles of tilt**					
		0^0	5^0	10^0	15^0	20^0	25^0
1.5	10	9.3610	9.4422	9.6035	9.7247	9.8460	9.9672
2.0	10	10.8997	11.0322	11.1647	11.2972	11.4297	11.5622
2.5	10	12.4385	12.5822	12.7260	12.8697	13.0135	13.1572
3.0	10	13.9772	14.1322	14.2872	14.4422	14.5972	14.7522
3.5	10	15.5160	15.6822	15.8485	16.0147	16.1810	16.3472
4.0	10	17.0547	17.2322	17.4097	17.5872	17.7647	17.9422

Table A2.18: Variations in percentage Fe(II) oxidised at a constant liquid flowrate of 11 litres per minute and various angles of tilt based on linear model $y=b_0 + b_1x_1 + b_2x_2 + b_3x_3 + b_4x_1x_2 + b_5x_1x_3 + b_6x_2x_3$

Vapour rate	**Liquid rate**	**Y, % Fe(II) oxidised at various angles of tilt**					
		0^0	5^0	10^0	15^0	20^0	25^0
1.5	11	9.4667	9.5985	9.7302	9.8620	9.9937	10.1255
2.0	11	11.0942	11.2372	11.3802	11.5232	11.6662	11.8092
2.5	11	12.7217	12.8760	13.0302	13.1845	13.3387	13.4930
3.0	11	14.3492	14.5147	14.6802	14.8457	15.0112	15.1767
3.5	11	15.9767	16.1535	16.3302	16.5070	16.6837	16.8605
4.0	11	17.6042	17.7922	17.9802	18.1682	18.3562	18.5442

Table A2.19: Variations in percentage Fe(II) oxidised at a constant liquid flowrate of 3 litres per minute and various angles of tilt based on quadratic model $y=b_0 + b_1x_1 + b_2x_2 + b_3x_3 + b_4x_1^2 + b_5x_2^2 + b_6x_3^2$

Vapour rate	**Liquid rate**	**Y, % Fe(II) oxidised at various angles of tilt**					
		0^0	5^0	10^0	15^0	20^0	25^0
1.5	3	7.9921	7.9031	7.9441	8.1151	8.4161	8.8471
2.0	3	6.1689	6.0799	6.1209	6.2919	6.5929	7.1239
2.5	3	6.1440	6.0550	6.0960	6.2670	6.5680	6.9990
3.0	3	7.9172	7.8282	7.8692	8.0402	8.3412	8.7722
3.5	3	11.4887	11.3997	11.4407	11.6117	11.9127	12.3437
4.0	3	16.8583	16.7693	16.8103	16.9813	17.2823	17.7133

Table A2.20: Variations in percentage Fe(II) oxidised at a constant liquid flowrate of 4 litres per minute and various angles of tilt based on quadratic model $y=b_0 + b_1x_1 + b_2x_2 + b_3x_3 + b_4x_1^2 + b_5x_2^2 + b_6x_3^2$

Vapour rate	**Liquid rate**	**Y, % Fe(II) oxidised at various angles of tilt**					
		0^0	5^0	10^0	15^0	20^0	25^0
1.5	4	9.7837	9.6947	9.7357	9.9067	10.2077	10.6387
2.0	4	7.9605	7.8715	7.9125	8.0835	8.3845	8.8185
2.5	4	7.9356	7.8466	7.8876	8.0586	8.3596	8.7906
3.0	4	9.7088	9.6198	9.6608	9.8318	10.1328	10.5638
3.5	4	13.2803	13.1913	13.2323	13.4033	13.7043	14.1353
4.0	4	18.6499	18.5609	18.6019	18.7729	19.0739	19.5049

Table A2.21: Variations in percentage Fe(II) oxidised at a constant liquid flowrate of 5 litres per minute and various angles of tilt based on quadratic model $y=b_0 + b_1x_1 + b_2x_2 + b_3x_3 + b_4x_1^2 + b_5x_2^2 + b_6x_3^2$

Vapour rate	**Liquid rate**	**Y, % Fe(II) oxidised at various angles of tilt**					
		0^0	5^0	10^0	15^0	20^0	25^0
1.5	5	11.2363	11.1473	11.1883	11.3593	11.6603	12.0913
2.0	5	9.4131	9.3241	9.3651	9.5361	9.8371	10.2681
2.5	5	9.3882	9.2992	9.3402	9.5112	9.8122	10.2432
3.0	5	11.1614	11.0724	11.1134	11.2844	11.5854	12.0164
3.5	5	14.7329	14.6439	14.6849	14.8559	15.1569	15.5879
4.0	5	20.1025	20.0135	20.0545	20.2255	20.5265	20.9575

Table A2.22: Variations in percentage Fe(II) oxidised at a constant liquid flowrate of 6 litres per minute and various angles of tilt based on quadratic model $y=b_0 + b_1x_1 + b_2x_2 + b_3x_3 + b_4x_1^2 + b_5x_2^2 + b_6x_3^2$

Vapour rate	**Liquid rate**	**Y, % Fe(II) oxidised at various angles of tilt**					
		0^0	5^0	10^0	15^0	20^0	25^0
1.5	6	12.3499	12.2609	12.3019	12.4729	12.7739	13.2049
2.0	6	10.5267	10.4377	10.4787	10.6497	10.9507	11.3817
2.5	6	10.5018	10.4128	10.4538	10.6248	10.9258	11.3568
3.0	6	12.2750	12.1860	12.2270	12.3980	12.6990	13.1300
3.5	6	15.8465	15.7575	15.7985	15.9695	16.2705	16.7015
4.0	6	21.2161	21.1271	21.1681	21.3391	21.6401	22.0711

Table A2.23: Variations in percentage Fe(II) oxidised at a constant liquid flowrate of 7 litres per minute and various angles of tilt based on quadratic model $y=b_0 + b_1x_1 + b_2x_2 + b_3x_3 + b_4x_1^2 + b_5x_2^2 + b_6x_3^2$

Vapour rate	**Liquid rate**	**Y, % Fe(II) oxidised at various angles of tilt**					
		0^0	5^0	10^0	15^0	20^0	25^0
1.5	7	13.1245	13.0355	13.0765	13.2475	13.5485	13.9795
2.0	7	11.3013	11.2123	11.2533	11.4243	11.7253	12.1563
2.5	7	11.2764	11.1874	11.2284	11.3994	11.7004	12.1314
3.0	7	13.0496	12.9606	13.0016	13.1726	13.4736	13.9046
3.5	7	16.6211	16.5321	16.5731	16.7441	17.0451	17.4761
4.0	7	21.9907	21.9017	21.9427	22.1137	22.4147	22.8457

Table A2.24: Variations in percentage Fe(II) oxidised at a constant liquid flowrate of 8 litres per minute and various angles of tilt based on quadratic model $y=b_0 + b_1x_1 + b_2x_2 + b_3x_3 + b_4x_1^2 + b_5x_2^2 + b_6x_3^2$

Vapour rate	**Liquid rate**	**Y, % Fe(II) oxidised at various angles of tilt**					
		0^0	5^0	10^0	15^0	20^0	25^0
1.5	8	13.5601	13.4711	13.5121	13.6831	13.9841	14.4151
2.0	8	11.7369	11.6479	11.6889	11.8599	12.1609	12.5919
2.5	8	11.7120	11.6230	11.6640	11.8350	12.1360	12.5670
3.0	8	13.4852	13.3962	13.4372	13.6082	13.9092	14.3402
3.5	8	17.0567	16.9677	17.0087	17.1797	17.4807	17.9117
4.0	8	22.4263	22.3373	22.3783	22.5493	22.8503	23.2813

Table A2.25: Variations in percentage Fe(II) oxidised at a constant liquid flowrate of 9 litres per minute and various angles of tilt based on quadratic model $y=b_0 + b_1x_1 + b_2x_2 + b_3x_3 + b_4x_1^2 + b_5x_2^2 + b_6x_3^2$

Vapour rate	Liquid rate	Y, % Fe(II) oxidised at various angles of tilt					
		0^0	5^0	10^0	15^0	20^0	25^0
1.5	9	13.6567	13.5677	13.6087	13.7797	14.0807	14.5117
2.0	9	11.8335	11.7445	11.7855	11.9565	12.2575	12.6885
2.5	9	11.8086	11.7196	11.7606	11.9316	12.2326	12.6636
3.0	9	13.5818	13.4928	13.5338	13.7048	14.0058	14.4368
3.5	9	17.1533	17.0643	17.1053	17.2763	17.5773	18.0083
4.0	8	22.4263	22.3373	22.3783	22.5493	22.8503	23.2813

Table A2.26: Variations in percentage Fe(II) oxidised at a constant liquid flowrate of 10 litres per minute and various angles of tilt based on quadratic model $y=b_0 + b_1x_1 + b_2x_2 + b_3x_3 + b_4x_1^2 + b_5x_2^2 + b_6x_3^2$

Vapour rate	Liquid rate	Y, % Fe(II) oxidised at various angles of tilt					
		0^0	5^0	10^0	15^0	20^0	25^0
1.5	10	13.4143	13.3253	13.3663	13.5373	13.8383	14.2693
2.0	10	11.5911	11.5021	11.5431	11.7141	12.0151	12.4461
2.5	10	11.5662	11.4772	11.5182	11.6892	11.9902	12.4212
3.0	10	13.3394	13.2504	13.2914	13.4624	13.7634	14.1944
3.5	10	16.9109	16.8219	16.8629	17.0339	17.3349	17.7659
4.0	10	22.2805	22.1915	22.2325	22.4035	22.7045	23.1355

Table A2.27: Variations in percentage Fe(II) oxidised at a constant liquid flowrate of 11 litres per minute and various angles of tilt based on quadratic model $y=b_0 + b_1x_1 + b_2x_2 + b_3x_3 + b_4x_1^2 + b_5x_2^2 + b_6x_3^2$

Vapour rate	Liquid rate	Y, % Fe(II) oxidised at various angles of tilt					
		0^0	5^0	10^0	15^0	20^0	25^0
1.5	11	12.8329	12.7439	12.7849	12.9559	13.2569	13.6879
2.0	11	11.0097	10.9207	10.9617	11.1327	11.4337	11.8647
2.5	11	10.9848	10.8958	10.9368	11.1078	11.4088	11.8398
3.0	11	12.7580	12.6690	12.7100	12.8810	13.1820	13.6130
3.5	11	16.3295	16.2405	16.2815	16.4525	16.7535	17.1845
4.0	11	21.6991	21.6101	21.6511	21.8221	22.1231	22.5541

Table A2.28: Variations in percentage Fe(II) oxidised at a constant liquid flowrate of 3 litres per minute and various angles of tilt based on quadratic model $y=b_0 + b_1x_1 + b_2x_2 + b_3x_3 + b_4x_1x_2 + b_5x_1x_3 + b_6x_2x_3 + b_7x_1^2 + b_8x_2^2 + b_9x_3^2$

Vapour rate	Liquid rate	Y, % Fe(II) oxidised at various angles of tilt					
		0^0	5^0	10^0	15^0	20^0	25^0
1.5	3	8.9831	8.6943	8.2756	7.7268	7.0481	6.2393
2.0	3	6.7824	6.5049	6.0974	5.5599	4.8929	4.0949
2.5	3	6.3800	6.1137	5.7175	5.1912	4.5350	3.7487
3.0	3	7.7757	7.5207	7.1357	6.6207	5.9757	5.2007
3.5	3	10.9697	10.7259	10.3522	9.8484	9.2147	8.4509
4.0	3	15.9618	15.7293	15.3668	14.8743	14.2518	13.4993

Table A2.29: Variations in percentage Fe(II) oxidised at a constant liquid flowrate of 4 litres per minute and various angles of tilt based on quadratic model $y=b_0 + b_1x_1 + b_2x_2 + b_3x_3 + b_4x_1x_2 + b_5x_1x_3 + b_6x_2x_3 + b_7x_1^2 + b_8x_2^2 + b_9x_3^2$

Vapour rate	Liquid rate	Y, % Fe(II) oxidised at various angles of tilt					
		0^0	5^0	10^0	15^0	20^0	25^0
1.5	4	10.5404	10.2622	9.8539	9.3157	8.6474	7.8492
2.0	4	8.4285	8.1615	7.7645	7.2375	6.5805	5.7935
2.5	4	8.1148	7.8591	7.4733	6.9576	6.3118	5.5361
3.0	4	9.5993	9.3548	8.9803	8.4758	7.8413	7.0768
3.5	4	12.8820	12.6488	12.2855	11.7923	11.1690	10.4158
4.0	4	17.9629	17.7409	17.3889	16.9069	16.2949	15.5529

Table A2.30: Variations in percentage Fe(II) oxidised at a constant liquid flowrate of 5 litres per minute and various angles of tilt based on quadratic model $y=b_0 + b_1x_1 + b_2x_2 + b_3x_3 + b_4x_1x_2 + b_5x_1x_3 + b_6x_2x_3 + b_7x_1^2 + b_8x_2^2 + b_9x_3^2$

Vapour rate	Liquid rate	Y, % Fe(II) oxidised at various angles of tilt					
		0^0	5^0	10^0	15^0	20^0	25^0
1.5	5	11.7588	11.4910	11.0933	10.5655	9.9078	9.1200
2.0	5	9.7356	9.4791	9.0926	8.5761	7.9296	7.1531
2.5	5	9.5107	9.2654	8.8902	8.3849	7.7497	6.9844
3.0	5	11.0839	10.8499	10.4859	9.9919	9.3679	8.6139
3.5	5	14.4554	14.2326	13.8799	13.3971	12.7844	12.0416
4.0	5	19.6250	19.4135	19.0720	18.6005	17.9990	17.2675

Table A2.31: Variations in percentage Fe(II) oxidised at a constant liquid flowrate of 6 litres per minute and various angles of tilt based on quadratic model $y=b_0 + b_1x_1 + b_2x_2 + b_3x_3 + b_4x_1x_2 + b_5x_1x_3 + b_6x_2x_3 + b_7x_1^2 + b_8x_2^2 + b_9x_3^2$

Vapour rate	Liquid rate	Y, % Fe(II) oxidised at various angles of tilt					
		0^0	5^0	10^0	15^0	20^0	25^0
1.5	6	12.6381	12.3809	11.9936	11.4764	10.8291	10.0519
2.0	6	10.7037	10.4577	10.0817	9.5757	8.9397	8.1737
2.5	6	10.5675	10.3328	9.9680	9.4733	8.8485	8.0938
3.0	6	12.2295	12.0060	11.6525	11.1690	10.5555	9.8120
3.5	6	15.6897	15.4775	15.1352	14.6630	14.0607	13.3285
4.0	6	20.9481	20.7471	20.4161	19.9551	19.3641	18.6431

Table A2.32: Variations in percentage Fe(II) oxidised at a constant liquid flowrate of 7 litres per minute and various angles of tilt based on quadratic model $y=b_0 + b_1x_1 + b_2x_2 + b_3x_3 + b_4x_1x_2 + b_5x_1x_3 + b_6x_2x_3 + b_7x_1^2 + b_8x_2^2 + b_9x_3^2$

Vapour rate	Liquid rate	Y, % Fe(II) oxidised at various angles of tilt					
		0^0	5^0	10^0	15^0	20^0	25^0
1.5	7	13.1785	12.9317	12.5550	12.0482	11.4115	10.6447
2.0	7	11.3328	11.0973	10.7318	10.2363	9.6108	8.8553
2.5	7	11.2854	11.0611	10.7069	10.2226	9.6084	8.8641
3.0	7	13.0361	12.8231	12.4801	12.0071	11.4041	10.6711
3.5	7	16.5851	16.3833	16.0516	15.5898	14.9981	14.2763
4.0	7	21.9322	21.7417	21.4212	20.9707	20.3902	19.6797

Table A2.33: Variations in percentage Fe(II) oxidised at a constant liquid flowrate of 8 litres per minute and various angles of tilt based on quadratic model $y=b_0 + b_1x_1 + b_2x_2 + b_3x_3 + b_4x_1x_2 + b_5x_1x_3 + b_6x_2x_3 + b_7x_1^2 + b_8x_2^2 + b_9x_3^2$

Vapour rate	Liquid rate	Y, % Fe(II) oxidised at various angles of tilt					
		0^0	5^0	10^0	15^0	20^0	25^0
1.5	8	13.3798	13.1436	12.7773	12.2811	11.6548	10.8986
2.0	8	11.6229	11.3979	11.0429	10.5579	9.9429	9.1979
2.5	8	11.6642	11.4505	11.1067	10.6330	10.0292	9.2955
3.0	8	13.5037	13.3012	12.9687	12.5062	11.9137	11.1912
3.5	8	17.1414	16.9502	16.6289	16.1777	15.5964	14.8852
4.0	8	22.5773	22.3973	22.0873	21.6473	21.0773	20.3773

Table A2.34: Variations in percentage Fe(II) oxidised at a constant liquid flowrate of 9 litres per minute and various angles of tilt based on quadratic model $y=b_0 + b_1x_1 + b_2x_2 + b_3x_3 + b_4x_1x_2 + b_5x_1x_3 + b_6x_2x_3 + b_7x_1^2 + b_8x_2^2 + b_9x_3^2$

Vapour rate	Liquid rate	Y, % Fe(II) oxidised at various angles of tilt					
		0^0	5^0	10^0	15^0	20^0	25^0
1.5	9	13.2422	13.0164	12.6607	12.1749	11.5592	10.8134
2.0	9	11.5740	11.3595	11.0150	10.5405	9.9360	9.2015
2.5	9	11.7041	11.5008	11.1676	10.7043	10.1111	9.3878
3.0	9	13.6323	13.4403	13.1183	12.6663	12.0843	11.3723
3.5	9	17.3588	17.1780	16.8673	16.4265	15.8558	15.1550
4.0	9	22.8834	22.7139	22.4144	21.9849	21.4254	20.7359

Table A2.35: Variations in percentage Fe(II) oxidised at a constant liquid flowrate of 10 litres per minute and various angles of tilt based on quadratic model $y=b_0 + b_1x_1 + b_2x_2 + b_3x_3 + b_4x_1x_2 + b_5x_1x_3 + b_6x_2x_3 + b_7x_1^2 + b_8x_2^2 + b_9x_3^2$

Vapour rate	Liquid rate	Y, % Fe(II) oxidised at various angles of tilt					
		0^0	5^0	10^0	15^0	20^0	25^0
1.5	10	12.7655	12.5503	12.2050	11.7298	11.1245	10.3893
2.0	10	11.1861	10.9821	10.6481	10.1841	9.5901	8.8661
2.5	10	11.4049	11.2122	10.8894	10.4367	9.8539	9.1412
3.0	10	13.4219	13.2404	12.9289	12.4874	11.9159	11.2144
3.5	10	17.2371	17.0669	16.7666	16.3364	15.7761	15.0859
4.0	10	22.8508	22.6915	22.4025	21.9835	21.4345	20.7555

Table A2.36: Variations in percentage Fe(II) oxidised at a constant liquid flowrate of 11 litres per minute and various angles of tilt based on quadratic model $y=b_0 + b_1x_1 + b_2x_2 + b_3x_3 + b_4x_1x_2 + b_5x_1x_3 + b_6x_2x_3 + b_7x_1^2 + b_8x_2^2 + b_9x_3^2$

Vapour rate	Liquid rate	Y, % Fe(II) oxidised at various angles of tilt					
		0^0	5^0	10^0	15^0	20^0	25^0
1.5	11	11.9499	11.7451	11.4104	10.9456	10.3509	9.6261
2.0	11	10.4592	10.2657	9.9422	9.4887	8.9052	8.1917
2.5	11	10.7668	10.5845	10.2723	9.8300	9.2578	8.5555
3.0	11	12.8725	12.7015	12.4005	11.9695	11.4085	10.7175
3.5	11	16.7765	16.6167	16.3270	15.9072	15.3575	14.6777
4.0	11	22.4786	22.3301	22.0516	21.6431	21.1046	20.4361

APPENDIX 3:

THE NULL HYPOTHESIS AND STATISTICAL INFERENCE

The p-values in the student's t-test are used as a tool to check the significance of each of the coefficients which in turn may indicate the pattern of the interactions between the variables. The smaller the p-value the more significant the corresponding coefficient. For model statistics, a variable coefficient is considered significant if the p value is less than or equal to 0.05 (at 95% confidence level). The null hypothesis H_0 is that the coefficient does not differ from zero and being significant means that H_0 is rejected. Thus non significant coefficients can be replaced by zero, meaning that elimination of the variable has no major impact on the model. For the analysis of variance, the null hypothesis H_0 is that the variations observed in y are not due to variations in x_1, x_2 and x_3 but they are coincidental. If any is significant, H_0 is rejected meaning that the variations in that variable are actually responsible for the changes observed in y. In statistical inference of observed data of a scientific experiment the null hypothesis refers to a general or default position: that there is no relationship between two measured phenomena, or that a potential treatment has no effect. Rejecting or disproving the null hypothesis – and thus concluding that there are grounds for believing that there is a relationship between two phenomena or that a potential treatment has a measurable

effect – is a central task in the modern practice of science, and gives a precise sense in which a claim is capable of being proven false (Wikipedia, 2013)

APPENDIX 4:

CATALOGUE OF DEVELOPED TRAYS AND FACILITIES FOR TRAY TESTING, DEVELOPMENT AND TROUBLE SHOOTING.

Recently Developed Trays.

The most recently introduced trays and improvements of existing tray hardware are presented here in reversed chronological order (newest at the top and oldest at the bottom). From this list it can be seen, that the last decade has seen interesting developments in tray technology. This has resulted from the competitive activities of the hardware manufacturers, who created a livelier tray market place by doing so.

(Please note: this listing is indicative and not exhaustive.)

UOP stands for "Universal Oil Processes"
SRP stands for "Separation Research Program"
DA stands for "Distillation and Absorption"

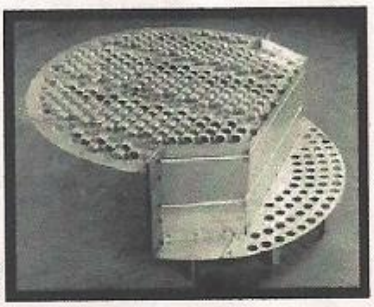

The ***Triton***™ high capacity tray was introduced during **1997** by **Norton Chemical Process Products Corp.,** Akron, Ohio, USA.

This tray combines a patented downcomer design (to increase the tray's contacting area) with a tray deck provided with proprietary fixed valves; the ***Provalve***™**.** Up to 45% greater capacity than conventional valve trays are claimed, while maintaining or improving mass transfer efficiency. This tray appears to be Norton's answer the competition.

A unique collaboration of **Nutter Engineering** and **UOP** resulted in the introduction of the new ***VG-MD*** tray, during the DA '97 Conference, september **1997** at Maastricht.

This tray is a further extension of the line of Multiple Downcomer trays of UOP. The ***VG-MD*** tray combines Multiple Downcomers with ***MVG*** tray decks (replacing the usual sieve tray decks). This tray type combines the characteristics of MD-trays and MVG-trays: a higher capacity and an improved turn down.

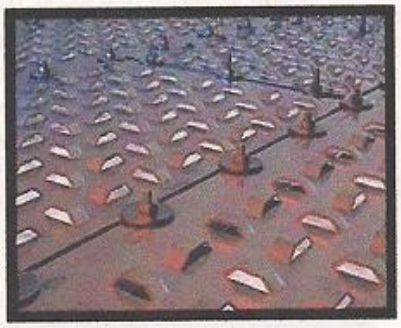

The ***Bi-FRAC*** ™ high capacity tray was introduced by **Koch Engineering** during **1997**.

A tray design engineered to minimize entrainment (by reducing gasvelocity) is the key to the claimed capacity increase of up to 30 % over conventional valve and sieve trays, without efficiency loss. (Another of Koch's competitors to Glitsch's Nye tray).

The tray floor is provided with fixed, open valves, which are positioned to create a bi-directional flow pattern, hence Bi-Frac.

The ***Vortex (Downcomer) Tray***™ was (re-) introduced by **Sulzer Metawa B.V.** (Tiel, the Netherlands) during the ACHEMA at Frankfurt, FRG in **1997**. This is an improved high capacity tray enabling capacity increases up to 30% over conventional trays, without losing separation efficiency (may even gain in efficiency). The special feature of this tray is in the design of the downcomers, which are cylindrical/conical with a seal pan underneath and three baffles on top. These baffles are placed in such a way, that liquid entering the downcomer induces a swirling motion on the liquid reservoir in the downcomer. This improves vapour disengagement and hence higher downcomer velocities are allowable. Reportedly, the first industrial applications have confirmed the advantages of this tray design and more applications are under study and being installed.

The (US 5453222) patent application for the ***SUPERFRAC***® tray of **Glitsch Inc**. was filed in **1994**. The new tray was described in a paper presented at the DA '97 conference, september **1997**, Maastricht. The basic concept of the improvement embodied in this tray is to transfer downcomer bottom area into contacting area by truncating the downcomer, so that contacting area can be maximized. Due to this increase vapour velocity decreases and entrainment will decrease, as well. The ***SUPERFRAC***® tray is specifically developed for large diameter (> 2m.) columns, which are heavily loaded with liquid.

In **1994 Stahl GmbH** (Mannheim/Viernheim, Germany) introduced during the ACHEMA their new ***Dualflex***™ tray. This is a high performance tray based on a downcomerless ('dual flow') tray provided with specially adapted ***Varioflex***™ valves. The main advantage of this tray is, that in situations where dual flow trays have to be applied, it gives a better tray efficiency and an improved turn down capability. See, Chemie-Ingenieur-Technik, 69(**1997**)5, 649-650.

In a **1994** paper presented in November at the Annual Meeting of the A.I.Ch.E. at San Francisco, **British Oxygen Company** and the **University of Nottingham** unveiled their newly developed ***Very High Capacity Expanded Metal tray.*** This tray was described in the European Patent 635,292, filed 12/07/94, which mentioned J.T. Lavin as inventor. This tray comprises a special combination of two Expanded Metal sheets (with different geometric specifications) which are 'piggy backed' together and make up the tray floor in the *contacting area*. In between these 'dual-sheet' tray floors of two successive trays, they mount, at a distance of some 0.15 m from the lower tray, a third Expanded Metal sheet, which collects and separates droplet entrainment and redirects this entrainment to a downcomer. The overal tray spacing could be made as low as 0.2 m. In a rectangular three tray air/water simulator (3inch wide and 4 ft flow path), they achieved a maximum air flowrate which was almost twice the maximum air flow rate expected for conventional sieve trays. Moreover, these trays showed a relative low pressure drop and also the separation performance (tray efficiency) was satisfactory, i.e. comparable to convential sieve trays. Apparently, this new tray type is under active development, at BOC.

In March **1994 Koch** Engineering Comp. Inc announced at the I.Chem.E. "Debottlenecking

Seminar" in London, that they had applied for the first time, with success, a new type of high capacity tray, specifically developed for heavily liquid loaded systems: the ***Ultra-Frac tray.*** For this tray, they claim at least a 20% capacity advantage, in comparison to the original UOP Multiple Downcomer trays, while this is combined with a comparable tray efficiency. They were enabled to do so, because several years earlier they had acquired access to Russian tray technology on cocurrent vortex tube contactors, as developed around 1978-1984 by Y.N. Lebedev, V.I. Sheinman and c.s.. See, paper by Kulov and Lebedev at 1992 Distillation and Absorption Conference at Birmingham. This Russian technology in combination with Koch's expertise and an additional development effort led to their ***Ultra-Frac tray.***

The ***MVG tray*** was introduced late in **1993** by **Nutter Engineering**. It was the logical further extension of the V-grid tray, which had two versions the SVG (Small V-Grid) and the LVG (Large V-Grid) to a still smaller size of the fixed-valve 'grid'; the Mini V-Grid. All three sizes are shown in the picture. Use of this type of plate in the *contacting area* of trays gives a 10 to 20% increase in the upper limit (when this limit is contrained by an excessive entrainment rate) *and* an (initially unexpected) decrease in the lower operating limit. Thus, increasing the turn down ratio to a value of about four, which makes this tray intermediate in flexibility, in comparison to conventional sieve trays (with a turndown ratio of ~2.5 to 3.0) and valve trays (5 and more). Since, their introduction Nutter Engineering has been selling these tray decks successfully, for a wide range of applications.

In **1992** the second commercial application of **UOP's *Enhanced Capacity Multiple Downcomer Trays*** came in use in a 18 ft. C3-splitter of Chevron Chemical Company at Port Arthur Texas, USA. UOP had been developing this tray technology since 1989. The first application had been in 1990 in a de-ethanizer owned by ÖMV Aktiengesellschaft, at Schwechat, Austria. The results of this application were described in a paper presented at the IChemE Distillation and Absorption Conference, Birmingham in **1992**. UOP's EMCD tray is a further development of their succesful MD-tray. Since the MD-tray was patented in 1968 by the Linde division of Union Carbide, by 1992 they had been installed in nearly 400 distillation columns, all over the world. The newly developed EMCD trays have a 20% increased upper limit for the vapour flow in comparison to the original MD trays. This may not sound spectacular, but financially can be highly attractive, because of the increased productivity of these large scale columns.

The ***Duo-Sorb tray*** is an example of a high efficiency and high turndown tray invented in **1992** by H.O. Ebeling (U.S. 5,116,393, US 5,514,305). The tray consists of a tray floor having a multitude of small bubble caps with random packing dumped on it and a special outlet downcomer construction. This tray was originally developed by **Latoka Engineering**, Tulsa, OK, USA, for a particular range of applications, viz. dehydration of natural with glycol at high pressure. The advantages of these trays resides in the far greater tray contacting area (greater efficiency), which lowers the number of actual trays, to be installed in a new column design (or existing columns might be shortened). This results in a reduced column height, which saves significantly on the cost of a high pressure column shell. Latoka Eng. has been selling these trays for some time now, successfully.

1989 and 1990 saw the patenting of a tray, which combined a sieve tray (or a tray floor made of closely spaced trapezoidal rods; a screen) with packing (or demistermat) on it. (U.S. Patent 4,842,778, 1989; European Patent 381,388, filed 26-01-90). This type of tray was invented and developed by G.K. Chen and K.T. Chuang at the University of Alberta, Edmonton, Canada. **Glitsch Inc.** acquired a license to this tray and initially they have been actively trying to sell it, under their trademark ***SCREEN TRAY***. The much improved efficiency of this type of tray could have made it attractive for many applications. Lately, this type of tray type is no longer actively promoted and has quitely disappeared from Glitsch's advertisements, for reasons which have not been made public.

The ***T-By tray*** was patented by B.M. Parker and T.J. Parker in **1988** (US 4,762,651) and test results were published in 1992. The ***T-By tray*** is a modified sieve tray using a system of transversal weirs with side baffles to approximate liquid plug flow across the tray. Vapour/liquid contact is modified by patterning the vapour sieve holes in parallel to the weirs and with the intermediate weirs forming circulation cells promoting liquid mixing and stabilizing the froth bed in the *contacting area*. The test results showed that the tray performance (efficiency) could be improved in significant ways. Additional studies were proposed, for further improvements.

In **1988** the ***Nye tray*** was applied for the first time in two deisobutanisers of different diameter. **Glitsch Inc.** acquired in 1991 the worldwide rights for the design, marketing and manufacturing of these trays, which were invented by James O. Nye. Since their introduction, Glitsch Inc. has had great success in selling these higher capacity trays. As of May 1994, they had been installed in 119 distillation columns, already. In existing columns that were modified, by installing these trays, Glitsch claims that capacity increases of 20% have been achieved by the 'Nye-tray' effect. The Nye tray achieves this increase in vapour capacity by shortening of the downcomers, in effect lifting them 2 to 3 inches up from the tray floor. In a way, trading off *downcomer area* for the enlargement of the *contacting area*. This reduces the vapour velocity in the contacting area and allows larger volumetric flowrates before entrainment or bed expansion limitations set in, again. This strategy works for both sieve tray decks and valve tray decks.

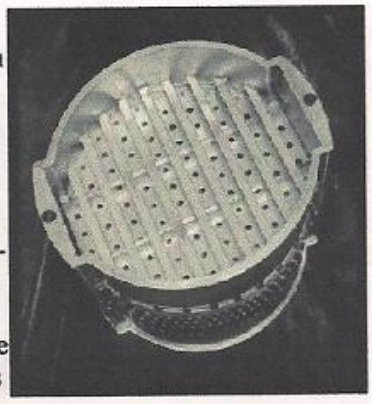

Already in **1982** William R. Trutna described in the U.S. Patent 4,361,469 (filed Feb. 17, 1981) a new device based on a combination of a special contacting tray with cocurrent upflow of vapour and liquid and a special liquid separation section. Relative to sieve trays this ***Trutna tray*** would have a 30 to 100% greater vapour handling capacity. A development programme has been in place at SRP, University of Texas, Austin, USA from **1989** onwards. From a SRP-publication in the Chemical Engineering Progress, June 1996, pp. 42-48, it can be learned, that this type of tray can double the upper limit of the vapour throughput and maintain the same separation efficiency. However, these trays are more complex to make and more expensive to install. In debottlenecking applications, the Trutna trays require about three to four times the replacement cost of convential sieve trays, which make them about as expensive as structured packing. By **1998**, **Jaeger Products., Inc.** had started to offer this tray under the trademark of ***CoFlo Tray.***

Last Updated: 18 december 1998

FACILITIES FOR TRAY TESTING, DEVELOPMENT AND TROUBLE SHOOTING

Some of the experimental facilities for research, development and troubleshooting work on absorption and distillation trays at various locations as listed by Wijn (1998) are given below:

- Koch Engineering, Wichita, USA operates a 0.20m reactive distillation pilot plant.
- Norton Chemical Process Products Corporation, USA has a 0.76m diameter column used for air/water simulation and gas absorption, and a 0.39m diameter distillation column which can be operated from high vacuum to 24 psia.
- Mitsui Engineering and Shipbuilding Co., Tamano, Japan has a 0.5m diameter distillation column capable of doing total reflux test runs with the cyclohexane/n-heptane system, at near atmospheric pressures.
- Shell Research and Technology Centre, Amsterdam, Netherlands operate a 0.45m distillation column capable of operating at sub- and super-atmospheric pressures.
- UOP Process Equipment, Tonawanda, NY, USA has a square 0.6m by 0.6m air/water simulator.
- Laboratory Equipment for the Chemical Process Industry at Delft Technical University, Netherlands operate a 0.45m distillation column.

- Separations Research Program, University of Texas, Austin, USA, has a 0.426m diameter air/water stripper and a 0.426m diameter distillation/extraction pilot plant.
- UMIST, Manchester, UK, has a 0.6m diameter distillation column operating with a methanol/water test system.
- University of Alberta, Dept. of Chemical Engineering, Edmonton, Canada has a 0.15m diameter air/water column, a 0.15m distillation column, a 0.30m air/water column, a 0.30m distillation column, and a 0.60m diameter air/water column.

APPENDIX 5:

ARCHIMEDES PRINCIPLE AND PRINCIPLE OF FLOTATION

The Archimedes principle states that when an object is wholly or partially immersed in a fluid, it experiences a weight loss or an Upthrust which is equal to the weight of the fluid displaced by the object. The following can be deduced from the above law;

- A body completely immersed in a liquid will displace a volume of liquid which is equal to the volume of the object. The mass of liquid thus displaced will be equal to the volume of the object times the density of the liquid. This mass can be converted to weight which is equal to Upthrust from Archimedes principle. The force exerted by 1 Kg is 9.81N.
- If a body is not completely immersed but partially, so that a fraction of the volume, say 1/6 is immersed, then mass of liquid displaced equals V/6 times the density of the liquid. The Upthrust is also obtained as stated previously.

The principle of flotation states that a body floats when the Upthrust exerted upon it by the fluid in which it floats is equal to the weight of the body.

APPENDIX 6:

CONSTRUCTION OF THE FACTORIAL DESIGN MATRICES.

A linear mathematical model is considered in the first phase of a research. Designing the first order regression model is the first phase of a study aimed at obtaining the interpolation model or function, the knowledge of which facilitates estimating response values in different points of the studied factorial space. A linear model is additionally used when moving to the optimum region, the same as when we use the steepest ascent method as an optimization technique. Later if necessary, the polynomial degree is increased. Accuracy and confidence of the obtained estimates for regression coefficients depend on the used design of experiments. Choice of the design of experiments has to do with determination of the number of experimental point-trials and such a distribution of those points in a factorial space that facilitates obtaining the necessary information with a minimal number of design point-trials. When selecting the design of experiments, a design matrix or a standard type table is constructed where all the conditions of doing the design points that are part of the chosen design are defined. Mostly in a design matrix, rows correspond to different design points-trials and columns to individual factors. Obtaining a linear model has to do with performing a Full Factorial Experiment or a Fractional Factorial Experiment, which is a definite part of the Full Factorial design. Full Factorial experiment is the experiment where all

possible combinations of levels of factors are realized and experiments are processed by applying statistical analysis. Full factorial experiment is called the design experiment of type 2^k and in cases where we have a large number of factors, it requires a large number of trials ($N=2^k$). When composing the factorial experiment matrices, coded factor values are used. Coding factors require linear transformation of the factor space coordinates with the coordinate beginning in the null point or experimental centre and defining the coordinate axis ratio in units of the factor variation interval.

Our design matrix has been constructed such that a mathematical modelling of the process has to be done according to the problem statement. A Full factorial experiment was used with double replication of design points. The 2^3 design matrix with 3 parallel design points in the experimental centre was used as a design matrix. These 3 parallel design points were used to estimate the experimental error that was necessary for checking the significance of the regression coefficients and lack of fit of the obtained regression.

It is characteristic for design of experiments that it uses polynomial models since the quality of the approximation may be improved by increasing a polynomial degree. Such models are especially suitable for solving optimization problems as it is possible to take into account the effects of interaction and a large number of

factors. Besides, it is easy to estimate the degree of lack of fit of polynomial models of different orders. This is the basis for the polynomial models used.

Based on the magnitude of the linear regression coefficients, one may speak about the strength of influence of associated factors on response. The higher the b_i value of the associated factor, the more intensively it affects the response. The sign of these coefficients also has to be accounted for. If b_i has a positive sign, the increase of the associated factor causes an increase in response; on the contrary, with a negative sign of the linear regression coefficient, an increase in its factor value causes a decrease in the optimization parameter.

A check of statistical significance must be done for the calculated regression coefficients and a check of lack of fit done for the regression model.

SECOND ORDER ROTATABLE DESIGN (BOX-WILSON DESIGN)

Second-order designs are used in practice in situations when the linear model is insufficient for a mathematical description of a research subject with an adequate precision. Then a mathematical model in the form of a second-order polynomial is formed. When describing a response surface by a second-order equation, varying a factor on only two levels does not offer the necessary information hence an experiment is designed so that factors are varied on three or more levels. One of such designs is the Second-order rotatable design (Box-Wilson design)

With second-order rotatable designs, we upgrade a Full Factorial Experiment or its fractional replica (usually half-replica) to get a second-order design by adding a certain number of “starlike/axial/star” and “null/centerpoints” points to the “core”. Starlike points are located on coordinate axes at a distance from the experimental centre given by $\alpha = 2^{k/4}$, while the centerpoints are created by setting all factors at their midpoints. In coded form, centerpoints all fall at the zero level, and act as a barometer of the variability in the system. The design matrix for a central Composite Rotatable Design for k = 3 is given in table 3.7.